

SKEIN AND CLUSTER ALGEBRAS OF UNPUNCTURED SURFACES FOR \mathfrak{sp}_4

TSUKASA ISHIBASHI AND WATARU YUASA

ABSTRACT. Continuing to our previous work [IY21] on the \mathfrak{sl}_3 -case, we introduce a skein algebra $\mathcal{S}_{\mathfrak{sp}_4, \Sigma}^q$ consisting of \mathfrak{sp}_4 -webs on a marked surface Σ with certain “clasped” skein relations at special points, and investigate its cluster nature. We also introduce a natural \mathbb{Z}_q -form $\mathcal{S}_{\mathfrak{sp}_4, \Sigma}^{\mathbb{Z}_q} \subset \mathcal{S}_{\mathfrak{sp}_4, \Sigma}^q$, while the natural coefficient ring \mathcal{R} of $\mathcal{S}_{\mathfrak{sp}_4, \Sigma}^q$ includes the inverse of the quantum integer $[2]_q$. We prove that its boundary-localization $\mathcal{S}_{\mathfrak{sp}_4, \Sigma}^{\mathbb{Z}_q}[\partial^{-1}]$ is included into a quantum cluster algebra $\mathcal{A}_{\mathfrak{sp}_4, \Sigma}^q$ that quantizes the function ring of the moduli space $\mathcal{A}_{\mathfrak{sp}_4, \Sigma}^\times$. Moreover, we obtain the positivity of Laurent expressions of elevation-preserving webs in a similar way to [IY21]. We also propose a characterization of cluster variables in the spirit of Fomin–Pylyavskyy [FP16] in terms of the \mathfrak{sp}_4 -webs, and give infinitely many supporting examples on a quadrilateral.

CONTENTS

1. Introduction	1
2. The \mathfrak{sp}_4 -skein algebra $\mathcal{S}_{\mathfrak{sp}_4, \Sigma}$ of an unpunctured marked surface	5
3. Generators and Laurent positivity for \mathfrak{sp}_4 -skein algebras	19
4. Quantum cluster algebras	30
5. Quantum cluster algebras and skein algebras	40
6. Gallery of web clusters in a quadrilateral	49
References	55

1. INTRODUCTION

We continue to investigate the relationship between the cluster and skein quantizations of the (decorated) G -character varieties of surfaces. The \mathfrak{sl}_2 -case is established by Muller [Mul16] and the \mathfrak{sl}_3 -case is investigated (via the \mathfrak{sl}_3 -skein algebra defined by [FS20]) in our previous paper [IY21]. In the present paper, we are going to deal with the \mathfrak{sp}_4 -case. Kuperberg [Kup96] has established the skein theory for rank two Lie algebras, including \mathfrak{sp}_4 . He gave a diagrammatic interpretation of categories of finite-dimensional representations of their quantum groups. The diagrammatic category of $U_q(\mathfrak{sp}_4)$ was further studied by Bodish [Bod20, Bod22], and that for $U_q(\mathfrak{sp}_{2n})$ by [BERT21]. On the other hand, the canonical cluster K_2 -structure on the moduli space $\mathcal{A}_{G, \Sigma}$ of decorated twisted G -local system on a marked surface Σ [FG06a] has been constructed by Le [Le19]

2020 *Mathematics Subject Classification.* 13F60, 57K31 (Primary), 57K20 (Secondary).

Key words and phrases. Cluster algebra; Skein algebra; Positivity.

(for classical types, and particular cluster charts) and [GS19] (for all semisimple types, and a more general class of cluster charts). Let $\mathfrak{s}(\mathfrak{g}, \Sigma)$ be the mutation class of seeds that encodes this structure, where $\mathfrak{g} = \text{Lie}(G)$.

1.1. Comparison of skein and cluster algebras. In this paper, we first define a skein algebra $\mathcal{S}_{\text{sp}_4, \Sigma}^q$ spanned by certain sp_4 -webs on an unpunctured marked surface Σ , subject to certain ‘‘clasped’’ skein relations (Definition 2.3) as well as the interior sp_4 -skein relations studied by Kuperberg. Here the coefficient ring of the skein algebra is $\mathcal{R} = \mathcal{R}_q := \mathbb{Z}[q^{\pm 1/2}, 1/[2]_q]$, which includes the inverse of the quantum integer $[2]_q$. We also introduce the set $\text{BWeb}_{\text{sp}_4, \Sigma} \subset \mathcal{S}_{\text{sp}_4, \Sigma}^q$ of *basis webs*, which gives an \mathcal{R} -basis (Theorem 2.15). Then we define the \mathbb{Z}_q -form $\mathcal{S}_{\text{sp}_4, \Sigma}^{\mathbb{Z}_q} \subset \mathcal{S}_{\text{sp}_4, \Sigma}^q$ to be the \mathbb{Z}_q -span of $\text{BWeb}_{\text{sp}_4, \Sigma}$, which turns out to be closed under the multiplication (Lemma 3.12).

On the other hand, we construct quantum clusters associated with decorated triangulations as *web clusters* in the skein algebra $\mathcal{S}_{\text{sp}_4, \Sigma}^q$, and show that they are mutation-equivalent to each other as a comparison between the quantum exchange and skein relations (Proposition 5.2). Hence the associated quantum seeds give rise to a canonical mutation class $\mathfrak{s}_q(\text{sp}_4, \Sigma)$ that quantizes $\mathfrak{s}(\text{sp}_4, \Sigma)$, which defines a quantum (upper) cluster algebras $\mathcal{A}_{\text{sp}_4, \Sigma}^q \subset \mathcal{U}_{\text{sp}_4, \Sigma}^q$ over $\mathbb{Z}_q = \mathbb{Z}[q^{\pm 1/2}]$ in the skew-field $\text{Frac} \mathcal{S}_{\text{sp}_4, \Sigma}^q$ of fractions.

The following is our first result, which gives a comparison of skein and cluster algebras:

Theorem 1 (Comparison of skein and cluster algebras: Sections 5.2 and 5.3). *For any connected (triangulable) unpunctured marked surface Σ , we have an inclusion $\mathcal{S}_{\text{sp}_4, \Sigma}^{\mathbb{Z}_q}[\partial^{-1}] \subset \mathcal{U}_{\text{sp}_4, \Sigma}^q$. Here $\mathcal{S}_{\text{sp}_4, \Sigma}^{\mathbb{Z}_q}[\partial^{-1}]$ denotes the boundary-localization of the \mathbb{Z}_q -form of sp_4 -skein algebra (Definition 2.7). Moreover if Σ has at least two special points, then we have inclusions*

$$\mathcal{S}_{\text{sp}_4, \Sigma}^{\mathbb{Z}_q}[\partial^{-1}] \subset \mathcal{A}_{\text{sp}_4, \Sigma}^q \subset \mathcal{U}_{\text{sp}_4, \Sigma}^q.$$

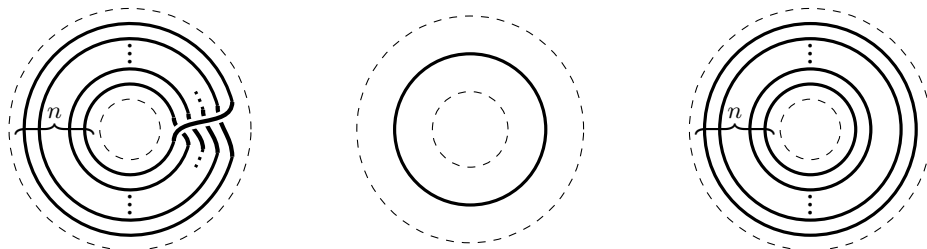
Moreover,

- the inclusions are mapping class group equivariant;
- the bar-involution on $\mathcal{U}_{\text{sp}_4, \Sigma}^q$ restricts to the mirror-reflections on $\mathcal{S}_{\text{sp}_4, \Sigma}^{\mathbb{Z}_q}[\partial^{-1}]$;
- the ensemble grading of $\mathcal{U}_{\text{sp}_4, \Sigma}^q$ restricts to the endpoint grading of $\mathcal{S}_{\text{sp}_4, \Sigma}^{\mathbb{Z}_q}[\partial^{-1}]$.

As in our previous study on the \mathfrak{sl}_3 -case, the inclusion $\mathcal{S}_{\text{sp}_4, \Sigma}^{\mathbb{Z}_q}[\partial^{-1}] \subset \mathcal{U}_{\text{sp}_4, \Sigma}^q$ is provided by the *cutting trick* (Lemma 3.1), which is the way to obtain the Laurent expression of a given web in a web cluster. The stronger inclusion $\mathcal{S}_{\text{sp}_4, \Sigma}^{\mathbb{Z}_q}[\partial^{-1}] \subset \mathcal{A}_{\text{sp}_4, \Sigma}^q$ is provided by the *sticking trick* (Lemma 3.2), by which we can reduce the generators of the localized skein algebra into those corresponding to cluster variables. Actually, we show that the boundary-localized \mathbb{Z}_q -form can be generated by the set $\text{SimpWil}_{\text{sp}_4, \Sigma}^{\varpi_1}$ (Theorem 3.13), which consists of the quantum counterpart of the matrix coefficients of *simple Wilson lines* [IOS22] in the vector representation. Then it is easy to see that they are actually cluster variables up to boundary webs (cf. [IOS22, Proposition 4.12]).

Conjecture 2. *For any connected (triangulable) unpunctured marked surface Σ , we have the equalities*

$$\mathcal{S}_{\text{sp}_4, \Sigma}^{\mathbb{Z}_q}[\partial^{-1}] = \mathcal{A}_{\text{sp}_4, \Sigma}^q = \mathcal{U}_{\text{sp}_4, \Sigma}^q.$$



the geometric n -bracelet of γ a simple loop γ the n -bangle of γ

FIGURE 1.1. The middle shows a tubular neighborhood of a simple loop γ . The *geometric n -bracelet* (resp. *n -bangle*) along γ is obtained by replacing it with the graph shown in the left (right) colored by a fundamental representation of \mathfrak{sp}_4 .

When $\Sigma = T$ is a triangle, this conjecture is true (Proposition 5.5). The classical counterpart $q = 1$ of this conjecture is proved by Ishibashi–Oya–Shen [IOS22]. In particular, $\text{BWeb}_{\mathfrak{sp}_4, \Sigma}$ provides a \mathbb{Z} -basis of the classical cluster algebra $\mathcal{A}_{\mathfrak{sp}_4, \Sigma}$.

We also obtain the following positivity result.

Theorem 3 (Quantum Laurent positivity of webs: Theorem 5.10). *Any elevation-preserving web with respect to an ideal triangulation Δ is expressed as a Laurent polynomial with coefficients in $\mathcal{R}_+ = \mathbb{Z}_+[q^{\pm 1/2}, 1/[2]_q]$ in the quantum cluster associated with any decorated triangulation $\mathbf{\Delta} = (\Delta, m_{\Delta}, \mathbf{s}_{\Delta})$ over Δ . In particular, the following webs are quantum GS-universally positive Laurent polynomials (Definition 5.9)*

- over \mathbb{Z}_q : descending loops/arcs of type 1 with or without legs (see Definition 3.4);
- over \mathcal{R} : the geometric bracelets or the bangles (Figure 1.1) of type 2 along simple loops.

Here the webs in the first item form a subset $\text{Desc}_{\mathfrak{sp}_4, \Sigma}^{\varpi_1}$ (see Definition 3.5) that contains geometric bracelets/bangles of type 1 and give a generating set of $\mathcal{S}_{\mathfrak{sp}_4, \Sigma}^{\mathbb{Z}_q}[\partial^{-1}]$ (Theorem 3.13).

1.2. Characterization of cluster variables. Among its possible benefits, the interplay between the skein and cluster theory is expected to provide a topological model for cluster variables. In the simplest case $\mathfrak{g} = \mathfrak{sl}_2$, the cluster variables are actually in a one-to-one correspondence with the simple arcs in the \mathfrak{sl}_2 -skein algebra. In the other cases, the mutation class $\mathfrak{s}(\mathfrak{g}, \Sigma)$ is typically of infinite mutation type. Namely, it contains infinitely many distinct exchange matrices (*i.e.*, it includes “infinitely complicated” combinatorics), so it is a very hard problem to uniformly understand all the cluster variables. In the \mathfrak{sl}_3 -case, Fomin–Pylyavskyy [FP16] proposed a series of insightful conjectures on the characterization of cluster variables in terms of \mathfrak{sl}_3 -webs.

We are going to discuss a conjectural characterization of the cluster variables in our \mathfrak{sp}_4 -case, in the same spirit as Fomin–Pylyavskyy. Let

- $\text{EWeb}_{\mathfrak{sp}_4, \Sigma} \subset \text{BWeb}_{\mathfrak{sp}_4, \Sigma}$ be the set of *elementary webs*;

In Section 6, we give a gallery of examples of web clusters on a quadrilateral, including an infinite sequence.

Acknowledgements. T. I. is supported by JSPS KAKENHI Grant Number JP20K22304. W. Y. is supported by JSPS KAKENHI Grant Numbers JP19J00252 and JP19K14528.

Notation on marked surfaces and their triangulations. A *marked surface* (Σ, \mathbb{M}) is a compact oriented surface Σ with boundary equipped with a fixed non-empty finite set $\mathbb{M} \subset \partial\Sigma$ of *special points*. In particular, we do not allow interior marked points (“punctures”) in this paper. We also call (Σ, \mathbb{M}) an *unpunctured marked surface* when we emphasize the absence of punctures. When the choice of \mathbb{M} is clear from the context, we simply denote a marked surface by Σ . Moreover, assume the following conditions:

- (1) Each boundary component has at least one special point.
- (2) $n(\Sigma) := -3\chi(\Sigma) + 2|\mathbb{M}| > 0$, and Σ is not a disk with two special points (a biangle).

These conditions ensure that the marked surface Σ has an ideal triangulation, that is, the isotopy class of a collection Δ of simple arcs connecting special points whose interiors are mutually disjoint, which decomposes Σ into triangles. The number $n(\Sigma)$ gives the number of edges of any ideal triangulation Δ . We call a connected component of the punctured boundary $\partial^*\Sigma := \partial\Sigma \setminus \mathbb{M}$ a *boundary interval*. Each boundary interval belongs to any ideal triangulation Δ . We call an edge of Δ an *interior edge* if it is not a boundary interval. Denote the set of edges (resp. interior edges, triangles) of Δ by $e(\Delta)$ (resp. $e_{\text{int}}(\Delta)$, $t(\Delta)$).

More generally, we can consider an *ideal cell decomposition* of Σ , which is a decomposition of Σ into a union of polygons. When it is obtained from an ideal triangulation by removing k interior edges, it is said to be of *deficiency* k . In this paper, we only use an ideal cell decomposition of deficiency 0 or 1. The ideal cell decomposition of deficiency 1 obtained from an ideal triangulation Δ by removing one interior edge E is denoted by $(\Delta; E)$.

Finally, a *decorated triangulation* is a triple $\mathbf{\Delta} = (\Delta, m_{\Delta}, \mathbf{s}_{\Delta})$, where

- Δ is an ideal triangulation of Σ ;
- $m_{\Delta} : t(\Delta) \rightarrow \mathbb{M}$ is a choice of a vertex of each triangle;
- $\mathbf{s}_{\Delta} : t(\Delta) \rightarrow \{+, -\}$ is a choice of a sign at each triangle.

The data m_{Δ} is indicated by the symbol $*$ in the figures. A typical seed in the mutation class $\mathfrak{s}(\mathfrak{sp}_4, \Sigma)$ will be associated with such a decorated triangulation [GS19].

2. THE \mathfrak{sp}_4 -SKEIN ALGEBRA $\mathcal{S}_{\mathfrak{sp}_4, \Sigma}$ OF AN UNPUNCTURED MARKED SURFACE

In this section, we define the \mathfrak{sp}_4 -skein algebra $\mathcal{S}_{\mathfrak{sp}_4, \Sigma} = \mathcal{S}_{\mathfrak{sp}_4, \Sigma}^v$ for a surface Σ with special points $\mathbb{M} \subset \partial\Sigma$ by introducing the skein relation at a special point. We also give some basic definitions and properties related to $\mathcal{S}_{\mathfrak{sp}_4, \Sigma}$. In what follows, we use a ring $\mathcal{R} = \mathcal{R}_v := \mathbb{Z}[v^{\pm 1/2}, 1/[2]_v]$ of coefficients with a formal variable $v^{1/2}$ where a quantum integer is defined by $[n] = [n]_v := (v^n - v^{-n})/(v - v^{-1})$.

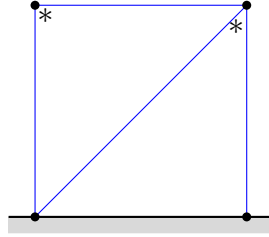


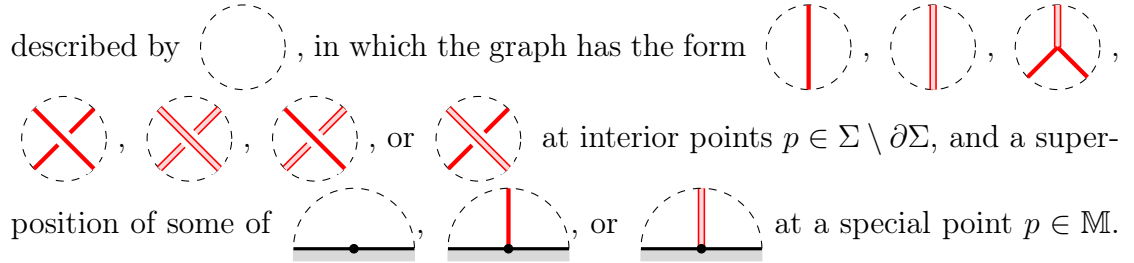
FIGURE 1.2. A local picture of a datum (Δ, m_Δ) . By convention, a portion of $\partial\Sigma$ is drawn by a thick line together with a gray region indicating the “outer side” of Σ .

2.1. **The skein relations for \mathfrak{sp}_4 .** Let us introduce the \mathfrak{sp}_4 -webs and its skein relation introduced by Kuperberg [Kup96]. We firstly define tangled graphs for \mathfrak{sp}_4 on an unpunctured marked surface.

Definition 2.1 (tangled \mathfrak{sp}_4 -graphs). (1) A *tangled \mathfrak{sp}_4 -graph diagram* on Σ is a map (or its image) from a uni-trivalent graph to Σ whose edges are colored by fundamental representations ϖ_1 (called *type 1 edges*) or ϖ_2 (called *type 2 edges*) of \mathfrak{sp}_4 . Moreover:

- We assume that each triple of edges incident to a common trivalent vertex consists of two type 1 edges and a type 2 edge, and the only self-intersections in the interior of Σ are transverse double points of edges (called *internal crossings*). The image of the graph only intersects with $\partial\Sigma$ at special points.
- The transverse double points of edges in the interior have over/under-passing information. For each $p \in \mathbb{M}$, the set of half-edges incident to p has a total order called the *elevation* at p .

In pictures, an edge of type 1 (resp. type 2) is described by a single (resp. double) line. Each point of the image of a tangled \mathfrak{sp}_4 -graph diagram has a neighborhood described by



position of some of --- , --- , or --- at a special point $p \in \mathbb{M}$. Here an edge with a gap at the intersection point is under-passing. The elevation is indicated by the distance from p (see Figure 2.1).

- (2) Two tangled \mathfrak{sp}_4 -graphs are *equivalent* if these graphs are related by a finite sequence of the Reidemeister moves (R1'), (R2), (R3), (R4), (bR) (see diagrams in Lemma 2.5) and isotopies of Σ relative to $\partial\Sigma$. We call the equivalence class of a tangled \mathfrak{sp}_4 -graph diagram a *tangled \mathfrak{sp}_4 -graph* on Σ . Let $\text{Tang}_{\mathfrak{sp}_4, \Sigma}$ be the set of tangled \mathfrak{sp}_4 -graphs on Σ . It has a multiplication defined by superposition of their diagrams: the product $G_1 G_2$ of $G_1, G_2 \in \text{Tang}_{\mathfrak{sp}_4, \Sigma}$ is defined by a superposing G_1

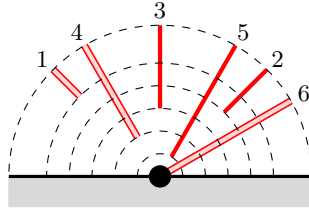


FIGURE 2.1. Elevation at a special point. The labeling by natural numbers represents the total order.

on G_2 so that G_1 passes over G_2 at all intersection points and the half-edges of G_1 has higher elevation than those of G_2 at any $p \in \mathbb{M}$.

We define the following skein relations for formal linear combinations of tangled \mathfrak{sp}_4 -graphs.

Definition 2.2 (the internal \mathfrak{sp}_4 -skein relations [Kup94, Kup96]).

$$\text{Red circle} = -\frac{[2][6]}{[3]} \text{Dashed circle} \tag{2.1}$$

$$\text{Red concentric circles} = \frac{[5][6]}{[2][3]} \text{Dashed concentric circles} \tag{2.2}$$

$$\text{Red circle with vertical line} = 0 \tag{2.3}$$

$$\text{Red circle with vertical line and red vertical line} = -[2] \text{Red vertical line} \tag{2.4}$$

$$\text{Red triangle} = 0, \tag{2.5}$$

$$\text{Red arcs} - [2] \text{Red Y-junction} = \text{Red arcs} - [2] \text{Red X-junction} \tag{2.6}$$

$$\begin{aligned} \text{Red crossing} &= \frac{v^2}{[2]} \text{Red arcs} + v^{-1} \text{Red arcs} + \text{Red Y-junction} \\ &= v \text{Red arcs} + \frac{v^{-2}}{[2]} \text{Red arcs} + \text{Red Y-junction} \end{aligned} \tag{2.7}$$

$$\text{Red crossing with red lines} = v \text{Red Y-junction} + v^{-1} \text{Red Y-junction} \tag{2.8}$$

$$\text{Red crossing with red lines} = v \text{Red Y-junction} + v^{-1} \text{Red Y-junction} \tag{2.9}$$

$$\text{Red crossing with red lines} = v^2 \text{Red arcs} + v^{-2} \text{Red arcs} + \text{Red square} \tag{2.10}$$

Let us further introduce the ‘‘clasped’’ skein relations among half-edges incident to a special point.

Definition 2.3 (the clasped \mathfrak{sp}_4 -skein relations).

$$\begin{array}{c} \text{Diagram 1} = v \text{ Diagram 2}, \quad \text{Diagram 3} = v^2 \text{ Diagram 4}, \\ \text{Diagram 5} = v \text{ Diagram 6}, \quad \text{Diagram 7} = v \text{ Diagram 8}, \end{array} \quad (2.11)$$

$$\begin{array}{c} \text{Diagram 9} = \text{Diagram 10}, \quad \text{Diagram 11} = \text{Diagram 12}, \\ \text{Diagram 13} = \frac{1}{[2]} \text{Diagram 14}, \quad \text{Diagram 15} = 0, \end{array} \quad (2.12)$$

$$\begin{array}{c} \text{Diagram 16} = 0, \quad \text{Diagram 17} = 0, \quad \text{Diagram 18} = 0, \end{array} \quad (2.13)$$

$$\begin{array}{c} \text{Diagram 19} = 0, \quad \text{Diagram 20} = 0. \end{array} \quad (2.14)$$

In the above definition, we have drawn half-edges with the same elevation (called *simultaneous crossings*), which is defined as follows.

Definition 2.4 (simultaneous crossings).

$$\text{Diagram 21} := v^{-\frac{1}{2}} \text{Diagram 22}, \quad (2.15)$$

$$\text{Diagram 23} := v^{-\frac{1}{2}} \text{Diagram 24}, \quad \text{Diagram 25} := v^{-\frac{1}{2}} \text{Diagram 26}, \quad (2.16)$$

$$\text{Diagram 27} := v^{-1} \text{Diagram 28}, \quad (2.17)$$

For a local diagram of a tangled \mathfrak{sp}_4 -graph, one can show the following by using the (clasped) \mathfrak{sp}_4 -skein relations.

Lemma 2.5. *The following Reidemeister moves are obtained by \mathfrak{sp}_4 -skein relations.*

$$\begin{array}{ccc} \text{Diagram 29} \xleftrightarrow{(R1')} \text{Diagram 30}, & \text{Diagram 31} \xleftrightarrow{(R2)} \text{Diagram 32}, \\ \text{Diagram 33} \xleftrightarrow{(R3)} \text{Diagram 34}, & \text{Diagram 35} \xleftrightarrow{(R4)} \text{Diagram 36}, \\ \text{Diagram 37} \xleftrightarrow{(bR)} \text{Diagram 38}. \end{array}$$

Here the edge coloring is arbitrary under the condition in Definition 2.1 at trivalent vertices. One can also show those moves obtained by exchanging type 1 and type 2 edges for some strands, or reversing all the over/under-passing information and the elevation.

Proof. The moves (R1'), (R2), (R3), and (R4) have been proved by Kuperberg [Kup94, Kup96]. One can prove (bR) by straightforward calculation using the skein relations in Definitions 2.2 and 2.3. \square

Definition 2.6 (the (clasped) \mathfrak{sp}_4 -skein algebra of an unpunctured marked surface). Let Σ be a marked surface with special points $\mathbb{M} \subset \partial\Sigma$. The (clasped) \mathfrak{sp}_4 -skein algebra $\mathcal{S}_{\mathfrak{sp}_4, \Sigma} = \mathcal{S}_{\mathfrak{sp}_4, \Sigma}^v$ is the quotient of the free \mathcal{R} -module $\mathcal{RTang}_{\mathfrak{sp}_4, \Sigma}$ modulo the \mathfrak{sp}_4 -skein relations in Definition 2.2 and the clasped \mathfrak{sp}_4 -skein relations in Definition 2.3. The multiplication of $\mathcal{S}_{\mathfrak{sp}_4, \Sigma}$ is induced from $\mathcal{Tang}_{\mathfrak{sp}_4, \Sigma}$.

We call an element of $\mathcal{S}_{\mathfrak{sp}_4, \Sigma}$ coming from $\mathcal{Tang}_{\mathfrak{sp}_4, \Sigma}$ a *tangled \mathfrak{sp}_4 -graphs in $\mathcal{S}_{\mathfrak{sp}_4, \Sigma}$* , and a general element (a linear combination of tangled \mathfrak{sp}_4 -graphs) of $\mathcal{S}_{\mathfrak{sp}_4, \Sigma}$ an *\mathfrak{sp}_4 -web*. A *flat \mathfrak{sp}_4 -graph* in $\mathcal{S}_{\mathfrak{sp}_4, \Sigma}$ is a tangled \mathfrak{sp}_4 -graph in $\mathcal{S}_{\mathfrak{sp}_4, \Sigma}$ without internal crossings, and only with simultaneous crossings at special points. A *boundary \mathfrak{sp}_4 -web* is a tangled \mathfrak{sp}_4 -graph in $\mathcal{S}_{\mathfrak{sp}_4, \Sigma}$ represented by an arc of any type parallel to a boundary interval. We denote the set of boundary webs by $\partial_\Sigma \subset \mathcal{S}_{\mathfrak{sp}_4, \Sigma}$.

Any boundary web v -commutes with any \mathfrak{sp}_4 -webs in $\mathcal{S}_{\mathfrak{sp}_4, \Sigma}$ by the clasped skein relations in Definition 2.3. Therefore it is easy to see that the multiplicatively closed subset

$$\text{mon}(\partial_\Sigma) := \{v^{\frac{k}{2}}[\prod_{\alpha \in \partial_\Sigma} \alpha^{f(\alpha)}] \mid f: \partial_\Sigma \rightarrow \mathbb{N}, k \in \mathbb{Z}\}$$

of $\mathcal{S}_{\mathfrak{sp}_4, \Sigma}$ becomes a left and right Ore set of $\mathcal{S}_{\mathfrak{sp}_4, \Sigma}$. It guarantees the existence of the following localization of $\mathcal{S}_{\mathfrak{sp}_4, \Sigma}$ at $\text{mon}(\partial_\Sigma)$.

Definition 2.7 (the boundary-localized \mathfrak{sp}_4 -skein algebra). The boundary-localized \mathfrak{sp}_4 -skein algebra $\mathcal{S}_{\mathfrak{sp}_4, \Sigma}[\partial^{-1}]$ is the Ore localization of $\mathcal{S}_{\mathfrak{sp}_4, \Sigma}$ at $\text{mon}(\partial_\Sigma)$.

The clasped skein relations preserve the number of edges of each type incident to $p \in \mathbb{M}$. Hence, the \mathfrak{sp}_4 -skein algebra has the following gradings.

Definition 2.8 (the endpoint grading). For a tangled \mathfrak{sp}_4 -graph G and $p \in \mathbb{M}$, associated is the vector $\text{deg}_p(G) = (c_p^1, c_p^2) \in \mathbb{N} \times \mathbb{N}$, where c_p^s is the number of type s edges of G incident to p , for $s = 1, 2$. It defines the *endpoint grading* $\text{deg}(G) = (\text{deg}_p(G)) \in (\mathbb{N} \times \mathbb{N})^{\mathbb{M}}$ of $G \in \mathcal{S}_{\mathfrak{sp}_4, \Sigma}$ for any tangled \mathfrak{sp}_4 -graph G .

Definition 2.9 (the mirror-reflection). The *mirror-reflection* G^\dagger of a tangled \mathfrak{sp}_4 -graph G is defined by reversing the ordering of the univalent vertices on each special point and exchanging the over-/under-passing information at each internal crossing. The mirror-reflection is extended to an anti-involution $\dagger: \mathcal{S}_{\mathfrak{sp}_4, \Sigma} \rightarrow \mathcal{S}_{\mathfrak{sp}_4, \Sigma}$ by \mathbb{Z} -linearly and by setting $(v^{\pm 1/2})^\dagger := v^{\mp 1/2}$.

2.2. Basis webs, elementary webs, and web clusters. In [Kup96], Kuperberg introduced a 4-valent vertex to define a basis for a certain space of \mathfrak{sp}_4 -webs. We rescale it and call it a “crossroad” in this paper.

Definition 2.10 (crossroads and rungs). A *crossroad* is a 4-valent vertex defined by

$$\begin{array}{c} \text{Crossroad} \\ \text{(circle with four red lines meeting at center)} \end{array} := \begin{array}{c} \text{Rung} \\ \text{(circle with two red lines meeting at top and bottom)} \end{array} - \frac{1}{[2]} \begin{array}{c} \text{Crossroad} \\ \text{(circle with two red arcs)} \end{array} = \begin{array}{c} \text{Crossroad} \\ \text{(circle with two red lines meeting at left and right)} \end{array} - \frac{1}{[2]} \begin{array}{c} \text{Crossroad} \\ \text{(circle with two red arcs)} \end{array}.$$

A *rung* is a type 2 edge in a tangled \mathfrak{sp}_4 -graph which does not touch special points. A subset S of rungs in a tangled \mathfrak{sp}_4 -graph is *essential* if the tangled \mathfrak{sp}_4 -graph obtained by removing all rungs in S becomes zero in the skein algebra. An \mathfrak{sp}_4 -web in $\mathcal{S}_{\mathfrak{sp}_4, \Sigma}$ is a *crossroad web* if it can be represented by a tangled \mathfrak{sp}_4 -graph diagram on Σ with crossroads and no rungs. The *crossroad web associated with an \mathfrak{sp}_4 -web G* is a crossroad web obtained by formally replacing all the rungs of G with crossroads.

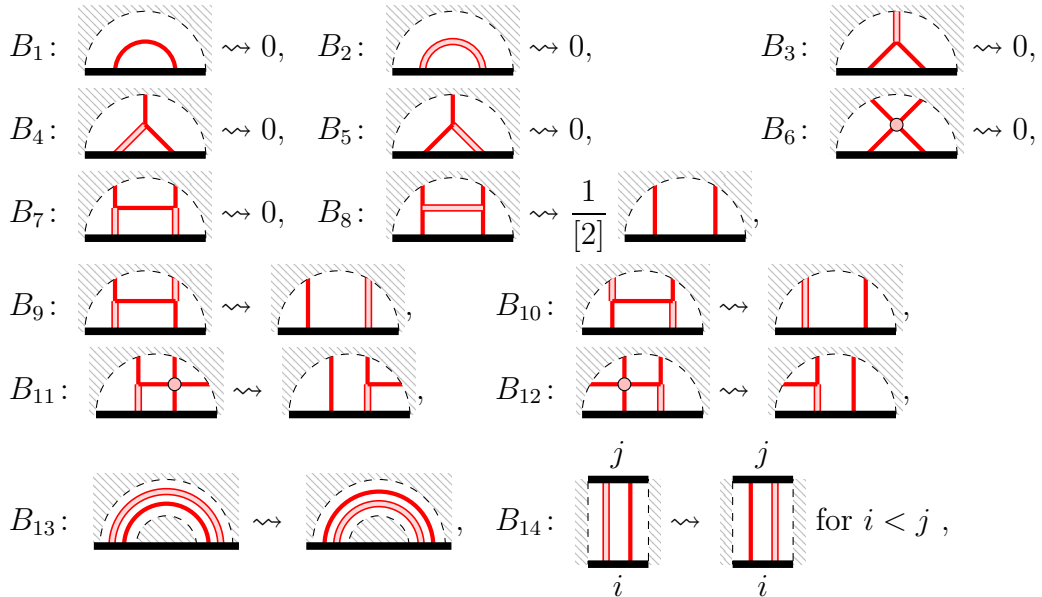
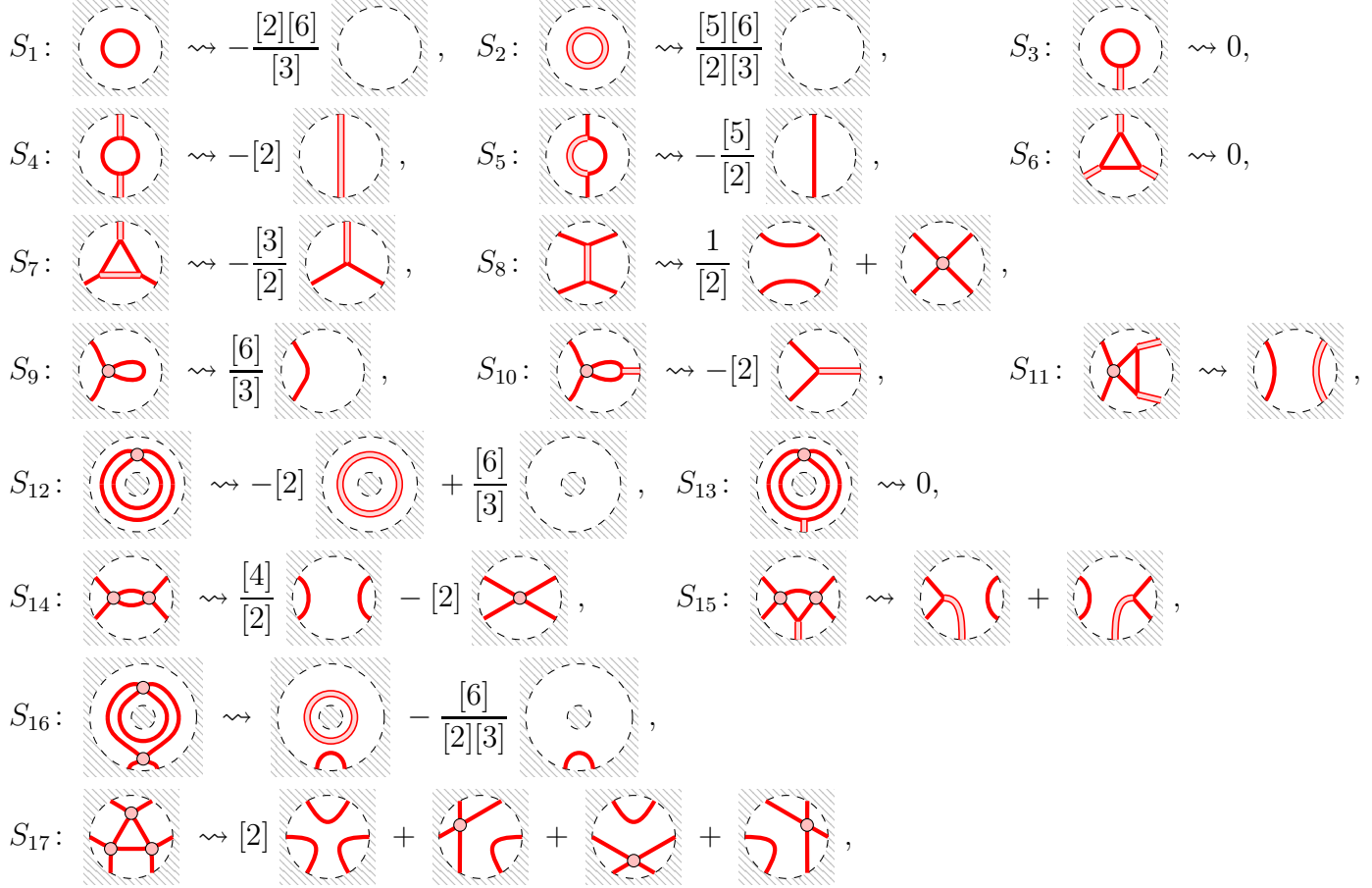
We remark here that a simple loop or arc of either type is also a crossroad web.

In order to define a basis of $\mathcal{S}_{\mathfrak{sp}_4, \Sigma}$, let us apply the confluence theory for skein modules in Sikora–Westbury [SW07] to our \mathfrak{sp}_4 -skein algebra $\mathcal{S}_{\mathfrak{sp}_4, \Sigma}$. Roughly speaking, the confluence theory is a general method to obtain a basis of the quotient of a free module spanned by graphs (in a manifold) with diagrammatic relations. A skein module of a surface is a typical example: let us consider such a module obtained as the quotient of the free \mathcal{R} -module spanned by certain diagrams on Σ modulo certain skein relations $\langle X_i - Y_i \rangle_{i \in I}$ corresponding to “reduction rules $\{S_i: X_i \rightsquigarrow Y_i\}_{i \in I}$ ”. In the terminology in [SW07], the statement is as follows:

Theorem 2.11 (Sikora–Westbury [SW07]). *If the reduction rules $\{S_i\}_{i \in I}$ is terminal and locally confluent, then the set of irreducible graphs on Σ gives a basis for the skein module.*

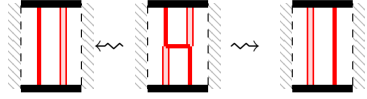
We roughly explain the confluence theory in the case of the our skein algebra $\mathcal{S}_{\mathfrak{sp}_4, \Sigma}$. A *reduction rule* $S: X \rightsquigarrow Y$ is a specific pair of X and Y in $\mathcal{R}\text{Diag}_{\mathfrak{sp}_4, \Sigma}$ which gives a relation $X - Y = 0$ where $\text{Diag}_{\mathfrak{sp}_4, \Sigma}$ is the set of isotopy classes of tangled graph diagrams. Examples of reduction rules for $\mathcal{R}\text{Diag}_{\mathfrak{sp}_4, \Sigma}$ are the left-hand sides to the right-hand sides in (2.1)–(2.5). We will give the precise set of reduction rules $\{S_i\}_{i \in I}$ soon below. A fixed set $\{S_i: X_i \rightsquigarrow Y_i\}_{i \in I}$ of reduction rules is *locally confluent* if for a tangled \mathfrak{sp}_4 -graph diagram $\Gamma \in \text{Diag}_{\mathfrak{sp}_4, \Sigma}$ having two reduction rules $S: \Gamma \rightsquigarrow Z$ and $T: \Gamma \rightsquigarrow W$, the diagrams Z and W have a common descendant via sequences of reduction rules in $\{S_i\}_{i \in I}$. An *irreducible \mathfrak{sp}_4 -graph diagram* is a \mathfrak{sp}_4 -graph diagram which admits no reductions. We define reduction rules for $\mathcal{R}\text{Diag}_{\mathfrak{sp}_4, \Sigma}$ by adding reduction rules in [SW07, Section 6]. It is useful for us to replace each marked point with a small interval which we call an *external clasp* (shown by a thick black line), and describe an \mathfrak{sp}_4 -graph as a diagram with distinct ends on external clasps. In fact, the skein relations in Definition 2.3 correspond to relations at external clasps in the sense of Kuperberg [Kup96]. We will use such a description using external clasps in Definition 2.12 and Proposition 2.24.

Definition 2.12 (reduction rules for $\mathcal{R}\text{Diag}_{\mathfrak{sp}_4, \Sigma}$). Let (Σ, \mathbb{M}) be an unpunctured marked surface, and fix an enumeration $\{1, 2, \dots, |\mathbb{M}|\} \xrightarrow{\sim} \mathbb{M}$ of special points.



$$\begin{aligned}
C_1: & \quad \begin{array}{c} \text{Diagram 1} \\ \text{Diagram 2} \end{array} \rightsquigarrow v \begin{array}{c} \text{Diagram 3} \\ \text{Diagram 4} \end{array} + v^{-1} \begin{array}{c} \text{Diagram 5} \\ \text{Diagram 6} \end{array} + \begin{array}{c} \text{Diagram 7} \\ \text{Diagram 8} \end{array}, \\
C_2: & \quad \begin{array}{c} \text{Diagram 9} \\ \text{Diagram 10} \end{array} \rightsquigarrow v \begin{array}{c} \text{Diagram 11} \\ \text{Diagram 12} \end{array} + v^{-1} \begin{array}{c} \text{Diagram 13} \\ \text{Diagram 14} \end{array}, \\
C_3: & \quad \begin{array}{c} \text{Diagram 15} \\ \text{Diagram 16} \end{array} \rightsquigarrow v \begin{array}{c} \text{Diagram 17} \\ \text{Diagram 18} \end{array} + v^{-1} \begin{array}{c} \text{Diagram 19} \\ \text{Diagram 20} \end{array}, \\
C_4: & \quad \begin{array}{c} \text{Diagram 21} \\ \text{Diagram 22} \end{array} \rightsquigarrow v^2 \begin{array}{c} \text{Diagram 23} \\ \text{Diagram 24} \end{array} + v^{-2} \begin{array}{c} \text{Diagram 25} \\ \text{Diagram 26} \end{array} + \begin{array}{c} \text{Diagram 27} \\ \text{Diagram 28} \end{array}.
\end{aligned}$$

Here for instance, the reduction rule B_1 is related to the first relation in (2.14). B_{13} is a reduction rule related to arcs incident to a special point. It moves arcs of type 2 towards inside of other arcs of type 1. The rule B_{14} moves arcs of type 2 towards the right of other arcs of type 1, referring to the labels of the relevant special points (or external clasps). We need reduction rules B_{13} and B_{14} because an overlap between two applications of B_9 is not locally confluent as shown below:



Lemma 2.13. *The set $\{S_1, \dots, S_{17}, B_1, \dots, B_{14}, C_1, \dots, C_4\}$ of reduction rules introduced above is locally confluent and terminal.*

Proof. Each reduction rule decreases a quintuple of the number of crossings, the total number of trivalent vertices and crossroads, the number of connected components, and the number of type 2 arcs lying in the left-side or outer-side of another type 1 arcs. Any descending path of the reduction rules is terminal because the quintuple belongs to $(\mathbb{Z}_{\geq 0})^5$ with the lexicographic order. One can also confirm that all “overlaps” are locally confluent in a similar way to [SW07, Section 6]. For example, the previous overlap between B_9 and itself is locally confluent thanks to B_{13} or B_{14} . \square

We call faces bounded by edges (resp. and an external clasp) appearing in the left-hand sides of S_1 to S_{17} (resp. B_1 to B_{12}) *elliptic faces* (cf. [Kup96, SW07]).

Definition 2.14 (basis webs). A *basis web* is a flat crossroad web without elliptic faces. We denote the set of all basis webs in $\mathcal{S}_{\mathfrak{sp}_4, \Sigma}$ by $\mathbf{BWeb}_{\mathfrak{sp}_4, \Sigma}$.


Theorem 2.15. $\mathbf{BWeb}_{\mathfrak{sp}_4, \Sigma}$ is an \mathcal{R} -basis of $\mathcal{S}_{\mathfrak{sp}_4, \Sigma}$.

Proof. One can apply Theorem 2.11 to $\mathcal{R}\text{Diag}_{\mathfrak{sp}_4, \Sigma} / \langle S_i, B_j, C_k \rangle$, thanks to Lemma 2.13. We can confirm that the \mathfrak{sp}_4 -webs in both sides of these reduction rules are related by skein relations in Definitions 2.2 and 2.3. Thus, the \mathcal{R} -submodule $\langle S_i, B_j, C_k \rangle$ is equal to the \mathcal{R} -submodule generated by the \mathfrak{sp}_4 -skein relations. It concludes that the irreducible \mathfrak{sp}_4 -graph diagrams with respect to the reduction rules in Definition 2.12 give an \mathcal{R} -basis of $\mathcal{S}_{\mathfrak{sp}_4, \Sigma}$. Note that if \mathfrak{sp}_4 -graphs in the left hand side of B_{13} or B_{14} has no elliptic faces,

then the right has also no elliptic faces. However, these \mathfrak{sp}_4 -graphs determine the same element in $\mathcal{S}_{\mathfrak{sp}_4, \Sigma}$. It concludes that $\mathbf{BWeb}_{\mathfrak{sp}_4, \Sigma}$ is an \mathcal{R} -basis of $\mathcal{S}_{\mathfrak{sp}_4, \Sigma}$. \square

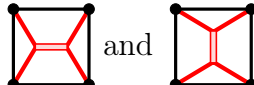
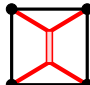
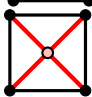
Definition 2.16 (elementary webs). An *elementary web* G is a flat \mathfrak{sp}_4 -graph satisfying the following:

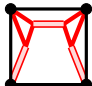
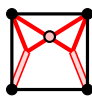
- all subsets of rungs of G are essential,
- G is indecomposable to a product of more than two basis webs, and
- the associated crossroad web is a basis web.


It is said to be of weight $d = 2$ if the number $\epsilon(\deg_p(G)) \in \mathbb{N}$ is even for all $p \in \mathbb{M}$, and $d = 1$ otherwise. Here $\epsilon(c^1, c^2) := c^1 + 2c^2$. An elementary web is *tree-type* if it is represented by a tangled tree G (i.e., an \mathfrak{sp}_4 -graph whose underlying graph is a tree) up to a power of $v^{1/2}$ such that any rung of G is adjacent to a triangle  bounded by type 1 edges. We call such a tangled tree G a *lift* of the tree-type elementary web. We denote the set of all elementary webs in $\mathcal{S}_{\mathfrak{sp}_4, \Sigma}$ by $\mathbf{EWeb}_{\mathfrak{sp}_4, \Sigma}$, and the subset of tree-type ones by $\mathbf{Tree}_{\mathfrak{sp}_4, \Sigma} \subset \mathbf{EWeb}_{\mathfrak{sp}_4, \Sigma}$.

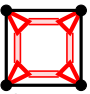
Remark 2.17. Any elementary web is, in fact, equal to its associated crossroad web in $\mathcal{S}_{\mathfrak{sp}_4, \Sigma}$ by definition of the essential rung and the crossroad. Hence, one obtain inclusions $\mathbf{Tree}_{\mathfrak{sp}_4, \Sigma} \subset \mathbf{EWeb}_{\mathfrak{sp}_4, \Sigma} \subset \mathbf{BWeb}_{\mathfrak{sp}_4, \Sigma}$.

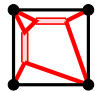
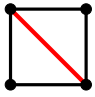
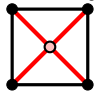
Example 2.18. Let Σ be a quadrilateral.

- (1) The \mathfrak{sp}_4 -graphs  and  are indecomposable. Their common associated crossroad web  belongs to $\mathbf{BWeb}_{\mathfrak{sp}_4, \Sigma}$. However, they are not elementary because their rungs are not essential.

- (2) The flat \mathfrak{sp}_4 -graph  belongs to $\mathbf{Tree}_{\mathfrak{sp}_4, \Sigma}$ with its associated crossroad web  in $\mathbf{BWeb}_{\mathfrak{sp}_4, \Sigma}$. It will correspond to a cluster variable via the inclusion $\mathcal{S}_{\mathfrak{sp}_4, \Sigma}^{\mathbb{Z}_q} \subset \mathcal{A}_{\mathfrak{sp}_4, \Sigma}^q$ given in Theorem 5.6.

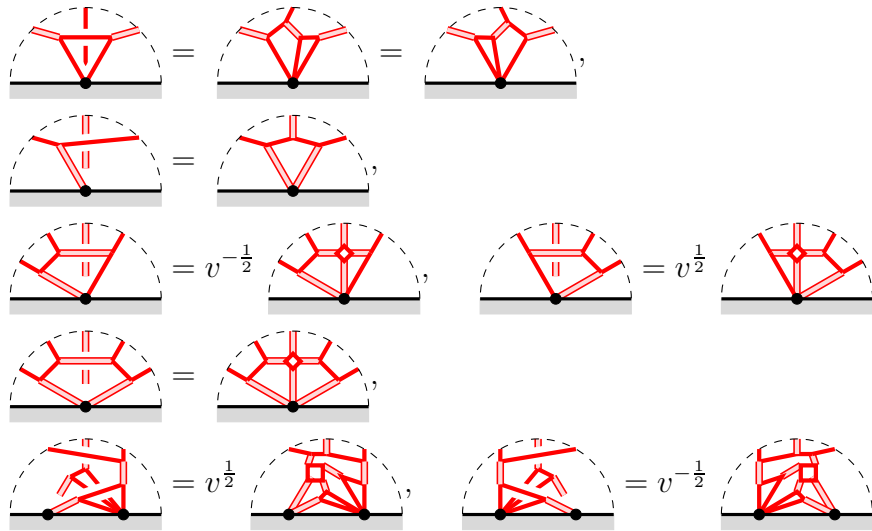
- (3) The indecomposable \mathfrak{sp}_4 -graph  has the same associated crossroad web as the previous example. However, it is not an elementary web because its rung is not essential.

- (4) The elementary web  is not tree-type, and it is invariant under the $\pi/2$ -rotations of the quadrilateral, which is the cluster Donaldson–Thomas transformation in this case: see (1.1).

- (5) The underlying graph of the flat \mathfrak{sp}_4 -graph  is a tree. However, it decomposes into the product of  and .

Certain decompositions of \mathfrak{sp}_4 -webs into products of elementary webs are obtained by the following *arborization relations*, which are similar to those introduced by Fomin–Pylyavskyy [FP16] for \mathfrak{sl}_3 -webs.

Lemma 2.19 (arborization relations for \mathfrak{sp}_4 -webs). *For \mathfrak{sp}_4 -webs, we have the following relations*



which we call the arborization relations.

Proof. One can easily prove them by the skein relations except for the final relation. The final relation follow from Lemma 2.20 in below. \square

Lemma 2.20.



Proof. The first is obtained by replacing the horizontal rung with a vertical one by using (2.6). In the left-hand side of the second equation, we replace a short edge of type 2 by using (2.6), and resolve the left crossing. Then, one can apply the first equality to obtain the second equality. \square

If a lift \tilde{G} of a tree-type elementary web G only has internal crossings appearing in the arborization relations, then any tangled tree \tilde{G}' related to \tilde{G} by crossing changes is also a lift of G . Hence we expect the following.

Conjecture 2.21. *Let \tilde{G} and \tilde{G}' be any tangled tree diagrams such that \tilde{G} is related to \tilde{G}' by crossing changes. If \tilde{G} is a lift of a tree-type elementary web $G \in \text{Tree}_{\mathfrak{sp}_4, \Sigma}$, then \tilde{G}' is also a lift of G .*

We remark that the above conjecture is trivial in the classical case $v = 1$. We believe that this conjecture is closely related to Conjecture 4.

The following notion will be related to the clusters.

Definition 2.22 (web clusters). A web cluster of $\mathcal{S}_{\mathfrak{sp}_4, \Sigma}$ is a v -commutative subset of $\text{EWeb}_{\mathfrak{sp}_4, \Sigma}$ with cardinality $\#I_{\mathfrak{sp}_4}(\Delta)$. We denote the set of web clusters by $\text{CWeb}_{\mathfrak{sp}_4, \Sigma}$.

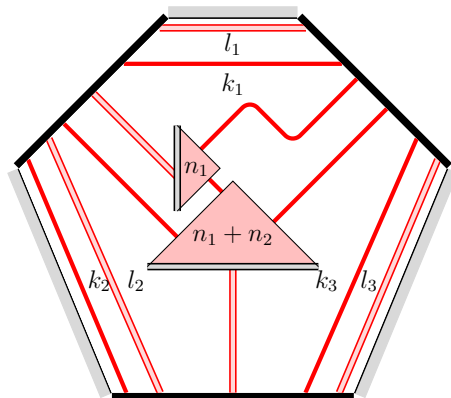
Definition 2.23. For two elementary webs $G_1, G_2 \in \text{EWeb}_{\mathfrak{sp}_4, \Sigma}$ contained in a common web cluster, define an integer $\Pi(G_1, G_2) \in \mathbb{Z}$ by

$$G_1 G_2 = v^{\Pi(G_1, G_2)} G_2 G_1.$$

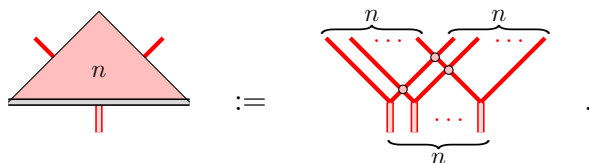
Below, we begin to investigate the cluster nature of our skein algebra $\mathcal{S}_{\mathfrak{sp}_4, \Sigma}$ by discussing the web clusters of triangles.

2.3. \mathfrak{sp}_4 -webs in a triangle. Let T be a triangle, *i.e.* a disk with three special points. In some of the figures below, each special point is “stretched” and shown by a thick black segment (like an *external clasp* of Kuperberg).

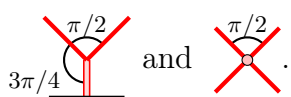
Proposition 2.24. $\text{BWeb}_{\mathfrak{sp}_4, T}$ consists of the \mathfrak{sp}_4 -webs represented by the following diagram (and its rotations and reflections along the vertical axis):



where $k_1, k_2, k_3, l_1, l_2, l_3, n_1, n_2 \in \mathbb{Z}_{\geq 0}$. Here an edge with a positive integer k represents the k -parallelization of the edge, and a triangle with n represents the crossroad web defined by



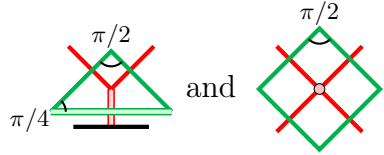
Proof. We use a formula on the angular defects of a flat crossroad web developed in [Kup96]. For a trivalent vertex and a crossroad, we assign angles between their edges by



n_1	1	2	3	4	5	\dots
(1) $n_2 = 0$	-	-	0	$-\pi/2$	$-\pi$	\dots
(2) $n_2 = 1$	-	-	$-\pi/4$	$-3\pi/4$	$-5\pi/4$	\dots
(3) $n_2 = 2$	-	0	$-\pi/2$	$-\pi$	$-3\pi/2$	\dots
(4) $n_2 = 0$	-	$\pi/2$	0	$-\pi/2$	$-\pi$	\dots
(5) $n_2 = 1$	$3\pi/4$	$\pi/4$	$-\pi/4$	$-3\pi/4$	$-5\pi/4$	\dots
(6) $n_2 = 2$	$\pi/2$	0	$-\pi/2$	$-\pi$	$-3\pi/2$	\dots

TABLE 1. Entries are angular defect $3\pi/2 - \pi(n + n_1)/4$ at external vertices where $n = n_1 + n_2$. Yellow-colored cells have positive defects.

Let G be a connected component of a basis web in a triangle whose ends are located on the three external clasps. We consider the dual graph G^* , as shown in green:



A non-elliptic face of G corresponds to an interior vertex of G^* which has $n > 4$ edges of type 1, or an exterior vertex of G^* which has n_1 edges of type 1 and n_2 edges of type 2. Then, n_1 and n_2 satisfy either

- (1) $n_1 \geq 3$ and $n_2 = 0$,
- (2) $n_1 \geq 3$ and $n_2 = 1$, or
- (3) $n_1 \geq 2$ and $n_2 = 2$

for the vertex bounded by an external clasp, and either

- (4) $n_1 \geq 2$ and $n_2 = 0$,
- (5) $n_1 \geq 1$ and $n_2 = 1$, or
- (6) $n_1 \geq 1$ and $n_2 = 2$

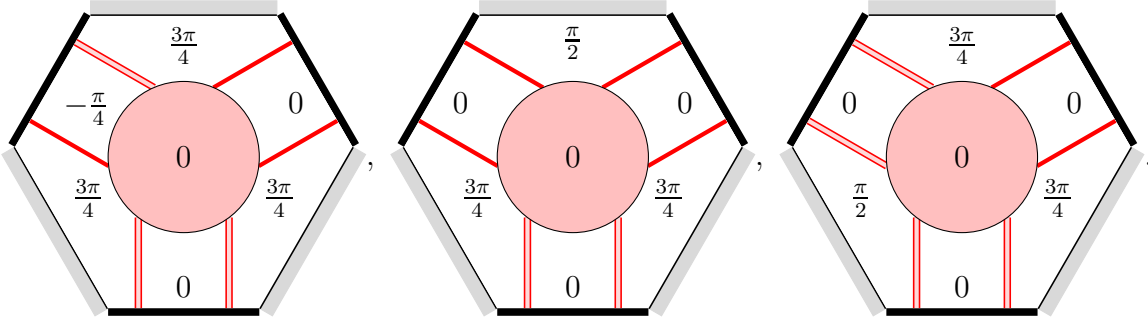
for the vertex bounded by a boundary interval. By the Gauss-Bonnet theorem, the total angular defect should be equal to 2π . Hence, one obtains the following formula:

$$2\pi = \sum_{n \geq 4} v_n^{\text{int}} \left(2\pi - \frac{\pi}{2}n \right) + \sum_{n_1, n_2} v_{n_1, n_2}^{\text{ex}} \left(\frac{3\pi}{2} - \frac{\pi}{4}(n + n_1) \right) + \sum_{n_1, n_2} v_{n_1, n_2}^{\text{cl}} \left(\frac{3\pi}{2} - \frac{\pi}{4}(n + n_1) \right),$$

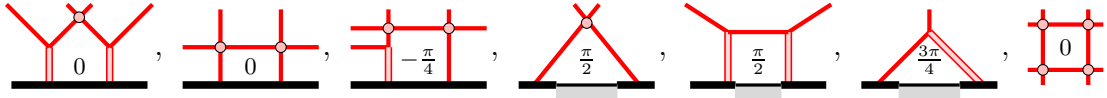
$$\sum_n v_n^{\text{ex}} = 3,$$

where v_n^{int} , v_{n_1, n_2}^{ex} , and v_{n_1, n_2}^{cl} are the number of interior vertices with valency n , exterior vertices with valency $n = n_1 + n_2$ bounded by boundary intervals, and exterior vertices with valency $n = n_1 + n_2$ bounded by external clasps, respectively. In the right-hand side of the first formula, the first term related to the interior vertices is non-negative, and the summand $3\pi/2 - \pi(n + n_1)/4$ in the second and the third terms are shown in Table 1. The angular defect at an internal vertex belongs to $\{0, -\pi/2, -\pi, \dots\}$. Therefore the

possibility of the total angular defect at each external clasps, boundary edges, and the interior is one of the following patterns (up to rotations and reflections):

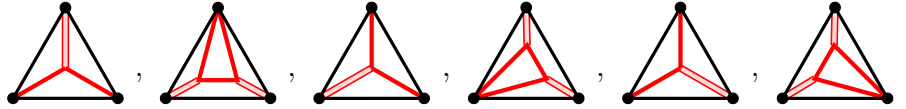


The faces of G corresponding to the vertices of G^* with the above angular defects are



As a consequence, we obtain the diagrams in the statement. The second and the third diagrams are the cases of $n_1 = 0$ and $n_2 = 0$, respectively. \square

Theorem 2.25. $\text{EWeb}_{\mathfrak{sp}_4, T}$ consists of the boundary webs in ∂_T and the following 6 webs:



and a \mathbb{Z}_v -subalgebra generated by these webs coincides with $\mathbb{Z}_v \text{BWeb}_{\mathfrak{sp}_4, T}$.

Proof. These webs are indecomposable because of the degrees at special points. One can see that a basis web decomposes into the above pieces by using the arborization relations in Lemma 2.19. In fact, a flat crossroad web represented by the diagram in Proposition 2.24 is decomposed into

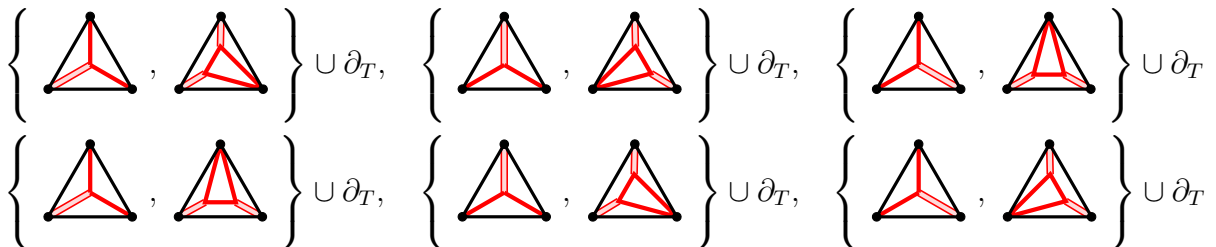
$$\prod_{i=1}^3 (e_i^{(1)})^{k_i} (e_i^{(2)})^{l_i} x^{n_1} y^{n_2}$$

up to multiplication by v , where $e_i^{(1)}$ (resp. $e_i^{(2)}$) are arcs corresponding to labels k_i (resp. l_i) and

$$x = \text{[web diagram]}, y = \text{[web diagram]} .$$

\square

Corollary 2.26. $\text{CWeb}_{\mathfrak{sp}_4, T}$ consists of the following 6 subsets of $\text{EWeb}_{\mathfrak{sp}_4, T}$:



Proof. For each set in above, one can confirm the v -commutativity by the arborization relations in Lemma 2.19. \square

2.4. $\mathcal{S}_{\mathfrak{sp}_4, \Sigma}$ is an Ore domain. In this section, we are going to see that $\mathcal{S}_{\mathfrak{sp}_4, \Sigma}$ is embedded into its skew-field of fractions $\text{Frac} \mathcal{S}_{\mathfrak{sp}_4, \Sigma}$. This is needed in studying the relationship between the localized \mathfrak{sp}_4 -skein algebra $\mathcal{S}_{\mathfrak{sp}_4, \Sigma}[\partial^{-1}]$ and the quantum cluster algebra $\mathcal{A}_{\mathfrak{sp}_4, \Sigma}^q$, where the latter will be naturally constructed in $\text{Frac} \mathcal{S}_{\mathfrak{sp}_4, \Sigma}$.

Proposition 2.27. *For a triangle T , the boundary-localized skein algebra $\mathcal{S}_{\mathfrak{sp}_4, T}[\partial^{-1}]$ is an Ore domain.*

This proposition follows from the isomorphism between $\mathcal{S}_{\mathfrak{sp}_4, T}[\partial^{-1}]$ and the quantum cluster algebra $\mathcal{A}_{\mathfrak{sp}_4, T}^q$ (Proposition 5.5). In what follows, we prove that $\mathcal{S}_{\mathfrak{sp}_4, \Sigma}[\partial^{-1}]$ is an Ore domain for any unpunctured marked surface, assuming that the triangle case is established. The proof is based on a relation to the *reduced stated \mathfrak{sp}_4 -skein algebra* and its splitting property. The stated \mathfrak{sp}_4 -skein algebra $\mathcal{S}_{\mathfrak{sp}_4}^{\text{st}}(\Sigma)$ and its reduced version $\mathcal{S}_{\mathfrak{sp}_4}^{\text{st}}(\Sigma)_{\text{rd}}$ is introduced in [IY22]. In that paper, we construct an isomorphism

$$\Phi_{\Sigma} : \mathcal{S}_{\mathfrak{sp}_4}^{\text{st}}(\Sigma)_{\text{rd}} \rightarrow \mathcal{S}_{\mathfrak{sp}_4, \Sigma}[\partial^{-1}]$$

and an injective homomorphism

$$\theta_{\alpha}^{\text{rd}} : \mathcal{S}_{\mathfrak{sp}_4}^{\text{st}}(\Sigma)_{\text{rd}} \hookrightarrow \mathcal{S}_{\mathfrak{sp}_4}^{\text{st}}(\Sigma')_{\text{rd}}$$

called the *splitting homomorphism* (cf. [Lê18] for \mathfrak{sl}_2 , [Hig20] for \mathfrak{sl}_3 , [LS22] for \mathfrak{sl}_n), where a marked surface Σ is obtained from another marked surface Σ' by gluing two distinct boundary intervals, which project to a common ideal arc α in Σ . We remark that if Σ' consists of two connected components Σ_1 and Σ_2 , then $\mathcal{S}_{\mathfrak{sp}_4}^{\text{st, rd}}(\Sigma') \cong \mathcal{S}_{\mathfrak{sp}_4}^{\text{st}}(\Sigma_1)_{\text{rd}} \otimes \mathcal{S}_{\mathfrak{sp}_4}^{\text{st}}(\Sigma_2)_{\text{rd}}$.

Theorem 2.28. *For any unpunctured marked surface Σ , the skein algebra $\mathcal{S}_{\mathfrak{sp}_4, \Sigma}$ is an Ore domain. Moreover, $\text{Frac} \mathcal{S}_{\mathfrak{sp}_4, \Sigma}$ is isomorphic to the skew-field of fractions of a quantum torus.*

Proof. Given an ideal triangulation $\Delta = \{\alpha_1, \alpha_2, \dots, \alpha_n\}$ of Σ , one can decompose $\mathcal{S}_{\mathfrak{sp}_4}^{\text{st}}(\Sigma)_{\text{rd}}$ into $\mathcal{S}_{\mathfrak{sp}_4}^{\text{st}}(\sqcup_{T \in t(\Delta)} T)_{\text{rd}} \cong \bigotimes_{T \in t(\Delta)} \mathcal{S}_{\mathfrak{sp}_4}^{\text{st}}(T)_{\text{rd}}$ via the composite $\theta_{\Delta}^{\text{rd}} := \theta_{\alpha_n}^{\text{rd}} \circ \dots \circ \theta_{\alpha_2}^{\text{rd}} \circ \theta_{\alpha_1}^{\text{rd}}$ of splitting homomorphisms. Then we get the following sequence of homomorphisms:

$$\mathcal{S}_{\mathfrak{sp}_4, \Sigma} \hookrightarrow \mathcal{S}_{\mathfrak{sp}_4, \Sigma}[\partial^{-1}] \xrightarrow[\Phi_{\Sigma}^{-1}]{\cong} \mathcal{S}_{\mathfrak{sp}_4}^{\text{st}}(\Sigma)_{\text{rd}} \xrightarrow[\theta_{\Delta}^{\text{rd}}]{\hookrightarrow} \bigotimes_{T \in t(\Delta)} \mathcal{S}_{\mathfrak{sp}_4}^{\text{st}}(T)_{\text{rd}} \xrightarrow[\bigotimes_T \Phi_T]{\cong} \bigotimes_{T \in t(\Delta)} \mathcal{S}_{\mathfrak{sp}_4, T}[\partial^{-1}].$$

The right-most algebra is an Ore domain by Proposition 2.27. Then we have an embedding of $\mathcal{S}_{\mathfrak{sp}_4, \Sigma}$ into an Ore domain, which implies that $\mathcal{S}_{\mathfrak{sp}_4, \Sigma}$ is a domain. Then we can apply [LY20, Proposition 2.2] to the domain $\mathcal{S}_{\mathfrak{sp}_4, \Sigma}$ and the quantum plane $\langle \mathcal{C}_{\Delta} \rangle_{\text{alg}}$ generated by a web cluster \mathcal{C}_{Δ} as in Theorem 3.14, where the hypothesis there is satisfied thanks to Theorem 3.14. It concludes that $\mathcal{S}_{\mathfrak{sp}_4, \Sigma}$ is an Ore domain, and $\text{Frac} \mathcal{S}_{\mathfrak{sp}_4, \Sigma}$ is isomorphic to the skew-field of fraction of the quantum torus generated by the web cluster \mathcal{C}_{Δ} . \square

Corollary 2.29. *We have inclusions $\mathcal{S}_{\mathfrak{sp}_4, \Sigma} \subset \mathcal{S}_{\mathfrak{sp}_4, \Sigma}[\partial^{-1}] \subset \text{Frac} \mathcal{S}_{\mathfrak{sp}_4, \Sigma}$.*

3. GENERATORS AND LAURENT POSITIVITY FOR \mathfrak{sp}_4 -SKEIN ALGEBRAS

3.1. **Cutting and Sticking tricks.** Let us introduce two fundamental lemmas on “the sticking trick” and “the cutting trick”, which will turn out to be useful techniques to investigate the relation between our skein algebra and the quantum cluster algebra. In [IY21], the authors showed that the sticking trick could be used to expand a \mathfrak{sl}_3 -web into a Laurent polynomial in the boundary-localized \mathfrak{sl}_3 -skein algebra. The cutting trick was used to prove the positivity of the coefficients for cluster expansions of elevation-preserving \mathfrak{sl}_3 -webs in the same paper. These tricks will play a similar role in the current case of \mathfrak{sp}_4 .

Lemma 3.1 (The cutting trick).

$$\begin{aligned}
 \text{Diagram 1} &= v^2 \text{Diagram 2} + v \text{Diagram 3} + v^{-1} \text{Diagram 4} + v^{-2} \text{Diagram 5}
 \end{aligned}
 \tag{3.1}$$

$$\begin{aligned}
 \text{Diagram 6} &= v^4 \text{Diagram 7} + v^2 \text{Diagram 8} \\
 &+ [2] \text{Diagram 9} + v^{-2} \text{Diagram 10} + v^{-4} \text{Diagram 11}
 \end{aligned}
 \tag{3.2}$$

Proof. Apply skein relations to crossings. □

Lemma 3.2 (The sticking trick).

$$\text{Diagram 12} = v \text{Diagram 13} - v^2 \text{Diagram 14} + v^3 \text{Diagram 15} - v^4 \text{Diagram 16},
 \tag{3.3}$$

$$\begin{aligned}
 \text{Diagram 17} &= v^2 \text{Diagram 18} - v^4 \text{Diagram 19} \\
 &+ v^4 [2] \text{Diagram 20} - v^4 \text{Diagram 21} + v^7 \text{Diagram 22}.
 \end{aligned}
 \tag{3.4}$$

Proof. These formulas are derived from the cutting trick. In Lemma 3.1, glue the bottom ends of the left and right boundary intervals and consider the returning arc obtained by bending the middle line. Then the statement follows by a straightforward calculation. The following formulas are useful in the calculation:

$$\begin{aligned}
 \text{Diagram 23} &= -v^2 \text{Diagram 24}, & \text{Diagram 25} &= -v^{-1} \text{Diagram 26}, & \text{Diagram 27} &= v^{-4} \text{Diagram 28}, & \text{Diagram 29} &= v^{-4} \text{Diagram 30}.
 \end{aligned}$$

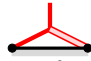

□

Remark 3.3. The sticking trick in this form corresponds to the sticking trick in the stated \mathfrak{sp}_4 -skein algebra via an isomorphism constructed in [IY22].

3.2. A generating set of the \mathfrak{sp}_4 -skein algebra. Roughly speaking, in order to construct an inclusion of the boundary-localized \mathfrak{sp}_4 -skein algebra into the quantum cluster algebra, we need to write an \mathfrak{sp}_4 -web as a (not necessarily positive) polynomial of \mathfrak{sp}_4 -webs that correspond to cluster variables. For this, let us first prepare some classes of \mathfrak{sp}_4 -graph diagrams that give rise to nice generating sets of $\mathcal{S}_{\mathfrak{sp}_4, \Sigma}$ and $\mathcal{S}_{\mathfrak{sp}_4, \Sigma}[\partial^{-1}]$.

Definition 3.4. A *tangled loop (resp. arc) diagram* on Σ is a tangled \mathfrak{sp}_4 -graph diagram given by a map from a circle (resp. interval) of type 1 or type 2. A *tangled loop (resp. arc) diagram with legs* on Σ is a connected tangled \mathfrak{sp}_4 -graph diagram on Σ obtained by connecting a tangled loop (resp. arc) diagram of type 1 to special points by attaching several edges of type 2 (called *legs*). A *tangled triad diagram* on Σ is a tangled arc diagram of type 1 with only one leg. We say that a tangled \mathfrak{sp}_4 -graph diagram is *simple* if it has no internal crossings. A tangled arc diagram on Σ is said to be *descending* if one passes every self-crossing points through an over-pass first, following some fixed orientation. A tangled loop diagram on Σ with a basepoint is said to be *descending* if an oriented tangled arc starting from the basepoint satisfies the descending property. A tangled loop or arc diagram with legs on Σ is said to be *descending* if its legs have no internal crossings, and the diagram obtained by removing the legs is descending.

Definition 3.5. (1) We denote by $\text{Desc}_{\mathfrak{sp}_4, \Sigma}^{\varpi_1}$ the set of all the descending loop/arc diagrams of type 1 with or without legs. (Here notice that it is possible that their ends share a common special point.)

(2) A *stated end* of type 1 means an end of either types  ,  , or  .

(3) The set $\text{SimpWil}_{\mathfrak{sp}_4, \Sigma}^{\varpi_1}$ of *simple Wilson lines of type 1* consists of all simple \mathfrak{sp}_4 -graphs obtained by connecting two stated ends on distinct boundary intervals by a simple arc of type 1.

Remark 3.6. A simple Wilson line of type 1 corresponds to a matrix entry of a simple Wilson line ([IOS22]) in the representation $V(\varpi_1)$, up to boundary webs. See also [IY22].

We are going to discuss a generating set of the \mathfrak{sp}_4 -skein algebra. For example, $\mathcal{S}_{\mathfrak{sp}_4, T}$ is generated $\text{SimpWil}_{\mathfrak{sp}_4, T}^{\varpi_1}$ by Theorem 2.25 for a triangle T .

Proposition 3.7. *For any unpunctured marked surface Σ , any basis web is expressed as a polynomial in elements of $\text{Desc}_{\mathfrak{sp}_4, \Sigma}^{\varpi_1}$, simple loops and arcs of type 2 in $\mathcal{S}_{\mathfrak{sp}_4, \Sigma}$ with coefficients in \mathbb{Z}_v . In particular, $\text{Desc}_{\mathfrak{sp}_4, \Sigma}^{\varpi_1}$ generates $\mathcal{S}_{\mathfrak{sp}_4, \Sigma}$ as an \mathcal{R} -algebra.*

Proof. Let us define the *complexity* $|G|$ of a crossroad diagram G to be the number of crossroads and internal crossings of G , where a *crossroad diagram* is a tangled \mathfrak{sp}_4 -graph with 4-valent vertices corresponding to crossroads and internal crossings and no rungs. Note that if a connected crossroad diagram G has the complexity $|G| = 0$, then G is a simple loop or arc diagram with or without legs. We claim that a connected flat crossroad diagram G is written as a \mathbb{Z}_v -linear combination of XG' and flat crossroad diagrams

with complexity less than $|G|$, where $X \in \text{Desc}_{\mathfrak{sp}_4, \Sigma}^{\varpi_1}$ and G' is a flat crossroad diagram with $|G'| < |G|$. Then by induction on the complexity, one can show that any basis web is written as a polynomial in $\text{Desc}_{\mathfrak{sp}_4, \Sigma}^{\varpi_1}$ over \mathbb{Z}_v because a basis web is represented as a product of connected flat crossroad diagrams. It concludes that $\text{Desc}_{\mathfrak{sp}_4, \Sigma}^{\varpi_1}$ generates $\mathcal{S}_{\mathfrak{sp}_4, \Sigma}$ as an \mathcal{R} -algebra.

Let G be any connected flat crossroad diagram on Σ , and choose its basepoint on a type 1 edge. Here if G has a type 1 edge incident to a special point, then we take the basepoint on such an edge. We start from the basepoint, and arriving at a crossroad, replace it with an internal crossing by:

$$\begin{array}{c} \text{---} \times \text{---} \\ \text{---} \times \text{---} \end{array} = \begin{array}{c} \text{---} \times \text{---} \\ \text{---} \times \text{---} \end{array} - v \begin{array}{c} \text{---} \text{---} \\ \text{---} \text{---} \end{array} - v^{-1} \begin{array}{c} \text{---} \text{---} \\ \text{---} \text{---} \end{array}. \quad (3.5)$$

Here we choose the crossing in such a way that our chosen path becomes an over-passing subarc. This operation produces two extra diagrams with complexity less than $|G| - 1$: see the lower two diagrams in the middle column in Figure 3.1. We repeat this procedure until we return to the basepoint or arrive at a special point. See diagrams in the top route in Figure 3.1. If one arrives at a type 2 edge (incident to a special point) in this procedure, turn at the vertex there and go to the other type 1 edge.

By construction, our trail X becomes a descending loop or an arc diagram with/without legs, and another component is a flat crossroad diagram G' with $|G'| < |G|$ since X removes at least one crossroad from G . Although crossroad diagrams other than XG' arise in this procedure, they have complexity less than $|G|$. These redundant crossroad diagrams become a \mathbb{Z}_v -linear combination of $\text{BWeb}_{\mathfrak{sp}_4, \Sigma}$ by the reduction rules in Definition 2.12 and (3.5), since the reduction rules related to crossroads and (3.5) all have coefficients in \mathbb{Z}_v and do not increase the complexity. Consequently, we can decompose G into $XG' + \sum_i \lambda_i G_i$ such that $X \in \text{Desc}_{\mathfrak{sp}_4, \Sigma}^{\varpi_1}$, G' and G_i are flat crossroad diagrams with $|G'| < |G|$ and $|G_i| < |G|$. Thus the first assertion is proved.

We can exclude simple loops and arcs of type 2 from generators of $\mathcal{S}_{\mathfrak{sp}_4, \Sigma}$ as \mathcal{R} -algebra. Indeed, one can produce a bigon by deforming a simple loop of type 2 using (2.4) and apply it to the algorithm above (notice that this produces a factor $[2]^{-1}$). In a similar way, we consider a simple arc of type 2 as a trivial loop with two legs. Thus the second assertion is proved. \square

Remark 3.8. In the proof of Proposition 3.7, we can choose a basepoint of a descending loop diagram (with legs) on an arbitrary subarc. Indeed, if G and G' are two descending loop diagrams with the same projection to Σ such that their basepoints are incident to each other across a single subarc, then these two descending loop diagrams are related by

$$\begin{array}{c} \text{---} \times \text{---} \\ \text{---} \times \text{---} \end{array} - \begin{array}{c} \text{---} \times \text{---} \\ \text{---} \times \text{---} \end{array} = (v - v^{-1}) \left(\begin{array}{c} \text{---} \text{---} \\ \text{---} \text{---} \end{array} - \begin{array}{c} \text{---} \text{---} \\ \text{---} \text{---} \end{array} \right). \quad (3.6)$$

Hence, the complexities of tangled graph diagrams appearing in the difference between G and G' are less than $|G|$. In a similar way to the proof in Proposition 3.7, the generator G can be replaced by G' .

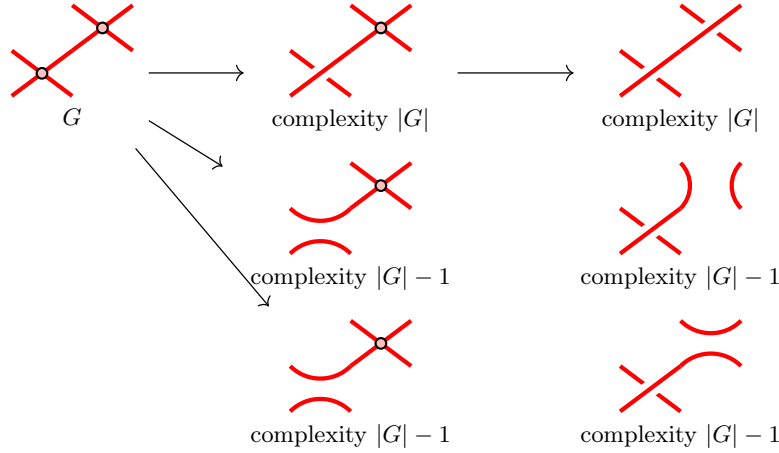


FIGURE 3.1. The top route removes a descending loop or arc X from a flat crossroad diagram G . The other resulting graphs are described as a \mathbb{Z}_v -linear combination of crossroad diagrams with complexity less than $|G|$.

One can obtain simple generators of the boundary-localized skein algebra $\mathcal{S}_{\mathfrak{sp}_4, \Sigma}[\partial^{-1}]$ by refining descending generators in $\text{Desc}_{\mathfrak{sp}_4, \Sigma}^{\varpi_1}$.

Theorem 3.9. *Let Σ be a connected unpunctured marked surface with at least two special points. Then, any element in $\text{Desc}_{\mathfrak{sp}_4, \Sigma}^{\varpi_1}$ and simple loops/arcs of type 2 are expressed as polynomials in $\text{SimpWil}_{\mathfrak{sp}_4, \Sigma}^{\varpi_1} \cup \partial_{\Sigma}^{-1}$ with coefficients in \mathbb{Z}_v , where ∂_{Σ}^{-1} is the set of inverses of boundary webs in $\mathcal{S}_{\mathfrak{sp}_4, \Sigma}[\partial^{-1}]$. In particular, $\text{SimpWil}_{\mathfrak{sp}_4, \Sigma}^{\varpi_1} \cup \partial_{\Sigma}^{-1}$ is a generating set of $\mathcal{S}_{\mathfrak{sp}_4, \Sigma}[\partial^{-1}]$ as \mathcal{R} -algebra.*

Proof. We are going to use the sticking tricks to further expand an element in $\text{Desc}_{\mathfrak{sp}_4, \Sigma}^{\varpi_1}$ or a simple loop/arc of type 2.

Firstly, by using the following relation and (3.6), we can expand a descending arc of type 2 to a polynomial of descending arcs of type 1 with or without legs:

$$\begin{array}{c} \bullet \\ \text{---} \\ \bullet \end{array} \begin{array}{c} \bullet \\ \text{---} \\ \bullet \end{array} = \begin{array}{c} \bullet \\ \text{---} \\ \bullet \end{array} \begin{array}{c} \bullet \\ \text{---} \\ \bullet \end{array} - v^{-1} \begin{array}{c} \bullet \\ \text{---} \\ \bullet \end{array} \begin{array}{c} \bullet \\ \text{---} \\ \bullet \end{array} .$$

Secondly, for a simple loop of type 2, stick it to a boundary interval E by (3.4). Then the resulting \mathfrak{sp}_4 -graphs in the first and final terms in (3.4) are descending arcs of type 2, which we have discussed. The second and fourth terms in (3.4) can be replaced with descending arcs with or without legs by

$$\begin{array}{c} \bullet \\ \text{---} \\ \bullet \end{array} \begin{array}{c} \bullet \\ \text{---} \\ \bullet \end{array} = \begin{array}{c} \bullet \\ \text{---} \\ \bullet \end{array} \begin{array}{c} \bullet \\ \text{---} \\ \bullet \end{array} - v^{-1} \begin{array}{c} \bullet \\ \text{---} \\ \bullet \end{array} \begin{array}{c} \bullet \\ \text{---} \\ \bullet \end{array} , \text{ or} \\ \begin{array}{c} \bullet \\ \text{---} \\ \bullet \end{array} \begin{array}{c} \bullet \\ \text{---} \\ \bullet \end{array} = \begin{array}{c} \bullet \\ \text{---} \\ \bullet \end{array} \begin{array}{c} \bullet \\ \text{---} \\ \bullet \end{array} - v^{-1} \begin{array}{c} \bullet \\ \text{---} \\ \bullet \end{array} \begin{array}{c} \bullet \\ \text{---} \\ \bullet \end{array} .$$

Observe that the above procedure can be applied for any given interval E .

Let us fix a boundary interval E and denote the corresponding boundary web of type s by e_s for $s = 1, 2$. Given a descending loop diagram G with or without legs, we can take its basepoint on a subarc γ between two crossing points of G such that γ and E share

the same face in $\Sigma \setminus G$ by Remark 3.8. Then, one can apply the sticking trick (3.3) to γ by multiplying $e_1 e_2$ to G to expand it into a \mathbb{Z}_v -linear combination of descending arc diagrams with/without legs. Then it remains to consider a descending arc diagram G with/without legs. For each leg of G , one can apply the sticking trick (3.3) as follows:

$$\begin{aligned}
 & \text{Diagram with arrow} = v \text{Diagram}_1 - v^2 \text{Diagram}_2 + v^3 \text{Diagram}_3 - v^4 \text{Diagram}_4 \\
 & = v^3 \text{Diagram}_5 - v^3 \text{Diagram}_6,
 \end{aligned}$$

where G is descending along the arrow in the first diagram. Observe that the resulting diagrams have stated ends on the interval E . In other words, G is expanded into a polynomial in $\text{DescWil}_{\mathfrak{sp}_4, \Sigma}^{\varpi_1}$ up to boundary webs. Let us denote by $S_n \subset \text{DescWil}_{\mathfrak{sp}_4, \Sigma}^{\varpi_1}$ the subset of descending Wilson lines whose minimal diagram has n self-crossing points. We remark that $S_0 = \text{SimpWil}_{\mathfrak{sp}_4, \Sigma}^{\varpi_1}$.

We then claim that any tangled graph in S_n can be written as a \mathbb{Z}_v -linear combination of the product of elements in $S_{<n} := \cup_{i < n} S_i$ and simple Wilson lines of type 1. For a tangled graph $G \in S_n$, we can describe a neighborhood of the subarc from an end to the first crossing of G by forgetting arcs that sit in the lower layer as follows:

and the left-turn version.

Apply the sticking trick to the under-passing subarc of the first crossing point of G . One can see that it becomes $G = \sum_i a_i \gamma_i G_i$ where $G_i \in S_{<n}$ and

$$\gamma_i =$$

where the filled area is one of the above ends. Finally, one can apply the sticking trick to the top subarc of γ_i and the other boundary interval (which exists since Σ has at least two special points), and the resulting graphs become simple Wilson line of type 1. By induction on n , we conclude that G is expressed as a \mathbb{Z}_v -linear combination of $\text{SimpWil}_{\mathfrak{sp}_4, \Sigma}^{\varpi_1}$. Observe that all the coefficients appearing in the above argument are in \mathbb{Z}_v . \square

Remark 3.10. See [IOS22, Corollary 3.20 and Proposition 2.1] for a closely related statement.

3.3. The \mathbb{Z}_v -form of the \mathfrak{sp}_4 -skein algebra. To compare the \mathfrak{sp}_4 -skein algebra $\mathcal{S}_{\mathfrak{sp}_4, \Sigma}[\partial^{-1}]$ with the quantum cluster algebra with its natural coefficient ring $\mathbb{Z}_v = \mathbb{Z}[v^{\pm 1/2}]$, we introduce the following notion.

Definition 3.11. The \mathbb{Z}_v -span $\mathcal{S}_{\mathfrak{sp}_4, \Sigma}^{\mathbb{Z}_v} := \mathbb{Z}_v \text{BWeb}_{\mathfrak{sp}_4, \Sigma} \subset \mathcal{S}_{\mathfrak{sp}_4, \Sigma}$ of the basis webs on Σ is called the \mathbb{Z}_v -form of the \mathfrak{sp}_4 -skein algebra $\mathcal{S}_{\mathfrak{sp}_4, \Sigma}$.





The following lemma implies that the \mathbb{Z}_v -form of $\mathcal{S}_{\mathfrak{sp}_4, \Sigma}$ is a \mathbb{Z}_v -subalgebra of $\mathcal{S}_{\mathfrak{sp}_4, \Sigma}$, namely, the product $G_1 G_2$ lies in $\mathcal{S}_{\mathfrak{sp}_4, \Sigma}^{\mathbb{Z}_v}$ for any basis webs $G_1, G_2 \in \mathbf{BWeb}_{\mathfrak{sp}_4, \Sigma}$.

Lemma 3.12. *Any crossroad web belongs to $\mathcal{S}_{\mathfrak{sp}_4, \Sigma}^{\mathbb{Z}_v}$.*

Proof. Let G be an \mathfrak{sp}_4 -graph diagram with crossroads whose legs have no internal crossings. We know that G reduces to a \mathcal{R} -linear combination of $\mathbf{BWeb}_{\mathfrak{sp}_4, \Sigma}$ by the reduction rules in Definition 2.12. Let us show that the coefficients in this expansion lie in \mathbb{Z}_v by induction on the *weighted crossing number* $c(G)$ defined as $c(G) := \# \text{ (crossing with two legs) } + 2\# \text{ (crossing with three legs) } + 2\# \text{ (crossing with four legs) } + 4\# \text{ (crossing with five legs) }$. We remark that $c(G)$ is invariant under the Reidemeister moves:

$$\begin{array}{ccc} \text{(crossing with two legs)} & \leftrightarrow & \text{(crossing with three legs)} \\ \text{(crossing with three legs)} & \leftrightarrow & \text{(crossing with four legs)} \end{array} \quad (3.7)$$

If G has no internal crossings, then it belongs to $\mathcal{S}_{\mathfrak{sp}_4, \Sigma}^{\mathbb{Z}_v}$ since those among the reduction rules S_i and B_i in Definition 2.12 used in this procedure have coefficients in \mathbb{Z}_v , thanks to the absence of rungs in G . Here note that $[4]/[2] = v^2 + v^{-2}$, $[6]/([2][3]) = v^2 - 1 + v^{-2} \in \mathbb{Z}_v$.

Let us consider the cases where G has an internal crossing (i) , (ii) , , or (iii) . We apply the reduction rule C_1 to the crossing (i), which expands G into a \mathbb{Z}_v -linear combination of crossroad webs with weighted crossing numbers less than $c(G)$. Since G has no rungs, the edge of type 2 in (ii) must be a tangled loop or an arc component. In the latter case, G is expanded as $G = vX + v^{-1}Y$ by the reduction rule C_2 or C_3 , where X and Y are crossroad webs with $c(X) < c(G)$ and $c(Y) < c(G)$. Observe that the resulting edges of type 2 are legs. In the former case, we expand similarly as $G = vX + v^{-1}Y$, where X and Y have rungs. These rungs are replaced by crossroads as follows:

$$\begin{aligned} \text{(crossing with two legs)} &= v \text{(crossing with two legs)} + v^{-1} \text{(crossing with two legs)} = v \text{(crossing with two legs)} + v^{-1} \text{(crossing with two legs)} \\ &= v \text{(crossing with two legs)} + v^{-1} \text{(crossing with two legs)} + \frac{v}{[2]} \text{(crossing with two legs)} + \frac{v^{-1}}{[2]} \text{(crossing with two legs)} \\ &= v \text{(crossing with two legs)} + v^{-1} \text{(crossing with two legs)} + \text{(crossing with two legs)}. \end{aligned}$$

Here we only use the Reidemeister move (3.7) in the second equation. The resulting crossroad webs have weighted intersection numbers less than $c(G)$. Let us consider an internal crossing (iii) of two tangled loops of type 2. We apply the skein relation (2.10) to the internal crossing of G :

$$\text{(crossing with two legs)} = v^2 \text{(crossing with two legs)} + v^{-2} \text{(crossing with two legs)} + \text{(crossing with two legs)}.$$

The first and second \mathfrak{sp}_4 -graphs are crossroad webs with the weighted crossing number less than $c(G)$. We are going to deform the third \mathfrak{sp}_4 -graph into a \mathbb{Z}_v -linear combination of crossroad webs. If the internal crossing is formed by different loop components, then:

$$\begin{aligned}
\begin{array}{c} \text{Diagram 1} \\ \text{Diagram 2} \end{array} &= \begin{array}{c} \text{Diagram 3} \\ \text{Diagram 4} \end{array} = \begin{array}{c} \text{Diagram 5} \\ \text{Diagram 6} \end{array} + \frac{1}{[2]} \begin{array}{c} \text{Diagram 7} \\ \text{Diagram 8} \end{array} \\
&= \begin{array}{c} \text{Diagram 9} \\ \text{Diagram 10} \end{array} - \begin{array}{c} \text{Diagram 11} \\ \text{Diagram 12} \end{array} = \begin{array}{c} \text{Diagram 13} \\ \text{Diagram 14} \end{array} - \begin{array}{c} \text{Diagram 15} \\ \text{Diagram 16} \end{array} \\
&= \begin{array}{c} \text{Diagram 17} \\ \text{Diagram 18} \end{array} + \frac{1}{[2]} \begin{array}{c} \text{Diagram 19} \\ \text{Diagram 20} \end{array} - \begin{array}{c} \text{Diagram 21} \\ \text{Diagram 22} \end{array} \\
&= \begin{array}{c} \text{Diagram 23} \\ \text{Diagram 24} \end{array} - \begin{array}{c} \text{Diagram 25} \\ \text{Diagram 26} \end{array} - \begin{array}{c} \text{Diagram 27} \\ \text{Diagram 28} \end{array}.
\end{aligned}$$

If it is a self-crossing, then:

$$\begin{aligned}
\begin{array}{c} \text{Diagram 1} \\ \text{Diagram 2} \end{array} &= \begin{array}{c} \text{Diagram 3} \\ \text{Diagram 4} \end{array} = \begin{array}{c} \text{Diagram 5} \\ \text{Diagram 6} \end{array} + \frac{1}{[2]} \begin{array}{c} \text{Diagram 7} \\ \text{Diagram 8} \end{array} \\
&= \begin{array}{c} \text{Diagram 9} \\ \text{Diagram 10} \end{array} - \begin{array}{c} \text{Diagram 11} \\ \text{Diagram 12} \end{array} \\
&= \begin{array}{c} \text{Diagram 13} \\ \text{Diagram 14} \end{array} + \frac{1}{[2]} \begin{array}{c} \text{Diagram 15} \\ \text{Diagram 16} \end{array} - \begin{array}{c} \text{Diagram 17} \\ \text{Diagram 18} \end{array} \\
&= \begin{array}{c} \text{Diagram 19} \\ \text{Diagram 20} \end{array} - \begin{array}{c} \text{Diagram 21} \\ \text{Diagram 22} \end{array} - \begin{array}{c} \text{Diagram 23} \\ \text{Diagram 24} \end{array}.
\end{aligned}$$

In both cases, the resulting crossroad webs have the weighted crossing number less than $c(G)$, and their coefficients lie in \mathbb{Z}_v . One can prove the same assertion for the cases where one or two of them are arcs rather than loops. Then we conclude that G belongs to $\mathcal{S}_{\mathfrak{sp}_4, \Sigma}^{\mathbb{Z}_v}$ by induction on $c(G)$. \square

For a subset $S \subset \mathcal{S}_{\mathfrak{sp}_4, \Sigma}$, let us denote by $\langle S \rangle_{\mathbb{Z}_v}[\partial^{-1}]$ a \mathbb{Z}_v -subalgebra generated by S and boundary webs $\partial_{\Sigma} \cup \partial_{\Sigma}^{-1}$ in $\mathcal{S}_{\mathfrak{sp}_4, \Sigma}^{\mathbb{Z}_v}[\partial^{-1}]$.

Theorem 3.13. $\mathcal{S}_{\mathfrak{sp}_4, \Sigma}^{\mathbb{Z}_v}[\partial^{-1}] = \langle \text{Desc}_{\mathfrak{sp}_4, \Sigma}^{\varpi_1} \rangle_{\mathbb{Z}_v}[\partial^{-1}] = \langle \text{SimpWil}_{\mathfrak{sp}_4, \Sigma}^{\varpi_1} \rangle_{\mathbb{Z}_v}[\partial^{-1}]$.

Proof. It is obvious that $\langle \text{SimpWil}_{\mathfrak{sp}_4, \Sigma}^{\varpi_1} \rangle_{\mathbb{Z}_v}[\partial^{-1}] \subset \mathcal{S}_{\mathfrak{sp}_4, \Sigma}^{\mathbb{Z}_v}[\partial^{-1}] = \text{BWeb}_{\mathfrak{sp}_4, \Sigma}$ because $\text{SimpWil}_{\mathfrak{sp}_4, \Sigma}^{\varpi_1} \subset \text{BWeb}_{\mathfrak{sp}_4, \Sigma}$. The inclusion $\mathcal{S}_{\mathfrak{sp}_4, \Sigma}^{\mathbb{Z}_v}[\partial^{-1}] \subset \langle \text{Desc}_{\mathfrak{sp}_4, \Sigma}^{\varpi_1} \rangle_{\mathbb{Z}_v}[\partial^{-1}]$ follows from Proposition 3.7 together with the argument on simple loops and arcs of type 2 discussed in the proof of Theorem 3.9. Moreover, Theorem 3.9 tells us that $\langle \text{Desc}_{\mathfrak{sp}_4, \Sigma}^{\varpi_1} \rangle_{\mathbb{Z}_v}[\partial^{-1}] \subset \langle \text{SimpWil}_{\mathfrak{sp}_4, \Sigma}^{\varpi_1} \rangle_{\mathbb{Z}_v}[\partial^{-1}]$. Consequently, we obtain a sequence of inclusions

$$\mathcal{S}_{\mathfrak{sp}_4, \Sigma}^{\mathbb{Z}_v}[\partial^{-1}] \subset \langle \text{Desc}_{\mathfrak{sp}_4, \Sigma}^{\varpi_1} \rangle_{\mathbb{Z}_v}[\partial^{-1}] \subset \langle \text{SimpWil}_{\mathfrak{sp}_4, \Sigma}^{\varpi_1} \rangle_{\mathbb{Z}_v}[\partial^{-1}] \subset \mathcal{S}_{\mathfrak{sp}_4, \Sigma}^{\mathbb{Z}_v}[\partial^{-1}],$$

which concludes the assertion. \square


3.4. Laurent expressions and positivity. The notion of “elevation-preserving” webs has been introduced in [IY21] for tangled \mathfrak{sl}_3 -webs. An elevation-preserving web is shown to have a Laurent expression with positive coefficients, based on the cutting trick in Lemma 3.1. Let us discuss the \mathfrak{sp}_4 -case here.

We first explain the expansion of a tangled \mathfrak{sp}_4 -graph based on the cutting trick in Lemma 3.1. For an ideal arc E connecting two special points p and q , denote the type s simple \mathfrak{sp}_4 -arc parallel to E by e_s for $s = 1, 2$.

Let us consider a tangled \mathfrak{sp}_4 -graph diagram G such that $E \setminus \{p, q\}$ has n_s transverse intersection points with type s edges of G for $s = 1, 2$. Then, one can easily see that $G(e_1 e_2)^{n_1} (e_1 e_2^2)^{n_2}$ is expanded into an \mathbb{Z}_v -linear combination of tangled graph diagrams with no intersection with $E \setminus \{p, q\}$. Applying this procedure to each edge of an ideal triangulation Δ of Σ , we can expand a tangled graph G into a \mathbb{Z}_v -linear combination of \mathfrak{sp}_4 -webs contained in triangles of Δ . Recall that any such \mathfrak{sp}_4 -web contained in triangles is expressed as a polynomial in $\cup_{T \in t(\Delta)} \mathbf{EWeb}_{\mathfrak{sp}_4, T}$ with coefficients in \mathcal{R} by Theorem 2.25. The coefficients can be restricted to \mathbb{Z}_v if G is a crossroad web because of Lemma 3.12. Moreover, it turns out that one can write G by only using the elementary webs associated with a fixed decorated triangulation:

Theorem 3.14 (web cluster expansions). *Let Δ be an ideal triangulation of an unpunctured marked surface Σ . Choosing a web cluster $\mathcal{C}_T \in \mathbf{CWeb}_{\mathfrak{sp}_4, T}$ for each $T \in t(\Delta)$, let $\mathcal{C}_\Delta := \cup_{T \in t(\Delta)} \mathcal{C}_T$ be the corresponding web cluster of $\mathcal{S}_{\mathfrak{sp}_4, \Sigma}$. For any tangled \mathfrak{sp}_4 -graph (resp. crossroad web) G in $\mathcal{S}_{\mathfrak{sp}_4, \Sigma}$ (resp. $\mathcal{S}_{\mathfrak{sp}_4, \Sigma}^{\mathbb{Z}_v}$), there exists a monomial J in \mathcal{C}_Δ such that GJ is a polynomial in \mathcal{C}_Δ with coefficients in \mathcal{R} (resp. \mathbb{Z}_v).*

Proof. From the above discussion, it suffices to see that any elementary web in a triangle T becomes a polynomial in \mathcal{C}_T after multiplying a monomial in \mathcal{C}_T . Let us consider the

web cluster \mathcal{C}_T consisting of , and the \mathfrak{sp}_4 -webs along the edges of T . The followings are verified straightforwardly by using the skein relations:

$$\begin{array}{ccc} \begin{array}{c} \text{Web 1} \\ \text{Web 2} \end{array} & = v \begin{array}{c} \text{Web 3} \\ \text{Web 4} \end{array} + v^{-1} \begin{array}{c} \text{Web 5} \\ \text{Web 6} \end{array}, & (3.8) \end{array}$$

$$\begin{array}{ccc} \begin{array}{c} \text{Web 1} \\ \text{Web 2} \end{array} & = v^{-\frac{1}{2}} \begin{array}{c} \text{Web 3} \\ \text{Web 4} \end{array} + v^{\frac{1}{2}} \begin{array}{c} \text{Web 5} \\ \text{Web 6} \end{array}, & (3.9) \end{array}$$

$$\begin{array}{ccc} \begin{array}{c} \text{Web 1} \\ \text{Web 2} \end{array} & = v^{\frac{1}{2}} \begin{array}{c} \text{Web 3} \\ \text{Web 4} \end{array} + v^{-\frac{1}{2}} \begin{array}{c} \text{Web 5} \\ \text{Web 6} \end{array}, & (3.10) \end{array}$$

$$\begin{array}{ccc} \begin{array}{c} \text{Web 1} \\ \text{Web 2} \end{array} & = v \begin{array}{c} \text{Web 3} \\ \text{Web 4} \end{array} + v^{-1} \begin{array}{c} \text{Web 5} \\ \text{Web 6} \end{array}. & (3.11) \end{array}$$

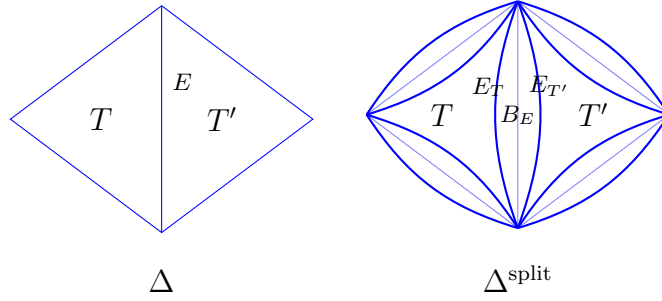


FIGURE 3.2. The split triangulation Δ^{split} associated with Δ . Here B_E is the biangle bounded by the two edges E_T and $E_{T'}$.

Using these relations, we see that each elementary web can be expanded into a polynomial in \mathcal{C}_T . Thus the assertion is proved. \square

One may notice that the coefficients in (3.1), (3.2), (3.8)–(3.11) are all positive, namely in the monoid $\mathbb{Z}_+[v^{\pm 1/2}] \subset \mathbb{Z}[v^{\pm 1/2}]$ of Laurent polynomials with non-negative coefficients. Globally, however, it is possible that we have to use skein relations which produce negative signs (such as (2.4)) in expanding a tangled \mathfrak{sp}_4 -graph. Let us introduce a class of tangled \mathfrak{sp}_4 -graphs whose expansions are ensured to have only positive coefficients.

For an ideal triangulation Δ , the associated *splitting triangulation* Δ^{split} is obtained by replacing each edge E of Δ with two parallel edges, as shown in Figure 3.2. The set of connected components of $\Sigma \setminus \Delta^{\text{split}}$ is divided into two subsets: the set $t(\Delta^{\text{split}})$ of triangles and the set $b(\Delta^{\text{split}})$ of biangles. We denote a triangle in $t(\Delta^{\text{split}})$ by the same symbol as the corresponding triangle in $t(\Delta)$, while the biangle corresponding to an edge $E \in e(\Delta)$ is denoted by $B_E \in b(\Delta^{\text{split}})$. For an edge $E \in e(\Delta)$ and a triangle $T \in t(\Delta)$ adjacent to E , let $E_T \in e(\Delta^{\text{split}})$ denote the edge shared by B_E and T .

Definition 3.15 (elevation-preserving \mathfrak{sp}_4 -webs). A tangled \mathfrak{sp}_4 -graph is said to be *elevation-preserving with respect to* Δ if it is represented by a diagram G on Σ satisfying the following conditions:

- For $B \in b(\Delta^{\text{split}})$ corresponding to an interior edge, $G \cap B$ consists of a braid between the two sides of B obtained by a superposition of arcs of either type. For $B \in b(\Delta^{\text{split}})$ corresponding to a boundary interval, $G \cap B$ consists of a braid between the interior side and special points. For any pair of strands β_1 and β_2 in the braid that intersects each other, one of them is required to have a higher elevation than the other throughout the way: we denote by $\beta_1 < \beta_2$ if β_2 passes over β_1 .
- For any $T \in t(\Delta^{\text{split}})$, $G \cap T$ consists of a superposition of the diagrams in

$$\left\{ \begin{array}{c} \text{Diagram 1: Triangle with red arcs} \\ \text{Diagram 2: Triangle with red arcs} \\ \text{Diagram 3: Triangle with red arcs} \end{array} , \text{ and their rotations} \right\}.$$

Similarly, the relative elevations between any two components are required to be fixed throughout the way if they have a crossing.

- For any $T \in t(\Delta^{\text{split}})$ and its adjacent bigon $B \in b(\Delta^{\text{split}})$, two components G_1, G_2 of the diagram in T satisfy $G_1 < G_2$ if $\beta_1 < \beta_2$, where β_i are strands of the braid in B connected to G_i for $i = 1, 2$.

Example 3.16. Elements in $\text{Desc}_{\text{sp}_4, \Sigma}^{\varpi_1}$, especially geometric n -bracelets and n -bangles in Figure 1.1, are elevation-preserving for any ideal triangulation Δ . Note that the legs of a descending loop or arc can avoid intersecting with the edges of Δ .

Theorem 3.17. Let Σ be any unpunctured marked surface, Δ its ideal triangulation, and \mathcal{C}_Δ the web cluster associated with a decorated triangulation Δ over Δ . For any elevation-preserving sp_4 -web G with respect to Δ , there exists a monomial J in \mathcal{C}_Δ such that $[2]^k G J$ is a polynomial in \mathcal{C}_Δ with coefficients in $\mathbb{Z}_+[v^{\pm 1/2}]$, where k is the total number of intersection points between type 2 edges of G and all the edges of the triangulation.

Proof. Let G be an elevation-preserving web with respect to an ideal triangulation Δ . We first expand G into sp_4 -webs in bigons and triangles in Δ^{split} by the cutting trick in Lemma 3.1, only producing positive coefficients by the discussion above. Here notice that the expansion of G can be obtained by expanding $G \cap T$ and $G \cap B$ for each $T \in t(\Delta^{\text{split}})$ and $B \in b(\Delta^{\text{split}})$ in the order from the webs in lower elevation to the higher, thanks to the elevation-preserving property. Then it remains to see how the local pieces shown below are glued in bigons B or triangles T :

$$\begin{aligned} X_1 &:= \text{diag}_1, & X_2 &:= \text{diag}_2, & X_3 &:= \text{diag}_3, & X_4 &:= \text{diag}_4, \\ Y_1 &:= \text{diag}_5, & Y_2 &:= \text{diag}_6, & Y_3 &:= \text{diag}_7, & Y_4 &:= \text{diag}_8, & Y_5 &:= \text{diag}_9. \end{aligned}$$

The gluing patterns are

$$\begin{aligned} B(X_i, X_j) &:= \text{bigon}_1, & B(Y_i, Y_j) &:= \text{bigon}_2, \\ T(X_i, X_j, \emptyset) &:= \text{triangle}_1, & T(Y_i, Y_j, \emptyset) &:= \text{triangle}_2, & T(Y_i, X_j, X_k) &:= \text{triangle}_3 \end{aligned}$$

up to symmetries of the bigon or the triangle. In the case of bigon, it is easy to see that

$$\begin{aligned} B(X_1, X_1) = B(X_4, X_4) &= \text{bigon}_3, & B(X_2, X_2) = B(X_3, X_3) &= \text{bigon}_4, \\ B(Y_1, Y_1) = B(Y_4, Y_4) &= \text{bigon}_5, & B(Y_2, Y_2) = B(Y_3, Y_3) &= \text{bigon}_6, \end{aligned}$$

and otherwise zero.

In the case of triangle, it is easy to confirm that

$$T(X_i, X_j, \emptyset) = T(Y_i, Y_j, \emptyset) = 0$$

for $i < j$, and

$$T(Y_i, X_1, X_4) = T(Y_1, X_3, X_k) = T(Y_1, X_4, X_k) = T(Y_2, X_4, X_k) = 0$$

for any $i \in \{1, \dots, 5\}$ and $k \in \{1, \dots, 4\}$. One can also see that X_i (resp. Y_i) coincides with X_{5-i} (resp. Y_{6-i}). Thus, $T(X_{5-j}, X_{5-i}, \emptyset)$, $T(Y_{6-j}, Y_{6-i}, \emptyset)$, and $T(Y_{6-i}, X_{5-j}, X_{5-k})$ are obtained from computations of $T(X_i, X_j, \emptyset)$, $T(Y_i, Y_j, \emptyset)$, and $T(Y_i, X_j, X_k)$, respectively. Then it remains to compute the following patterns, which are verified by straightforward calculation:

$$\begin{aligned}
 T(X_1, X_1, \emptyset) &= \text{triangle with red arc from top to bottom-right}, & T(X_2, X_1, \emptyset) &= \text{triangle with red arcs from top to both bottom vertices}, & T(X_2, X_2, \emptyset) &= \text{triangle with red arcs from both top vertices to bottom}, \\
 T(X_3, X_1, \emptyset) &= \text{triangle with red arcs from top to both bottom vertices and from top to bottom-right}, & T(X_3, X_2, \emptyset) &= \text{triangle with red arcs from top to both bottom vertices and from top to bottom-left}, & T(X_4, X_1, \emptyset) &= \text{triangle with red arcs from top to both bottom vertices and from top to bottom-left}, \\
 T(Y_1, Y_1, \emptyset) &= \text{triangle with red arcs from top to both bottom vertices and from top to bottom-right}, & T(Y_2, Y_1, \emptyset) &= \text{triangle with red arcs from top to both bottom vertices and from top to bottom-left}, & T(Y_2, Y_2, \emptyset) &= \text{triangle with red arcs from both top vertices to bottom}, \\
 T(Y_3, Y_1, \emptyset) &= \text{triangle with red arcs from top to both bottom vertices and from top to bottom-left}, & T(Y_3, Y_2, \emptyset) &= \text{triangle with red arcs from top to both bottom vertices and from top to bottom-right}, & T(Y_3, Y_3, \emptyset) &= \frac{1}{[2]} \text{triangle with red arcs from both top vertices to bottom}, \\
 T(Y_4, Y_1, \emptyset) &= \text{triangle with red arcs from top to both bottom vertices and from top to bottom-left}, & T(Y_4, Y_2, \emptyset) &= \left(\text{triangle with red arcs from top to both bottom vertices and from top to bottom-right} \right)^2, & T(Y_5, Y_1, \emptyset) &= \text{triangle with red arcs from top to both bottom vertices and from top to bottom-right}, \\
 T(Y_1, X_1, X_1) &= \text{triangle with red arcs from top to both bottom vertices and from top to bottom-right}, & T(Y_1, X_1, X_2) &= \text{triangle with red arcs from top to both bottom vertices and from top to bottom-left}, & T(Y_1, X_1, X_3) &= \text{triangle with red arcs from top to both bottom vertices and from top to bottom-right}, \\
 T(Y_1, X_2, X_1) &= \text{triangle with red arcs from top to both bottom vertices and from top to bottom-left}, & T(Y_1, X_2, X_2) &= \text{triangle with red arcs from top to both bottom vertices and from top to bottom-right}, & T(Y_1, X_2, X_3) &= \text{triangle with red arcs from top to both bottom vertices and from top to bottom-right}, \\
 T(Y_1, X_2, X_4) &= \text{triangle with red arcs from top to both bottom vertices and from top to bottom-right}, & T(Y_2, X_1, X_1) &= \text{triangle with red arcs from top to both bottom vertices and from top to bottom-left}, & T(Y_2, X_1, X_2) &= \left(\text{triangle with red arcs from top to both bottom vertices and from top to bottom-right} \right)^2, \\
 T(Y_2, X_1, X_3) &= \text{triangle with red arcs from top to both bottom vertices and from top to bottom-right}, & T(Y_2, X_2, X_1) &= \text{triangle with red arcs from top to both bottom vertices and from top to bottom-left}, \\
 T(Y_2, X_2, X_2) &= v^{-\frac{1}{2}} \text{triangle with red arcs from top to both bottom vertices and from top to bottom-right} \quad \text{triangle with red arcs from top to both bottom vertices and from top to bottom-left}, & T(Y_2, X_2, X_3) &= v^{\frac{1}{2}} \text{triangle with red arcs from top to both bottom vertices and from top to bottom-right} \quad \text{triangle with red arcs from top to both bottom vertices and from top to bottom-left},
 \end{aligned}$$

$$\begin{aligned}
T(Y_2, X_2, X_4) &= \text{triangle with red and blue edges} , & T(Y_2, X_3, X_1) &= \text{triangle with red and blue edges} , & T(Y_2, X_3, X_2) &= \text{triangle with red and blue edges} , \\
T(Y_2, X_3, X_3) &= \text{triangle with red and blue edges} , & T(Y_2, X_3, X_4) &= \text{triangle with red and blue edges} , & T(Y_3, X_1, X_1) &= \frac{1}{[2]} \text{triangle with red and blue edges} , \\
T(Y_3, X_1, X_2) &= \text{triangle with red and blue edges} , & T(Y_3, X_1, X_3) &= \text{triangle with red and blue edges} , & T(Y_3, X_2, X_1) &= \frac{1}{[2]} \text{triangle with red and blue edges} , \\
T(Y_3, X_2, X_2) &= \text{triangle with red and blue edges} + \frac{1}{[2]} \text{triangle with red and blue edges} , & T(Y_3, X_2, X_3) &= \left(\text{triangle with red and blue edges} \right)^2 , \\
T(Y_3, X_3, X_1) &= \frac{1}{[2]} \text{triangle with red and blue edges} , & T(Y_3, X_3, X_2) &= \text{triangle with red and blue edges} , & T(Y_3, X_4, X_1) &= \text{triangle with red and blue edges} .
\end{aligned}$$

Observe that all the coefficients are in $\mathbb{Z}^+[v^{\pm 1/2}]$, up to the appearance of $[2]^{-1}$ related to Y_3 . We remark that Y_3 appears only when we apply the cutting lemma to a type 2 edges. Hence, we see that $[2]^k G$ is expanded as a polynomial in $\cup_{T \in t(\Delta)} \mathbf{EWeb}_{\text{sp}_4, T}$ with coefficients in $\mathbb{Z}^+[v^{\pm 1/2}]$, where k is as in the statement. Finally, we can further expand the polynomial in $\cup_{T \in t(\Delta)} \mathbf{EWeb}_{\text{sp}_4, T}$ into a polynomial in \mathcal{C}_Δ with positive coefficients in the same way as in the proof of Theorem 3.14. \square

4. QUANTUM CLUSTER ALGEBRAS

In this section, we use a formal quantum parameter q and the coefficient ring $\mathbb{Z}_q = \mathbb{Z}[q^{\pm 1/2}]$.

4.1. Quantum cluster algebra. Recall that for a skew-symmetric form Π on a lattice L , the associated *based quantum torus* is the associative \mathbb{Z}_q -algebra T_Π such that

- T_Π has a free \mathbb{Z}_q -basis M^α parametrized by $\alpha \in L$, and
- the product of these basis elements is given by $M^\alpha \cdot M^\beta = q^{\Pi(\alpha, \beta)/2} M^{\alpha + \beta}$.

Fix a datum (I, I_{uf}, D) , where $I = \{1, \dots, N\}$ is a finite set of indices and $I_{\text{uf}} \subset I$ is a subset; $D = \text{diag}(d_i \mid i \in I)$ is a positive integral diagonal matrix. The indices in I_{uf} are called *unfrozen indices*, while those in the complement $I_f := I \setminus I_{\text{uf}}$ are called *frozen indices*. A *quantum seed* in \mathcal{F} is a quadruple $(B, \Pi, \hat{\Lambda}, M)$, where

- $B = (b_{ij})_{i, j \in I}$ is a matrix with half-integral entries such that DB is skew-symmetric, and $b_{ij} \in \mathbb{Z}$ unless $(i, j) \in I_f \times I_f$;
- $\Pi = (\pi_{ij})_{i, j \in I}$ is a skew-symmetric matrix with integral entries satisfying the *compatibility relation*

$$\sum_{k \in I} b_{ki} \pi_{kj} = \delta_{ij} \hat{d}_j$$

for all $i \in I_{\text{uf}}$ and $j \in I$, where \hat{d}_i is a positive integer for $i \in I_{\text{uf}}$.

- $\mathring{\Lambda} = \bigoplus_{i \in I} \mathbb{Z}f_i$ is a lattice, on which the matrix Π defines a skew-symmetric form by $\Pi(\mathbf{f}_i, \mathbf{f}_j) := \pi_{ij}$;
- $M : \mathring{\Lambda} \rightarrow \mathcal{F} \setminus \{0\}$ is a function such that

$$M(\alpha)M(\beta) = q^{\Pi(\alpha, \beta)/2} M(\alpha + \beta)$$

for $\alpha, \beta \in \mathring{\Lambda}$, and the \mathbb{Z}_q -span of $M(\mathring{\Lambda}) \subset \mathcal{F}$ is the based quantum torus of the form Π whose skew-field of fractions coincides with \mathcal{F} .

We call B the *exchange matrix*, Π the *compatibility matrix*, and M the *toric frame* of the quantum seed. When no confusion can occur, we omit the lattice $\mathring{\Lambda}$ from the notation and call the triple (B, Π, M) a quantum seed. The compatibility relation can be written as

$$\varepsilon \Pi = B^\top \Pi = (\widehat{D}, 0), \quad (4.1)$$

where $\widehat{D} := \text{diag}(\widehat{d}_i \mid i \in I_{\text{uf}})$ and 0 denotes the $I_{\text{uf}} \times I_{\text{f}}$ -zero matrix. By [BZ05, Lemma 4.4], a toric frame M is uniquely determined by the values $A_i := M(\mathbf{f}_i)$, which we call the (*quantum*) *cluster variable*, on the basis vectors \mathbf{f}_i for $i \in I$. Indeed, we have

$$M\left(\sum_{i \in I} x_i \mathbf{f}_i\right) = q^{\frac{1}{2} \sum_{l < k} x_k x_l \pi_{kl}} A_1^{x_1} \dots A_N^{x_N} \quad (4.2)$$

for all $(x_1, \dots, x_N) \in \mathbb{Z}^N$. Note that both sides are invariant under permutations of indices. Elements of the form $M(\alpha)$ for $\alpha \in \mathring{\Lambda}$ are called *cluster monomials*.

Given a quantum seed (B, Π, M) in \mathcal{F} and an unfrozen index $k \in I_{\text{uf}}$, the *quantum seed mutation* produces a new quantum seed $(B', \Pi', M') = \mu_k(B, \Pi, M)$ according to the following rule. Let $E_{k, \varepsilon} = (e_{ij})_{i, j \in I}$ and $F_{k, \varepsilon} = (f_{ij})_{i, j \in I}$ be the matrices defined by

$$e_{ij} := \begin{cases} \delta_{ij} & \text{if } j \neq k, \\ -1 & \text{if } i = k = j, \\ [-\varepsilon b_{ik}]_+ & \text{if } i \neq k = j, \end{cases}$$

and

$$f_{ij} := \begin{cases} \delta_{ij} & \text{if } i \neq k, \\ -1 & \text{if } i = k = j, \\ [\varepsilon b_{kj}]_+ & \text{if } i = k \neq j, \end{cases}$$

respectively for $\varepsilon \in \{+, -\}$. Then we define

$$B' = E_{k, \varepsilon} B F_{k, \varepsilon}, \quad (4.3)$$

$$\Pi' = E_{k, \varepsilon}^\top \Pi E_{k, \varepsilon}, \quad (4.4)$$

$$M'(\mathbf{f}'_i) = \begin{cases} M(\mathbf{f}_i) & \text{if } i \neq k, \\ M(-\mathbf{f}_k + \sum_{j \in I} [b_{jk}]_+ \mathbf{f}_j) + M(-\mathbf{f}_k + \sum_{j \in I} [-b_{jk}]_+ \mathbf{f}_j) & \text{if } i = k. \end{cases} \quad (4.5)$$

Here $(\mathbf{f}_i)_{i \in I}$ and $(\mathbf{f}'_i)_{i \in I}$ denote the basis vectors of the underlying lattices. The relation (4.5) is called the *quantum exchange relation*. It can be verified that (4.3) and (4.4) do

not depend on the sign ϵ [BZ05, Proposition 3.4]. The mutation rule (4.3) is the same one as the well-known matrix mutation formula. In this paper, the quantum exchange relation is often used in the following form:

Lemma 4.1. *The quantum exchange relation (4.5) is equivalent to*

$$A_k A'_k = q^{\frac{1}{2} \sum_{j \in I} [b_{jk}]_+ \pi_{kj}} \left(M \left(\sum_{j \in I} [b_{jk}]_+ \mathbf{f}_j \right) + q^{\frac{1}{2} \widehat{d}_k} M \left(\sum_{j \in I} [-b_{jk}]_+ \mathbf{f}_j \right) \right) \quad (4.6)$$

and $A'_i = A_i$ for $i \neq k$, where $A_j := M(\mathbf{f}_j)$ and $A'_j := M'(\mathbf{f}'_j)$ for $j \in I$.

The verification of the following lemma is also straightforward:

Lemma 4.2. *Let (B, Π, M) be a quantum seed in \mathcal{F} , $k \in I_{\text{uf}}$, and consider the exchange matrix $B' := E_{k, \epsilon} B F_{k, \epsilon}$ and the toric frame M' determined by (4.5). Let $\Pi' = (\pi'_{ij})_{i, j \in I}$ be the skew-symmetric matrix associated with M' , which is uniquely determined by the condition*

$$A'_i A'_j = q^{\pi'_{ij}} A'_j A'_i$$

for $i, j \in I$ with $A'_i := M'(\mathbf{f}'_i)$. Then the pair (B', Π') satisfies the compatibility relation.

Let

$$\mathfrak{S}_I^{\text{cl}} := \{\sigma \in \mathfrak{S}_I \mid \sigma(I_{\text{uf}}) = I_{\text{uf}}, d_{\sigma^{-1}(i)} = d_i \text{ for all } i \in I\}$$

denote the group of permutations that do not mix the unfrozen/frozen indices and that preserve the weights. For $\sigma \in \mathfrak{S}_I^{\text{cl}}$, a new quantum seed $(B', \Pi', M') = \sigma(B, \Pi, M)$ is defined by

$$b'_{ij} = b_{\sigma^{-1}(i), \sigma^{-1}(j)}, \quad \pi'_{ij} = \pi_{\sigma^{-1}(i), \sigma^{-1}(j)}, \quad A'_i = A_{\sigma^{-1}(i)}.$$

An $\mathfrak{S}_I^{\text{cl}}$ -orbit of quantum seeds is called a *quantum unlabeled seed*. Two quantum seeds in \mathcal{F} are said to be *mutation-equivalent* if they are transformed to each other by a finite sequence of seed mutations and permutations. An equivalence class of quantum seeds is called a *mutation class*. The relations among the quantum seeds in a given mutation class \mathfrak{s}_q can be encoded in the (*labeled*) *exchange graphs*:

Definition 4.3. The *labeled exchange graph* is a graph $\mathbb{E}\text{xch}_{\mathfrak{s}}$ with vertices v corresponding to the quantum seeds $\mathfrak{s}_q^{(v)}$ in \mathfrak{s}_q , together with labeled edges of the following two types:

- edges of the form $v \xrightarrow{k} v'$ whenever the quantum seeds $\mathfrak{s}_q^{(v)}$ and $\mathfrak{s}_q^{(v')}$ are related by the mutation μ_k for $k \in I_{\text{uf}}$;
- edges of the form $v \xrightarrow{\sigma} v'$ whenever the quantum seeds $\mathfrak{s}_q^{(v)}$ and $\mathfrak{s}_q^{(v')}$ are related by the transposition $\sigma = (j \ k)$ in $\mathfrak{S}_I^{\text{cl}}$.

The *exchange graph* is a graph $\text{Exch}_{\mathfrak{s}}$ with vertices ω corresponding to the quantum unlabeled seeds $\mathfrak{s}_q^{(\omega)}$ in \mathfrak{s}_q , together with (unlabeled, horizontal) edges corresponding to the mutations. There is a graph projection $\pi_{\mathfrak{s}} : \mathbb{E}\text{xch}_{\mathfrak{s}} \rightarrow \text{Exch}_{\mathfrak{s}}$.

When no confusion can occur, we simply denote a vertex of the labeled exchange graph by $v \in \mathbb{E}xch_s$ instead of $v \in V(\mathbb{E}xch_s)$, and similarly for the exchange graph. We remark that the (labeled) exchange graph depend only on the mutation class of the underlying exchange matrices. The absense of q in the notation will be explained in Remark 4.7.

Remark 4.4 (labelings). For a vertex $\omega \in \mathbb{E}xch_s$, picking up a lift $v \in \pi_s^{-1}(\omega)$ amounts to fixing a labeling of the unlabeled seed $\mathfrak{s}_q^{(\omega)}$. More generally, π_s can be trivialized over any subgraph $\Gamma \subset \mathbb{E}xch_s$ only with square faces (corresponding to the commutativity $\mu_i\mu_j = \mu_j\mu_i$ for $b_{ij} = 0$). Such a graph Γ can be uniquely lifted to a subgraph $\tilde{\Gamma} \subset \mathbb{E}xch_s$ if one fixes a labeling at a single vertex.

To each vertex $v \in \mathbb{E}xch_s$, associated is a based quantum torus

$$T_{(v)} = \text{span}_{\mathbb{Z}_q} M^{(v)}(\mathring{\Lambda}^{(v)}) \subset \mathcal{F}.$$

We also have the unlabeled version $T_{(\omega)} = \text{span}_{\mathbb{Z}_q} M^{(\omega)}(\mathring{\Lambda}^{(\omega)})$ for $\omega \in \mathbb{E}xch_s$, where the basis of $\Lambda^{(\omega)}$ is unordered. The unlabeled collection $\mathbf{A}_{(\omega)} := \{A_i^{(v)}\}_{i \in I}$ with $v \in \pi_s^{-1}(\omega)$ is called a *quantum cluster*. We also have the subcollection $\mathbf{A}_{(\omega)}^f := \{A_i^{(v)}\}_{i \in I_f}$ of frozen variables.

Definition 4.5. The *quantum cluster algebra* associated with a mutation class \mathfrak{s}_q of quantum seeds is the \mathbb{Z}_q -subalgebra $\mathcal{A}_{\mathfrak{s}_q} \subset \mathcal{F}$ generated by the union of the quantum clusters $\mathbf{A}_{(\omega)}$ and the inverses of frozen variables in $\mathbf{A}_{(\omega)}^f$ for $\omega \in \mathbb{E}xch_s$. The *quantum upper cluster algebra* is defined to be

$$\mathcal{U}_{\mathfrak{s}_q} := \bigcap_{\omega \in \mathbb{E}xch_s} T_{(\omega)} \subset \mathcal{F}.$$

For each vertex $\omega \in \mathbb{E}xch_s$, the *upper bound* at ω is defined to be

$$\mathcal{U}_{\mathfrak{s}_q}(\omega) := T_{(\omega)} \cap \bigcap_{\omega'} T_{(\omega')},$$

where $\omega' \in \mathbb{E}xch_s$ runs over the vertices adjacent to ω .

Theorem 4.6 (Quantum upper bound theorem [BZ05, Theorem 5.1]). *For any vertices $\omega, \omega' \in \mathbb{E}xch_s$, we have $\mathcal{U}_{\mathfrak{s}_q}(\omega) = \mathcal{U}_{\mathfrak{s}_q}(\omega')$. In particular, we have*

$$\mathcal{U}_{\mathfrak{s}_q} = \mathcal{U}_{\mathfrak{s}_q}(\omega)$$

for any $\omega \in \mathbb{E}xch_s$.¹

It in particular implies the inclusion $\mathcal{A}_{\mathfrak{s}_q} \subset \mathcal{U}_{\mathfrak{s}_q}$, which is called the *quantum Laurent phenomenon*. Again we remark that the quantum (upper) cluster algebra depends only on the mutation class of the compatibility pairs (B, Π) , up to automorphisms of the ambient skew-field. In other words, the choice of toric frames determines the way of realization of these algebras in some skew-field.

¹We remark here that the coprimality condition required in the classical setting ([BFZ05, Corollary 1.7]) is automatically satisfied in the quantum setting, since the existence of the compatibility matrix forces the exchange matrix to be full-rank.

Remark 4.7 (cluster algebras). Let $\overline{\mathcal{F}}$ be a field isomorphic to the field of rational functions on N variables with rational coefficients. A seed in $\overline{\mathcal{F}}$ is a pair (B, \mathbf{A}) , where B is an exchange matrix as above, and $\mathbf{A} = (A_i)_{i \in I}$ is a tuple of algebraically independent elements of $\overline{\mathcal{F}}$. The mutation of a seed for $k \in I_{\text{uf}}$ is defined by the matrix mutation rule (4.3) and

$$A' = \begin{cases} A_k^{-1} \left(\prod_{j \in I} A_j^{[b_{jk}]_+} + \prod_{j \in I} A_j^{[-b_{jk}]_+} \right) & \text{if } i = k, \\ A_i & \text{if } i \neq k, \end{cases}$$

which is the classical counterpart of (4.5). A mutation class \mathfrak{s} of seeds is similarly defined, and the *cluster algebra* is the subring $\mathcal{A}_{\mathfrak{s}} \subset \overline{\mathcal{F}}$ generated by all the cluster variables in \mathfrak{s} . The *upper cluster algebra* is defined to be the intersection $\mathcal{U}_{\mathfrak{s}} := \bigcap_{\omega \in \text{Exch}_{\mathfrak{s}}} \mathbb{Z}[\mathbf{A}^{(\omega)}] \subset \overline{\mathcal{F}}$ of Laurent polynomial rings.

When a mutation class \mathfrak{s}_q of quantum seeds and a mutation class \mathfrak{s} of seeds contain the same mutation class of exchange matrices, there is a graph isomorphism between the labeled exchange graph $\text{Exch}_{\mathfrak{s}}$ associated with \mathfrak{s}_q and a similar graph parametrizing the seeds in \mathfrak{s} . In particular the quantum cluster variables in \mathfrak{s}_q bijectively corresponds to the cluster variables in \mathfrak{s} . We say that \mathfrak{s}_q (resp. $\mathcal{A}_{\mathfrak{s}_q}$) is a *quantization* of \mathfrak{s} (resp. $\mathcal{A}_{\mathfrak{s}}$).

Bar-involution. For each $\omega \in \text{Exch}_{\mathfrak{s}}$, define a \mathbb{Z} -linear involution $\dagger : T_{(\omega)} \rightarrow T_{(\omega)}$ by

$$(q^{r/2} M^{(\omega)}(\alpha))^{\dagger} := q^{-r/2} M^{(\omega)}(\alpha)$$

for $r \in \mathbb{Z}$ and $\alpha \in \mathring{\Lambda}^{(\omega)}$. Then \dagger preserves the subalgebras $\mathcal{A}_{\mathfrak{s}_q} \subset \mathcal{U}_{\mathfrak{s}_q} \subset T_{(\omega)}$, and the induced involution does not depend on the choice of ω [BZ05, Proposition 6.2]. Following [BZ05], we call this anti-involution $\dagger : \mathcal{U}_{\mathfrak{s}_q} \rightarrow \mathcal{U}_{\mathfrak{s}_q}$ the *bar-involution*. Each quantum cluster variable is invariant under the bar-involution.

Exchange matrices and weighted quivers. It is useful to represent an exchange matrix $B = (b_{ij})_{i,j \in I}$ by a weighted quiver Q . For the correspondence, we use the convention in [IO21]. Let us define the *Fock–Goncharov exchange matrix* $\varepsilon = (\varepsilon_{ij})_{i,j \in I}$ by $\varepsilon_{ij} := b_{ji}$. Then the weighted quiver Q corresponding to B has vertices parametrized by the set I , and each vertex $i \in I$ is assigned the integer weight d_i . The structure matrix $\sigma = (\sigma_{ij})_{i,j \in I}$ of Q , whose (i, j) -entry indicates the number of arrows from i to j minus the number of arrows from j to i , is defined to be

$$\sigma_{ij} := d_i^{-1} \varepsilon_{ij} \gcd(d_i, d_j).$$

In figures, we draw n dashed arrows from i to j if $\sigma_{ij} = n/2$ for $n \in \mathbb{Z}$, where a pair of dashed arrows is replaced with a solid arrow. In this paper, we only deal with the weighted quivers whose vertices have weights 1 or 2. A vertex of weight 1 (resp. 2) is shown by a small circle (resp. a doubled circle).

Example 4.8. For the matrices $B = \begin{pmatrix} 0 & -1 \\ 2 & 0 \end{pmatrix}$ and $D = \text{diag}(2, 1)$, the matrix $DB = \begin{pmatrix} 0 & -2 \\ 2 & 0 \end{pmatrix}$ is skew-symmetric. We have $\varepsilon = B^\top = \begin{pmatrix} 0 & 2 \\ -1 & 0 \end{pmatrix}$ and $\sigma = \begin{pmatrix} 0 & 1 \\ -1 & 0 \end{pmatrix}$. The corresponding weighted quiver is given by

$$\textcircled{1} \longrightarrow \textcircled{2}.$$

The following lemma is useful to compute the mutations in terms of the weighted quivers:

Lemma 4.9 ([HIO21, Lemma 2.3]). *Assume that the weights d_i take only two values: $\{d_i\}_{i \in I} = \{1, d\}$ for some integer $d \geq 2$. Then for $B' = \mu_k B$, the corresponding mutation of the structure matrix $\sigma' = \mu_k \sigma$ is given by*

$$\sigma'_{ij} = \begin{cases} -\sigma_{ij} & i = k \text{ or } j = k, \\ \sigma_{ij} + ([\sigma_{ik}]_+ + [\sigma_{kj}]_+ - [-\sigma_{ik}]_+ - [-\sigma_{kj}]_+) \alpha_{ij}^k & \text{otherwise,} \end{cases}$$

where

$$\alpha_{ij}^k = \begin{cases} d & \text{if } d_i = d_j \neq d_k, \\ 1 & \text{otherwise.} \end{cases}$$

4.2. The cluster algebras related to the moduli space $\mathcal{A}_{Sp_4, \Sigma}$. Let Σ be a marked surface. Although the classical construction presented here works for any marked surface, we assume that Σ is unpunctured for simplicity.

Recall that a decorated triangulation $\Delta = (\Delta, m_\Delta, \mathbf{s}_\Delta)$ consists of an ideal triangulation Δ of Σ , together with a choice of a vertex $m_\Delta(T)$ and a sign $\mathbf{s}_\Delta(T)$ for each triangle $T \in t(\Delta)$. Given a decorated triangulation Δ , we define a weighted quiver Q^Δ as follows. Let $Q_{m,+}$ and $Q_{m,-}$ be the weighted quivers on a triangle shown in the left and right of Figure 4.1, respectively. Here notice that these weighed quivers are not symmetric for the rotations of the triangle, and depend on a chosen special point m . By convention, $Q_{m,\pm}$ are considered up to isotopy on T which preserves each edge set-wisely. In particular, we are allowed to move an interior vertex inside the triangle; move and swap the two vertices on a common edge.

For each triangle $T \in t(\Delta)$, we draw the quiver $Q_{m_\Delta(T), \mathbf{s}_\Delta(T)}$, and glue them via the *amalgamation* procedure [FG06b] to get a weighted quiver Q^Δ drawn on Σ . Here two vertices on a common interior edge with the same weight are identified; opposite half-arrows cancel together, and parallel half-arrows combine to give a solid arrow. Some examples are shown in Figure 4.2. By convention, Q^Δ is considered up to isotopy on Σ which preserves each boundary interval set-wisely.

The vertex set of Q^Δ is denoted by $I(\Delta) = I_{\mathfrak{sp}_4}(\Delta)$. It admits the following decompositions according to the properties of vertices:

- Let $I^{\text{edge}}(\Delta)$ (resp. $I^{\text{tri}}(\Delta)$) denote the subset of vertices on edges (resp. faces of triangles), so that $I(\Delta) = I^{\text{edge}}(\Delta) \sqcup I^{\text{tri}}(\Delta)$.

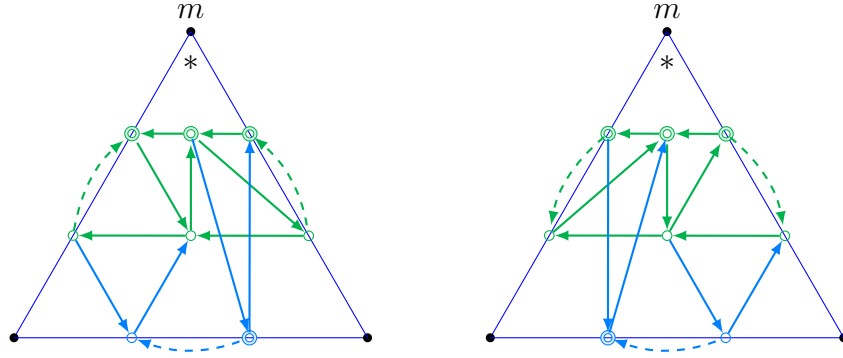


FIGURE 4.1. The quivers $Q_{(\Delta, m, +)}$ (left) and $Q_{(\Delta, m, -)}$ (right) placed on a triangle with a fixed special point m . Here the vertices on the opposite side of m and the arrows incident to them are colored blue for visibility.

- Let $I(\Delta)_f \subset I^{\text{edge}}(\Delta)$ be the subset of the vertices on $\partial\Sigma$, and $I(\Delta)_{\text{uf}}$ its complement, so that $I(\Delta) = I(\Delta)_{\text{uf}} \sqcup I(\Delta)_f$.
- Let $I_s(\Delta) \subset I(\Delta)$ be the subset of vertices of weight $s \in \{1, 2\}$, so that $I(\Delta) = I_1(\Delta) \sqcup I_2(\Delta)$.

Let $i_s(E) \in I(\Delta)$ denote the unique vertex on an edge $E \in e(\Delta)$ with weight $s \in \{1, 2\}$. Similarly, let $i_s(T) \in I(\Delta)$ denote the unique vertex on a triangle $T \in t(\Delta)$ with weight s .

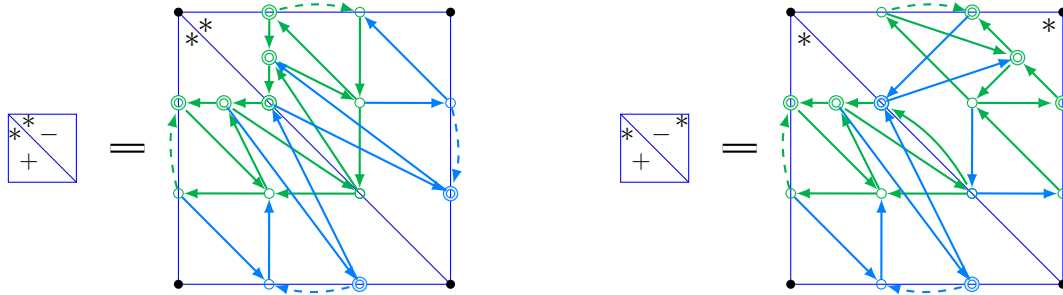


FIGURE 4.2. Two examples of weighted quivers associated with decorated triangulations of a quadrilateral. Here the pair of dashed arrows along the diagonal edge is canceled in the first example, while it is combined to a solid arrow in the second example.

Theorem 4.10 (cf. Goncharov–Shen [GS19, Section 8.5]). *For any two decorated triangulations Δ, Δ' of Σ , the two weighted quivers $Q^\Delta, Q^{\Delta'}$ are mutation-equivalent.*

Proof. Here we give an explicit mutation equivalence. Let us first consider the case $\Sigma = T$. In this case, we have six decorated triangulations. The associated weighted quivers are related as shown in Figure 4.3. Thus the assertion for the triangle case is proved. We remark here that $\mu_1\mu_2$ and $\mu_2\mu_1$ amount to the rotations of the distinguished vertex, and $\mu_1\mu_2\mu_1 = \mu_2\mu_1\mu_2$ amounts to the change of sign.

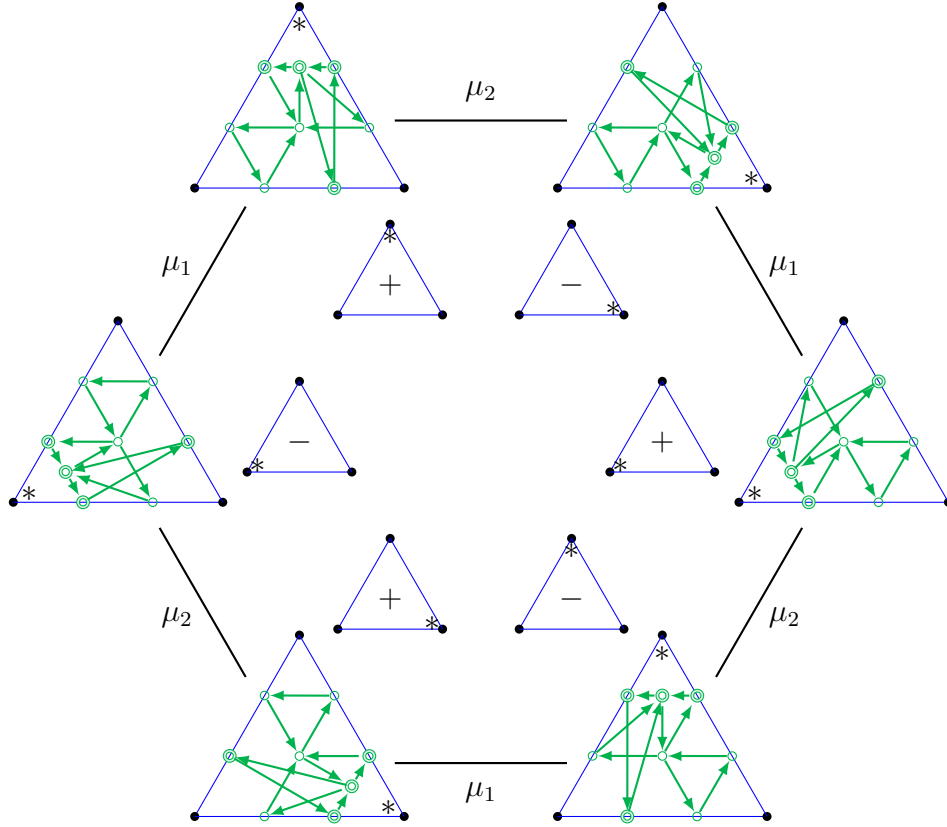


FIGURE 4.3. The exchange graph $\text{Exch}_{\mathfrak{s}(\mathfrak{sp}_4, T)}$ for a triangle T . Here μ_d denotes the mutation at the unique unfrozen vertex with weight $d \in \{1, 2\}$.

In the general case, a consequence of the previous paragraph is that the weighted quivers Q^Δ and $Q^{\Delta'}$ are mutation-equivalent if the underlying triangulations of Δ and Δ' are the same. It remains to consider the flips of ideal triangulations. Again by the previous paragraph, we can choose the decorations as shown in the left-most and right-most pictures in Figure 4.4. Then it is easily verified that the flip can be realized by $2 + 4 + 2$ mutations as shown there. Since any two ideal triangulations are transformed into each other by a finite sequence of flips, the assertion is proved. \square

For the construction of a seed $(Q^\Delta, \mathbf{A}^\Delta)$ in the field $\mathcal{K}(\mathcal{A}_{S_{\mathfrak{sp}_4, \Sigma}})$ of rational functions on the moduli space $\mathcal{A}_{S_{\mathfrak{sp}_4, \Sigma}}$, see [GS19] or Remark 4.12 below.

By Theorem 4.10 (and Remark 4.12), the mutation class $\mathfrak{s}(\mathfrak{sp}_4, \Sigma)$ of the weighted quivers Q^Δ (or the seeds $(Q^\Delta, \mathbf{A}^\Delta)$) defines a canonical cluster algebra $\mathcal{A}_{\mathfrak{s}(\mathfrak{sp}_4, \Sigma)}$ (inside the field $\mathcal{K}(\mathcal{A}_{S_{\mathfrak{sp}_4, \Sigma}})$). We will identify a decorated triangulation Δ with the corresponding vertex of the exchange graph $\text{Exch}_{\mathfrak{s}(\mathfrak{sp}_4, \Sigma)}$. Let us simplify the notation as

$$\mathcal{A}_{\mathfrak{sp}_4, \Sigma} := \mathcal{A}_{\mathfrak{s}(\mathfrak{sp}_4, \Sigma)}, \quad \mathcal{U}_{\mathfrak{sp}_4, \Sigma} := \mathcal{U}_{\mathfrak{s}(\mathfrak{sp}_4, \Sigma)}, \quad \text{and} \quad \text{Exch}_{\mathfrak{sp}_4, \Sigma} := \text{Exch}_{\mathfrak{s}(\mathfrak{sp}_4, \Sigma)}$$

A decorated cell decomposition (with deficiency 1) consists of the following data:

- An ideal cell decomposition $(\Delta; E)$ of deficiency 1 with the unique quadrilateral Q_E having E as a diagonal.

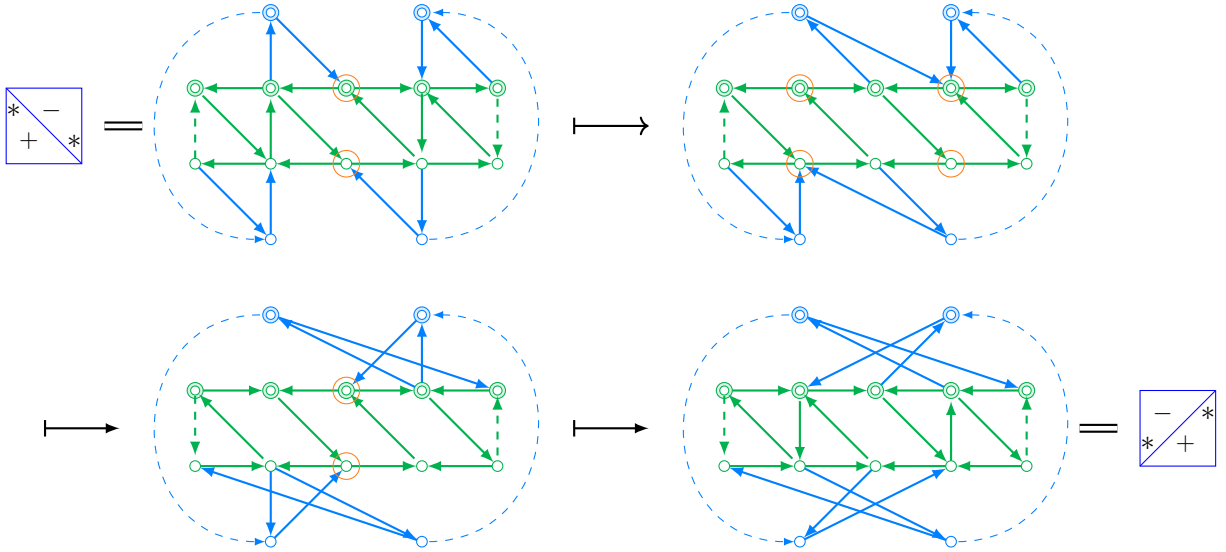


FIGURE 4.4. Mutation sequences that realize a flip of triangulation. Here we forget the boundary framing of the weighted quivers so that most parts are drawn planar. The vertices at which we perform mutations are shown in orange circles. Notice that the mutations at two vertices without arrows between them commute with each other.

- A decoration $(m(T), \mathbf{s}(T))$ for each triangle of $(\Delta; E)$.
- A choice of a weighed quiver among those appearing in the sequence Figure 4.4.

In particular, a decorated triangulation is a decorated cell decomposition.

Definition 4.11. Define the *surface subgraph* to be the subgraph $\text{Exch}'_{\text{sp}_4, \Sigma} \subset \text{Exch}_{\text{sp}_4, \Sigma}$ such that

- the vertices are the seeds corresponding to the decorated cell decompositions;
- the edges are mutations appearing in Figure 4.3 or Figure 4.4.

The exchange matrix $B^{(\omega)}$ for any vertex $\omega \in \text{Exch}'_{\text{sp}_4, \Sigma}$ is determined by the corresponding weighted quiver $Q^{(\omega)}$.

By the proof of Theorem 4.10, the surface subgraph is a connected graph on which the associated seeds are explicitly understood.

Here is a remark on the labeling. If we fix a labeling $\ell : I(\Delta) \xrightarrow{\sim} \{1, \dots, N\}$, then by Remark 4.4, the part of the exchange graph shown in Figure 4.3 or the part corresponding to Figure 4.4 can be lifted to a subgraph of $\mathbb{E}\text{xch}_{\text{sp}_4, \Sigma}$. We call the pair (Δ, ℓ) a *labeled decorated triangulation*. In other words, the index set $I(\Delta)$ can be commonly used for the seeds assigned to these parts when we locally discuss rotations in a triangle or a single flip in a quadrilateral.

Remark 4.12. Here are remarks on the geometry of the moduli space $\mathcal{A}_{\text{Sp}_4, \Sigma}$ of decorated twisted Sp_4 -local systems on Σ [FG06a, GS19] behind the constructions above. Let $G := \text{Sp}_4$ and $\mathfrak{g} := \mathfrak{sp}_4$.

- (1) For $\Sigma = T$, the moduli space $\mathcal{A}_{G,T}$ can be identified with the configuration space $\text{Conf}_3\mathcal{A}_G$ of three decorated flags, where $\mathcal{A}_G := G/U^+$. Such an identification

$$f_m : \mathcal{A}_{G,T} \xrightarrow{\sim} \text{Conf}_3\mathcal{A}_G$$

is determined by a choice of distinguished special point m . Moreover, a reduced word \mathbf{s} of the longest element $w_0 \in W(\mathfrak{g})$ determines a birational chart on $\text{Conf}_3\mathcal{A}_G$. We have only two reduced words $\mathbf{s}_+ := (1, 2, 1, 2)$, $\mathbf{s}_- := (2, 1, 2, 1)$ in the \mathfrak{sp}_4 -case. Let \mathbf{A}_+ , \mathbf{A}_- denote the corresponding charts (tuples of regular functions). Given a datum (m, ϵ) , we get a birational chart

$$\mathbf{A}_{m,\epsilon} := f_m^* \mathbf{A}_\epsilon : \mathcal{A}_{G,T} \rightarrow (\mathbb{G}_m)^N,$$

which gives rise to a seed $(Q_{m,\epsilon}, \mathbf{A}_{m,\epsilon})$ in the field $\mathcal{K}(\mathcal{A}_{G,T})$ of rational functions.

- (2) Given a decorated triangulation Δ of Σ , these coordinates collectively give a birational chart \mathbf{A}^Δ on $\mathcal{A}_{G,\Sigma}$ via restrictions to the triangle moduli spaces, which gives rise to a seed $(Q^\Delta, \mathbf{A}^\Delta)$ in the field $\mathcal{K}(\mathcal{A}_{G,\Sigma})$. It is known that these seeds are mutation-equivalent to each other [GS19, Section 8.5], where the equivalence corresponding to a flip is described by transformations of *double reduced words*. The mutation sequences in Figure 4.4 corresponds to specific transformations between the double reduced words

$$(1, 2, 1, 2, \bar{1}, \bar{2}, \bar{1}, \bar{2}) \quad \text{and} \quad (\bar{1}, \bar{2}, \bar{1}, \bar{2}, 1, 2, 1, 2)$$

of (w_0, w_0) .

- (3) We have $\mathcal{A}_{\mathfrak{sp}_4,\Sigma} = \mathcal{U}_{\mathfrak{sp}_4,\Sigma} = \mathcal{O}(\mathcal{A}_{Sp_4,\Sigma}^\times)$ if Σ has at least two special points [IOS22], where $\mathcal{A}_{Sp_4,\Sigma}^\times \subset \mathcal{A}_{Sp_4,\Sigma}$ is the open subspace obtained by imposing the genericity on consecutive pairs of decorated flags.

Ensemble grading of cluster algebras. Recall from [FG09, Section 2.3] that there is a natural $H_{\mathcal{A}}$ -action on the cluster variety \mathcal{A}_s . Here $H_{\mathcal{A}}$ is a split algebraic torus. Let $X^*(H_{\mathcal{A}})$ be its character lattice. It induces $X^*(H_{\mathcal{A}})$ -gradings of the (upper) cluster algebras $\mathcal{A}_s \subset \mathcal{U}_s = \mathcal{O}(\mathcal{A}_s)$, which can be lifted to gradings of any quantization $\mathcal{A}_{s_q} \subset \mathcal{U}_{s_q}$ such that each (quantum) cluster variable is homogeneous. We call these gradings the *ensemble gradings*, and denote by $\text{deg}_{\text{cl}}(A_i^{(\omega)}) \in X^*(H_{\mathcal{A}})$ the degree of a (quantum) cluster variable $A_i^{(\omega)}$. See also [IY21, Lemma-Definition 4.7].

In the case $\mathfrak{s} = \mathfrak{s}(\mathfrak{g}, \Sigma)$ related to the moduli space $\mathcal{A}_{G,\Sigma}$, the torus $H_{\mathcal{A}}$ covers the product $H^{\mathbb{M}}$ of Cartan subgroups $H \subset G$, one for each special point. Thus the grading lattice $X^*(H_{\mathcal{A}})$ contains the direct sum $\bigoplus_{\mathbb{M}} \mathbb{P}$ of weight lattices. For the triangle case $\Sigma = T$, we have the Peter–Weyl isomorphism

$$\mathcal{O}(\mathcal{A}_{G,T}) = \mathcal{O}(\text{Conf}_3\mathcal{A}_G) \cong \bigoplus_{\lambda,\mu,\nu} (V(\lambda) \otimes V(\mu) \otimes V(\nu))^G,$$

where $\lambda, \mu, \nu \in \mathbb{P}_+$ are dominant integral weights. The ensemble degree is nothing but the triple $(\lambda, \mu, \nu) \in \mathbb{P}_+^{\oplus 3}$ in this case. The ensemble degrees of the cluster variables arising from Goncharov–Shen’s construction can be computed from [GS19, Section 6.3], which we show in Figure 4.5. In particular, the ensemble degree of each cluster variable associated

with any decorated triangulation belongs to the submonoid $\bigoplus_{\mathbb{M}} \mathbb{P}_+$ of dominant integral weights.

Actually, the ensemble grading is one of our basic tools to find appropriate web clusters in the skein algebra. See Lemma 5.1.

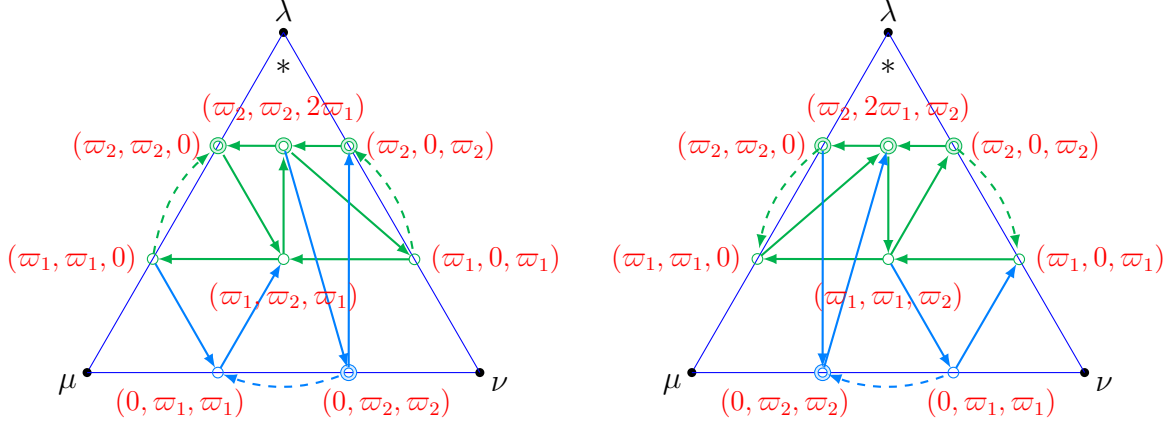


FIGURE 4.5. The ensemble degrees of cluster variables on a triangle.

5. QUANTUM CLUSTER ALGEBRAS AND SKEIN ALGEBRAS

5.1. Realization of the quantum cluster algebra inside the fraction of the skein algebra. In this section, we construct a mutation class $\mathfrak{s}_q(\mathfrak{sp}_4, \Sigma)$ of quantum seeds in the skew-field $\text{Frac} \mathcal{S}_{\mathfrak{sp}_4, \Sigma}^q$ of fractions of the skein algebra $\mathcal{S}_{\mathfrak{sp}_4, \Sigma}^q$, which defines a quantum cluster algebra $\mathcal{A}_{\mathfrak{sp}_4, \Sigma}^q \subset \text{Frac} \mathcal{S}_{\mathfrak{sp}_4, \Sigma}^q$. In what follows, we identify the quantum parameters as $q = v$.

For any vertex $\omega \in \text{Exch}'_{\mathfrak{sp}_4, \Sigma}$ of the surface subgraph, we are going to define a quantum seed $(B^{(\omega)}, \Pi^{(\omega)}, M^{(\omega)})$ in $\text{Frac} \mathcal{S}_{\mathfrak{sp}_4, \Sigma}^q$. The exchange matrix $B^{(\omega)}$ is the one already defined in Section 4.2. In order to define the remaining data, we consider a web cluster $C_{(\omega)} = \{e_i^{(\omega)} \mid i \in I(\omega)\}$ defined as follows (recall Definition 2.16). First consider the case where $\omega = \Delta$ is a decorated triangulation.

- For each edge E and $s \in \{1, 2\}$, let $e_{i_s(E)}^\Delta$ be the elementary web of weight s given by the type s arc along E .
- For each triangle T and $s \in \{1, 2\}$, let $e_{i_s(T)}^\Delta$ be the elementary web of weight s given in Figure 5.1, depending on the decoration data (m_T, \mathfrak{s}_T) on T .

See also Figure 5.4. By Corollary 2.26, these elementary webs indeed form a web cluster in $\mathcal{S}_{\mathfrak{sp}_4, \Sigma}^q$. If ω is a decorated cell decomposition over $(\Delta; E)$, then $C_{(\omega)} = \{e_i^{(\omega)} \mid i \in I(\omega)\}$ is defined as follows.

- The assignment of an elementary web $e_i^{(\omega)}$ for a vertex $i \in I(\omega)$ is the same as before unless i is contained in the interior of the unique quadrilateral Q_E .
- Recalling that the weighted quiver on Q_E is one of those appearing in the mutation sequence in Figure 4.4, let us assign the elementary webs $e_i^{(\omega)}$ to the six interior

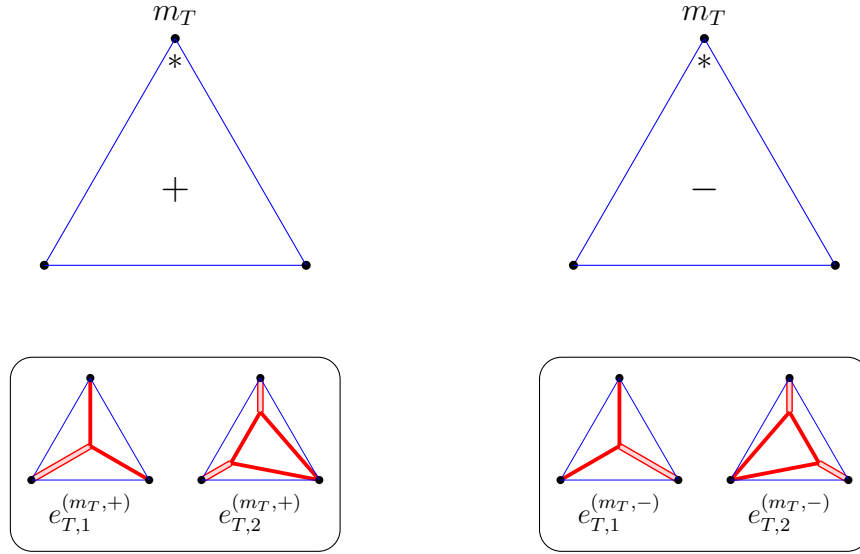


FIGURE 5.1. Assignment of a web cluster to a decorated triangle (T, m_T, \mathbf{s}_T) .

vertices as shown in Figure 5.5. Here they are auxiliary labeled so that one of weight $s = 1$ (resp. $s = 2$) is labeled by an odd (resp. even) number.

Then it is not hard to verify that they form a web cluster. Notice that in each of these cases, the weight of the elementary web $e_i^{(\omega)}$ in the sense of Definition 2.16 coincides with the weight s of the corresponding vertex of the weighted quiver.

Define the compatibility matrix $\Pi^{(\omega)} = (\pi_{ij}^{(\omega)})_{i,j \in I(\omega)}$ by

$$\pi_{ij}^{(\omega)} := \Pi(e_i^{(\omega)}, e_j^{(\omega)}).$$

Here recall Definition 2.23. Then $\Pi^{(\omega)}$ is evidently skew-symmetric.

We first verify that their degrees are correct. We identify the monoid \mathbf{P}_+ of dominant integral weights with $\mathbb{N} \times \mathbb{N}$ via

$$\mathbf{P}_+ \xrightarrow{\sim} \mathbb{N} \times \mathbb{N}, \quad c_1\varpi_1 + c_2\varpi_2 \mapsto (c_1, c_2). \quad (5.1)$$

Lemma 5.1. *For any decorated triangulation Δ and $i \in I(\Delta)$, the endpoint degree of the elementary web e_i^Δ coincides with the ensemble degree of the corresponding cluster variable A_i^Δ via (5.1). Namely, we have*

$$\deg_{\text{cl}}(A_i^\Delta) = \deg(e_i^\Delta).$$

Proof. It is verified by comparing Figure 4.5 with Figure 5.1. \square

Then the coincidence of the two degrees for the (web) clusters associated to general $\omega \in \text{Exch}'_{\mathfrak{sp}_4, \Sigma}$ will follow from the mutation-equivalence shown in Theorem 5.4 below.

Proposition 5.2. *For any decorated triangulation $\Delta = (\Delta, m_\Delta, \mathbf{s}_\Delta)$ with $\mathbf{s}_\Delta(T) = +$ for all $T \in t(\Delta)$, the pair (B^Δ, Π^Δ) satisfies the compatibility relation*

$$(B^\Delta)^\top \Pi^\Delta = (2D, 0).$$

Here $D = \text{diag}(d_i \mid i \in I(\Delta))$ is the diagonal matrix encoding the weights of vertices.

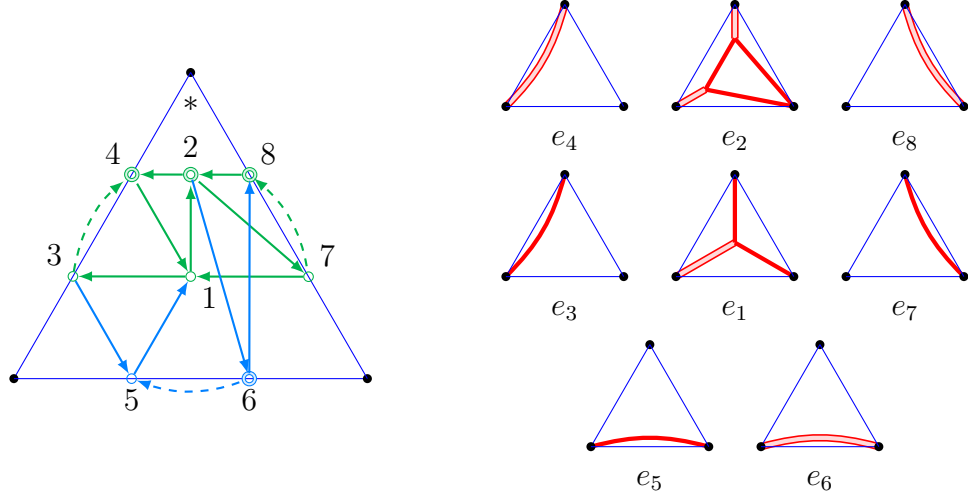


FIGURE 5.2. Labeling of quiver vertices and the corresponding elementary webs on a triangle.

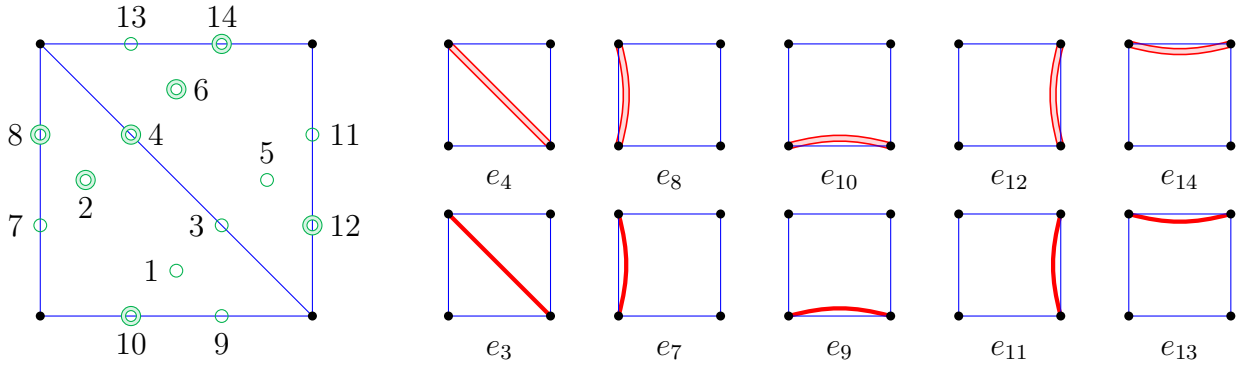


FIGURE 5.3. Labeling of quiver vertices and the corresponding elementary webs.

Proof. During the proof, we fix a decorated triangulation Δ and omit the superscript Δ . Let $\varepsilon := B^T$ denote the Fock–Goncharov exchange matrix associated with Δ . For $i \in I(\Delta)_{\text{uf}}$ and $j \in I(\Delta)$, we are going to compute $(\varepsilon\Pi)_{ij} = \sum_{k \in I(\Delta)} \varepsilon_{ik}\pi_{kj}$. For a fixed $i \in I(\Delta)_{\text{uf}}$, let us consider the Weyl-ordered Laurent monomial

$$X_i := \left[\prod_{k \in I(\Delta)} e_k^{\varepsilon_{ik}} \right].$$

Then we have

$$(\varepsilon\Pi)_{ij} = \sum_{k \in I(\Delta)} \varepsilon_{ik}\pi_{kj} = \sum_{k \in I(\Delta)} \varepsilon_{ik}\Pi(e_k, e_j) = \Pi(X_i, e_j).$$

From the very definition, we see that the ensemble degree of X_i is 0. Then by Lemma 5.1, its endpoint degree is also 0. On the other hand, observe that

- X_i only involves the elementary webs on the triangle T if $i = i_s(T) \in I^{\text{tri}}(\Delta)$, and
- X_i only involves the elementary webs on the quadrilateral Q_E with diagonal E if $i = i_s(E) \in I^{\text{edge}}(\Delta)$.

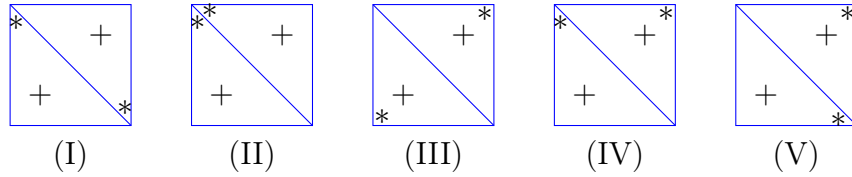
From these facts, we immediately get $(\varepsilon\Pi)_{ij} = \Pi(X_i, e_j) = 0$ for the vertices j not lying in the interior of T if $i = i_s(T)$, and for j not lying in the interior of Q_E if $i = i_s(E)$. Thus the problem is reduced to the triangle and quadrilateral cases.

Triangle case: Let us label the vertices of the weighted quiver and the corresponding elementary webs as shown in Figure 5.2. Then we have

$$\begin{aligned} \pi_{21} &= 1, \\ \pi_{13} &= \pi_{15} = \pi_{17} = \pi_{18} = 0, \quad \pi_{14} = 1, \quad \pi_{16} = -1, \\ \pi_{23} &= \pi_{24} = \pi_{26} = \pi_{28} = 0, \quad \pi_{25} = 1, \quad \pi_{27} = -1, \\ X_1 &= \begin{bmatrix} e_2 e_3 \\ e_4 e_5 e_7 \end{bmatrix}, \quad X_2 = \begin{bmatrix} e_4 e_6 e_7^2 \\ e_1^2 e_8 \end{bmatrix}. \end{aligned}$$

Then one can easily verify that $\Pi(X_1, e_2) = \Pi(X_2, e_1) = 0$, $\Pi(X_1, e_1) = 2$ and $\Pi(X_2, e_2) = 4$. Thus we have $(\varepsilon\Pi)_{ij} = 2d_i \delta_{ij}$ for $i = i_s(T)$.

Quadrilateral case: Up to symmetry, we need to consider the following five cases:



We use the common labeling as shown in Figure 5.3. The structure of the quiver depends on the cases (I)–(V), as well as the elementary webs e_1, e_2, e_5, e_6 . In particular, the Laurent monomials X_3, X_4 depend on the cases. They are listed as follows:

$$\begin{aligned} \text{(I): } e_1 &= \begin{array}{c} \bullet \\ \diagdown \quad \diagup \\ \bullet \end{array}, \quad e_2 = \begin{array}{c} \bullet \\ \diagup \quad \diagdown \\ \bullet \end{array}, \quad e_5 = \begin{array}{c} \bullet \\ \diagdown \quad \diagup \\ \bullet \end{array}, \quad e_6 = \begin{array}{c} \bullet \\ \diagup \quad \diagdown \\ \bullet \end{array}, \\ X_3 &= \begin{bmatrix} e_1 e_4 e_5 \\ e_2 e_6 \end{bmatrix}, \quad X_4 = \begin{bmatrix} e_2 e_6 \\ e_3^2 e_{10} e_{14} \end{bmatrix}. \\ \text{(II): } e_1 &= \begin{array}{c} \bullet \\ \diagdown \quad \diagup \\ \bullet \end{array}, \quad e_2 = \begin{array}{c} \bullet \\ \diagup \quad \diagdown \\ \bullet \end{array}, \quad e_5 = \begin{array}{c} \bullet \\ \diagdown \quad \diagup \\ \bullet \end{array}, \quad e_6 = \begin{array}{c} \bullet \\ \diagup \quad \diagdown \\ \bullet \end{array}, \\ X_3 &= \begin{bmatrix} e_1 e_4 e_{11} \\ e_2 e_5 \end{bmatrix}, \quad X_4 = \begin{bmatrix} e_2 e_5^2 \\ e_3^2 e_6 e_{10} \end{bmatrix}. \\ \text{(III): } e_1 &= \begin{array}{c} \bullet \\ \diagdown \quad \diagup \\ \bullet \end{array}, \quad e_2 = \begin{array}{c} \bullet \\ \diagup \quad \diagdown \\ \bullet \end{array}, \quad e_5 = \begin{array}{c} \bullet \\ \diagdown \quad \diagup \\ \bullet \end{array}, \quad e_6 = \begin{array}{c} \bullet \\ \diagup \quad \diagdown \\ \bullet \end{array}, \\ X_3 &= \begin{bmatrix} e_1 e_5 \\ e_4 e_9 e_{13} \end{bmatrix}, \quad X_4 = \begin{bmatrix} e_3^2 e_8 e_{12} \\ e_2 e_6 \end{bmatrix}. \end{aligned}$$

$$\begin{aligned}
\text{(IV): } e_1 &= \begin{array}{c} \bullet \\ \diagup \quad \diagdown \\ \bullet \end{array}, & e_2 &= \begin{array}{c} \bullet \\ \diagdown \quad \diagup \\ \bullet \end{array}, & e_5 &= \begin{array}{c} \bullet \\ \diagup \quad \diagdown \\ \bullet \end{array}, & e_6 &= \begin{array}{c} \bullet \\ \diagdown \quad \diagup \\ \bullet \end{array}, \\
X_3 &= \begin{bmatrix} e_5 e_7 \\ e_1 e_{13} \end{bmatrix}, & X_4 &= \begin{bmatrix} e_1^2 e_{12} \\ e_2 e_6 \end{bmatrix}. \\
\text{(V): } e_1 &= \begin{array}{c} \bullet \\ \diagup \quad \diagdown \\ \bullet \end{array}, & e_2 &= \begin{array}{c} \bullet \\ \diagdown \quad \diagup \\ \bullet \end{array}, & e_5 &= \begin{array}{c} \bullet \\ \diagup \quad \diagdown \\ \bullet \end{array}, & e_6 &= \begin{array}{c} \bullet \\ \diagdown \quad \diagup \\ \bullet \end{array}, \\
X_3 &= \begin{bmatrix} e_1 e_5 \\ e_2 e_{13} \end{bmatrix}, & X_4 &= \begin{bmatrix} e_2 e_{12} \\ e_6 e_{10} \end{bmatrix}.
\end{aligned}$$

We have $\pi_{21} = \pi_{65} = 1$ in each case. The other q -commutation relations among the variables appearing above can be easily computed from the clasped skein relations (Definition 2.3). For instance, $\pi_{34} = 0$, $\pi_{39} = 1$, $\pi_{4,10} = 2$. Then it is not hard to verify that $\Pi(X_i, e_j) = 2d_i \delta_{ij}$ holds for $i = 3, 4$ and $j = 1, 2, 3, 4, 5, 6$ in each case. \square

The check of the compatibility relation for a general $\omega \in \text{Exch}'_{\text{sp}_4, \Sigma}$ is postponed until the proof of Theorem 5.4 below. For any vertex $\omega \in \text{Exch}'_{\text{sp}_4, \Sigma}$, define a toric frame

$$M^{(\omega)} : \mathring{\Lambda}^{(\omega)} \rightarrow \text{Frac} \mathcal{S}_{\text{sp}_4, \Sigma}^q$$

by the formula

$$M^{(\omega)} \left(\sum_{i \in I} x_i \mathbf{f}_i^{(\omega)} \right) := \left[\prod_{i \in I} (e_i^{(\omega)})^{x_i} \right],$$

where we use the Weyl ordering (Definition 2.4). Observe that this is the same extension rule as (4.2). As a consequence, we get:

Lemma 5.3. *For any vertex $\omega \in \text{Exch}'_{\text{sp}_4, \Sigma}$, the pair $(\Pi^{(\omega)}, M^{(\omega)})$ satisfies*

$$M^{(\omega)}(\alpha) M^{(\omega)}(\beta) = q^{\Pi^{(\omega)}(\alpha, \beta)/2} M^{(\omega)}(\alpha + \beta)$$

for $\alpha, \beta \in \mathring{\Lambda}^{(\omega)}$.

Theorem 5.4. *For any vertex $\omega \in \text{Exch}'_{\text{sp}_4, \Sigma}$, the triple $(B^{(\omega)}, \Pi^{(\omega)}, M^{(\omega)})$ is a quantum seed in $\text{Frac} \mathcal{S}_{\text{sp}_4, \Sigma}^q$. These quantum seeds are mutation-equivalent to each other.*

Proof. By Proposition 5.2 and Lemma 5.3, the triple $(B^\Delta, \Pi^\Delta, M^\Delta)$ associated with a decorated triangulation $\omega = \Delta$ is a quantum seed. Here the condition $\text{Frac} T_\Delta = \text{Frac} \mathcal{S}_{\text{sp}_4, \Sigma}^q$ follows from Corollary 2.29. We have also seen that the exchange matrices $B^{(\omega)}$ are related to each other by matrix mutations.

We are going to first show that the toric frames $M^{(\omega)}$ are related to each other by the quantum exchange relations (4.5). Since the surface subgraph is connected, we only need to consider the mutation sequences lying in the exchange graph $\text{Exch}_{\text{s}(\text{sp}_4, T)}$ for a triangle T and those giving rise to a flip of triangulation. See Figures 5.4 and 5.5, respectively. Therefore the computation reduces to the triangle and quadrilateral cases:

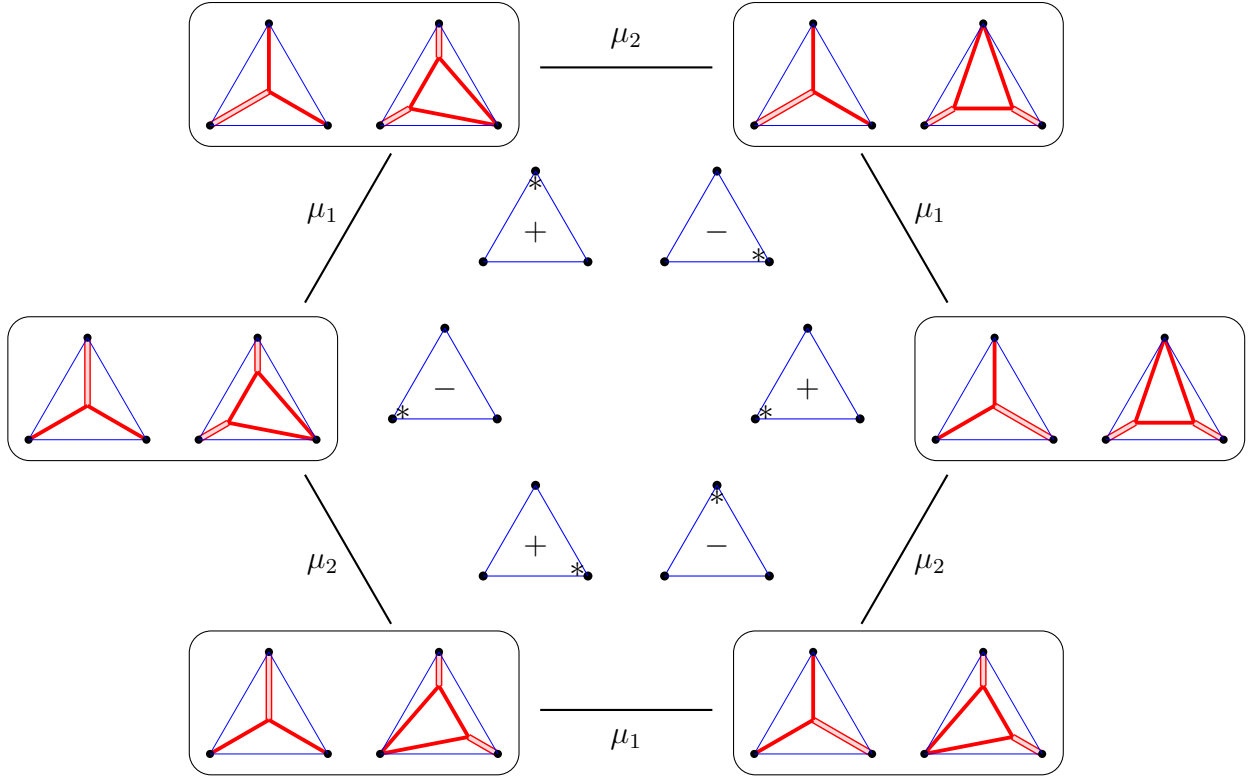


FIGURE 5.4. The six web clusters for a triangle T . Here μ_d denotes the mutation at the unique unfrozen vertex with weight $s \in \{1, 2\}$. The frozen variables (boundary webs) are omitted. Compare with Figure 4.3.

Triangle case: Let us consider the web cluster and the quiver shown at the top left in Figures 4.3 and 5.4, respectively, and the mutations μ_1, μ_2 from there. We also use the labeling in Figure 5.2. From the quantum exchange relation (4.6), we expect the relations

$$e_1 e'_1 = q^{-1/2}([e_2 e_3] + q[e_4 e_5 e_7]),$$

$$e_2 e'_2 = q^{-1}([e_4 e_6 e_7^2] + q^2[e_1^2 e_8])$$

to hold inside the skein algebra $\mathcal{S}_{\mathfrak{sp}_4, \Sigma}^q$. Indeed, the first (resp. second) one is exactly the skein relation (3.10) being rotated by 120° (resp. (3.11) with mirror reflection). By symmetry, it implies that all of the six quantum clusters on T are mutation-equivalent to each other.

Quadrilateral case (a flip): Let us use the labeling in Figure 5.3. Then the mutation sequence under consideration is written as $(\mu_3 \mu_4)(\mu_1 \mu_2 \mu_5 \mu_6)(\mu_3 \mu_4)$. Here each of the parenthesized subsequence does not depend on the order of mutations. In the first parenthesized step $\mu_3 \mu_4$, we expect:

$$e_3 e'_3 = q^0([e_1 e_5] + q[e_2 e_{11}]),$$

$$e_4 e'_4 = q^0([e_2 e_6] + q^2[e_5^2 e_{10}])$$

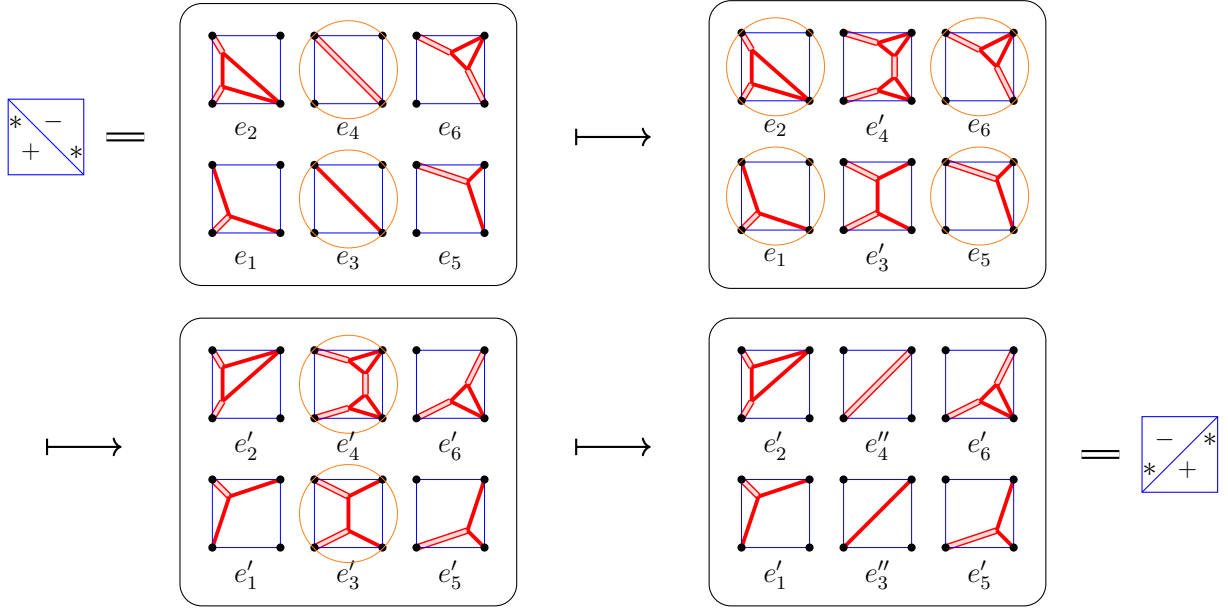


FIGURE 5.5. The web clusters along a flip. Compare with Figure 5.5. Here in each (web) cluster, the six elementary webs are assigned to the vertices of the weighted quiver at the corresponding position.

inside the skein algebra $\mathcal{S}_{\text{sp}_4, \Sigma}^q$. In the second parenthesized step $\mu_1\mu_2\mu_5\mu_6$,

$$\begin{aligned} e_1e'_1 &= q^0([e'_3e_7] + q^1[e_8e_9e_{10}]), \\ e_2e'_2 &= q^0([e'_4e_8] + q^2(e'_3)^2), \\ e_5e'_5 &= q^0([e'_3e_{13}] + qe'_4), \\ e_6e'_6 &= q^0([e'_4e_{14}] + q^2[e_{10}e_{12}e_{13}^2]). \end{aligned}$$

Here we used $e_1e'_3 = [e_1e'_3]$, $e_2e'_4 = [e_2e'_4]$, $e_5e'_3 = [e_5e'_3]$, $e_6e'_4 = [e_6e'_4]$ to obtain q^0 . It is not hard to verify that these relations are indeed satisfied by the elementary webs shown in Figure 5.5. The check for the third step $\mu_3\mu_4$ follows from the first step by turning the topside down.

Thus the toric frames $M^{(\omega)}$ are related to each other by the quantum exchange relations. Then it follows from Lemmas 4.2 and 5.3 that the pair $(B^{(\omega)}, \Pi^{(\omega)})$ satisfies the compatibility relation for all $\omega \in \text{Exch}'_{\text{sp}_4, \Sigma}$. The assertion is proved. \square

It follows from the above theorem that there exists a canonical mutation class $\mathfrak{s}_q(\text{sp}_4, \Sigma)$ containing the quantum seeds $(B^{(\omega)}, \Pi^{(\omega)}, M^{(\omega)})$ associated with the vertices $\omega \in \text{Exch}'_{\text{sp}_4, \Sigma}$, and we get the following algebras over \mathbb{Z}_q :

$$\mathcal{A}_{\text{sp}_4, \Sigma}^q \subset \mathcal{U}_{\text{sp}_4, \Sigma}^q \subset \text{Frac} \mathcal{S}_{\text{sp}_4, \Sigma}^q.$$

Here we write $\mathcal{A}_{\text{sp}_4, \Sigma}^q := \mathcal{A}_{\mathfrak{s}_q(\text{sp}_4, \Sigma)}$ and $\mathcal{U}_{\text{sp}_4, \Sigma}^q := \mathcal{U}_{\mathfrak{s}_q(\text{sp}_4, \Sigma)}$ by simplifying the notation. By construction, we already know that the cluster variables associated with the vertices $\omega \in \text{Exch}'_{\text{sp}_4, \Sigma}$ in the surface subgraph are realized in $\mathcal{S}_{\text{sp}_4, \Sigma}^{\mathbb{Z}_q}[\partial^{-1}]$.

5.2. **Inclusion $\mathcal{S}_{\mathfrak{sp}_4, \Sigma}^{\mathbb{Z}_q}[\partial^{-1}] \subseteq \mathcal{A}_{\mathfrak{sp}_4, \Sigma}^q$ via the sticking trick.**

Proposition 5.5. *When $\Sigma = T$ is a triangle, we have*

$$\mathcal{S}_{\mathfrak{sp}_4, T}^{\mathbb{Z}_q}[\partial^{-1}] = \mathcal{A}_{\mathfrak{sp}_4, T}^q = \mathcal{U}_{\mathfrak{sp}_4, T}^q.$$

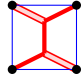
Proof. In this case, the six elementary webs in $\mathcal{S}_{\mathfrak{sp}_4, T}^q$ listed in Theorem 2.25 exactly correspond to the six quantum cluster variables in $\mathcal{A}_{\mathfrak{sp}_4, T}^q$. Moreover, observe that all the six elementary webs are simple Wilson lines. Hence

$$\mathcal{A}_{\mathfrak{sp}_4, T}^q = \langle \text{EWeb}_{\mathfrak{sp}_4, T} \rangle_{\mathbb{Z}_q}[\partial^{-1}] = \langle \text{Desc}_{\mathfrak{sp}_4, T}^{\varpi_1} \rangle_{\mathbb{Z}_q}[\partial^{-1}] = \mathcal{S}_{\mathfrak{sp}_4, T}^{\mathbb{Z}_q}[\partial^{-1}].$$

Since the mutation class $\mathfrak{s}_q(\mathfrak{sp}_4, T)$ is of acyclic exchange type, we have $\mathcal{A}_{\mathfrak{sp}_4, T}^q = \mathcal{U}_{\mathfrak{sp}_4, T}^q$ ([Mul16, Proposition 8.17]). Thus the assertion is proved. \square

Theorem 5.6. *For a connected unpunctured marked surface Σ with at least two special points, we have an inclusion*

$$\mathcal{S}_{\mathfrak{sp}_4, \Sigma}^{\mathbb{Z}_q}[\partial^{-1}] \subset \mathcal{A}_{\mathfrak{sp}_4, \Sigma}^q.$$

Proof. By Theorem 3.13, it suffices to prove that each element in $\text{SimpWil}_{\mathfrak{sp}_4, \Sigma}^{\varpi_1}$, namely each simple Wilson line α of type 1, is a cluster variable. From the definition, there exists a quadrilateral Q that contains α such that its interior is embedded, and the stated ends of α lie on opposite sides of Q . Here we allow one of the other side is collapsed so that Q is in fact a triangle in Σ . Then we find that α appears as a cluster variable in $\mathcal{A}_{\mathfrak{sp}_4, Q}^q$ from Figure 5.5 (the variables e_1, e_3, e'_1 and e'_3), except for the pattern . This one is also found in a cluster adjacent to the decorated triangulation (III) in the proof of Proposition 5.2. See Section 6. The assertion is proved. \square

Classical limit. At the classical limit $q = 1$, it is known that $\mathcal{A}_{\mathfrak{sp}_4, \Sigma} = \mathcal{U}_{\mathfrak{sp}_4, \Sigma}$ is generated by the matrix entries of simple Wilson lines in the vector representation $V(\varpi_1)$ of Sp_4 [IOS22, Theorem 1, Corollary 3.20 and Proposition 2.1]. Moreover, they correspond to elements in $\text{SimpWil}_{\mathfrak{sp}_4, \Sigma}^{\varpi_1}$ (recall Remark 3.6). Combining with Theorem 3.13, we get the following:

Theorem 5.7. *In the classical limit $q = 1$, we have*

$$\mathcal{S}_{\mathfrak{sp}_4, \Sigma}^{\mathbb{Z}}[\partial^{-1}] = \mathcal{A}_{\mathfrak{sp}_4, \Sigma} = \mathcal{U}_{\mathfrak{sp}_4, \Sigma}.$$

Here $\mathcal{S}_{\mathfrak{sp}_4, \Sigma}^{\mathbb{Z}} \subset \mathcal{S}_{\mathfrak{sp}_4, \Sigma}$ is the \mathbb{Z} -form defined as the \mathbb{Z} -span of $\text{BWeb}_{\mathfrak{sp}_4, \Sigma}$ in the classical skein algebra $\mathcal{S}_{\mathfrak{sp}_4, \Sigma}$.

5.3. **Inclusion $\mathcal{S}_{\mathfrak{sp}_4, \Sigma}^{\mathbb{Z}_q}[\partial^{-1}] \subseteq \mathcal{U}_{\mathfrak{sp}_4, \Sigma}^q$ via the cutting trick, quantum Laurent positivity.** Here we give a direct way to compute the inclusion $\mathcal{S}_{\mathfrak{sp}_4, \Sigma}^{\mathbb{Z}_q}[\partial^{-1}] \subset \mathcal{U}_{\mathfrak{sp}_4, \Sigma}^q$ based on the cluster expansion result (Theorem 3.14).

Theorem 5.8. *For any unpunctured marked surface Σ , we have an inclusion*

$$\mathcal{S}_{\mathfrak{sp}_4, \Sigma}^{\mathbb{Z}_q}[\partial^{-1}] \subseteq \mathcal{U}_{\mathfrak{sp}_4, \Sigma}^q.$$

We remark that this theorem also follows from the quantum Laurent phenomenon (Theorem 4.6) and Theorem 5.6 if we assume that Σ has at least two special points.

Proof. Let $\Delta \in \text{Exch}_{\text{sp}_4, \Sigma}$ be a decorated triangulation. Thanks to Theorem 4.6, it suffices to check the inclusion $\mathcal{S}_{\text{sp}_4, \Sigma}^{\mathbb{Z}_q}[\partial^{-1}] \subset \mathcal{U}_{\text{sp}_4, \Sigma}^q(\Delta)$ into the upper bound associated with Δ . It is a direct consequence of Theorem 3.14 that any element in $\mathcal{S}_{\text{sp}_4, \Sigma}^{\mathbb{Z}_q}[\partial^{-1}]$ has a Laurent expression with coefficients in \mathbb{Z}_q in the web cluster \mathcal{C}_Δ . Thus $\mathcal{S}_{\text{sp}_4, \Sigma}^{\mathbb{Z}_q}[\partial^{-1}] \subset T_\Delta$.

Observe that all the vertices of $\text{Exch}_{\text{sp}_4, \Sigma}$ adjacent to Δ are decorated cell decompositions. Indeed, the mutation at a face vertex preserves the underlying triangulation, and the mutation at an edge vertex lies in a flip sequence. Therefore it suffices to consider an ideal cell decomposition $(\Delta; E)$ and verify that any element $x \in \mathcal{S}_{\text{sp}_4, \Sigma}^{\mathbb{Z}_q}$ has a Laurent expression in each web cluster of the form

$$\mathcal{C}_{(\Delta; E)} := \bigcup_{T \in t(\Delta), T \not\ni E} \mathcal{C}_T \cup \mathcal{C}_{Q_E},$$

where Q_E denotes the unique quadrilateral containing E , \mathcal{C}_T (resp. \mathcal{C}_{Q_E}) is a web cluster in $\mathcal{S}_{\text{sp}_4, T}^q$ (resp. $\mathcal{S}_{\text{sp}_4, Q_E}^q$).

By the cutting trick (Lemma 3.1), there exists a monomial $J_{(\Delta; E)}$ of arcs along $\Delta \setminus \{E\}$ of either types such that the product $J_{(\Delta; E)}x$ is expanded into a linear combination of products of webs contained in $\mathcal{S}_{\text{sp}_4, T}^{\mathbb{Z}_q}[\partial^{-1}]$ or $\mathcal{S}_{\text{sp}_4, Q_E}^{\mathbb{Z}_q}[\partial^{-1}]$. Here each term in the expansion belongs to the \mathbb{Z}_q -form by Lemma 3.12. With a notice that each triangle T or the quadrilateral Q_E have at least two special points (since Σ has no punctures), we have inclusions

$$\begin{aligned} \mathcal{S}_{\text{sp}_4, T}^{\mathbb{Z}_q}[\partial^{-1}] &\subset \mathcal{A}_{\text{sp}_4, T}^q \subset \mathcal{U}_{\text{sp}_4, T}^q, \\ \mathcal{S}_{\text{sp}_4, Q_E}^{\mathbb{Z}_q}[\partial^{-1}] &\subset \mathcal{A}_{\text{sp}_4, Q_E}^q \subset \mathcal{U}_{\text{sp}_4, Q_E}^q \end{aligned}$$

by Theorem 5.6. Then it follows that each web appearing in the expression of $J_{(\Delta; E)}x$ has a Laurent expansion with coefficients in \mathbb{Z}_q in the web cluster $\mathcal{C}_{(\Delta; E)}$. Therefore so does x . Thus we get the inclusion $\mathcal{S}_{\text{sp}_4, \Sigma}^{\mathbb{Z}_q}[\partial^{-1}] \subset \mathcal{U}_{\text{sp}_4, \Sigma}^q(\Delta) = \mathcal{U}_{\text{sp}_4, \Sigma}^q$, as desired. \square

Now we complete the proof of Theorem 1.

Proof of Theorem 1. The algebra inclusions are already proved in Theorems 5.6 and 5.8. The mapping class group equivariance is clear from the construction (see [IY21] for more explanation). What remains are the comparison of gradings and anti-involutions. Thanks to the web cluster expansion result (Theorem 3.14), it suffices to compare these structures on the quantum torus T_Δ generated by the elementary webs associated with a single decorated triangulation Δ . Then the coincidence of the mirror-reflection and the bar-involution is clear from their definitions, and the coincidence of the endpoint grading and the ensemble grading has been shown in Lemma 5.1. \square

Definition 5.9. An element of $\mathcal{U}_{\text{sp}_4, \Sigma}^q \otimes \mathcal{R}$ is called a *quantum GS-universally positive Laurent polynomial over \mathbb{Z}_q (resp. \mathcal{R})* if it admits an expression as a Laurent polynomial

in the cluster \mathbf{A}^Δ associated with any decorated triangulation Δ of Σ with coefficients in $\mathbb{Z}_+[q^{\pm 1/2}]$ (resp. $\mathcal{R}_+ = \mathbb{Z}_+[q^{\pm 1/2}, 1/[2]_q]$).

Here ‘‘GS’’ stands for Goncharov–Shen. The quantum GS-universal positivity over \mathbb{Z}_q is weaker than the quantum universal positivity [FG09], which asks the positivity of Laurent expression for *any* cluster. The following is a rephrasing of Theorem 3.17:

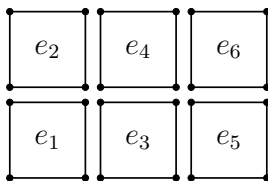
Theorem 5.10 (Quantum Laurent positivity of webs). *Any elevation-preserving web with respect to an ideal triangulation Δ is expressed as a Laurent polynomial with coefficients in \mathcal{R}_+ in the quantum cluster associated with any decorated triangulation $\Delta = (\Delta, m_\Delta, \mathbf{s}_\Delta)$ over Δ . In particular, by Example 3.16, the following webs are quantum GS-universally positive Laurent polynomials*

- over \mathbb{Z}_q : elements in $\text{Desc}_{\mathfrak{sp}_4, \Sigma}^{\varpi_1}$;
- over \mathcal{R} : the geometric bracelets or the bangles (Figure 1.1) of type 2 along simple loops.

6. GALLERY OF WEB CLUSTERS IN A QUADRILATERAL

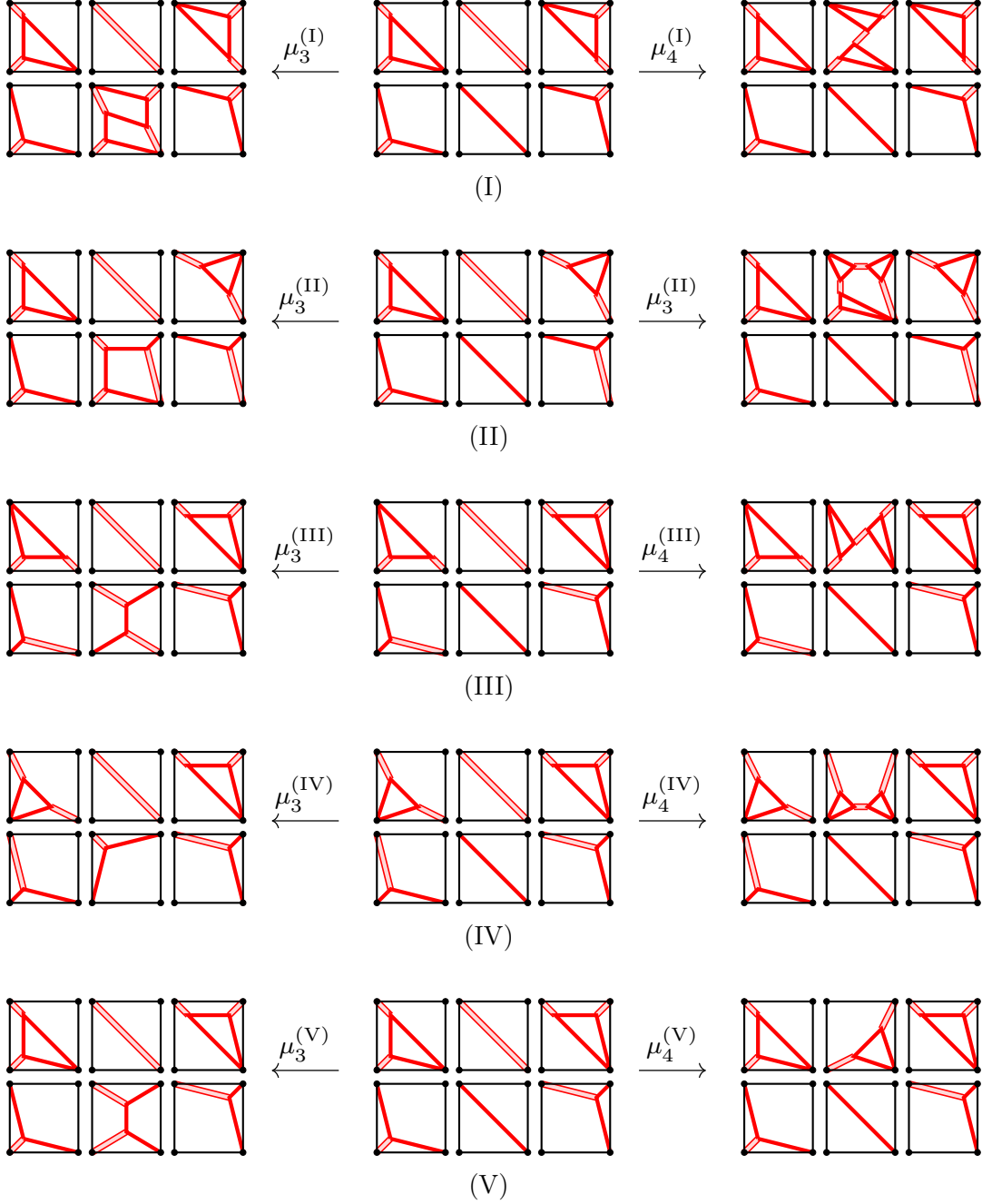
In this section, we present examples of web clusters in a quadrilateral that support Conjecture 4, and exchange relations among them. Indecomposability of elementary webs in this section follows from the injective homomorphism constructed in Theorem 5.6 and the indecomposability of cluster variables [GLS13]. Let Σ be a quadrilateral, which is a disk with four special points. We use the labeling in Figure 5.3 for boundary webs.

In the following presentation of web clusters of $\mathcal{S}_{\mathfrak{sp}_4, \Sigma}$, we display the 6 elementary webs other than boundary webs as follows.



Moreover, in the presentation of quantum exchange/skein relation upon each mutation μ_k , non-primed variables e_i , $i = 1, \dots, 6$ denote the elementary webs in the web cluster before that mutation and the primed one e'_k denotes the new elementary web appearing after the mutation.

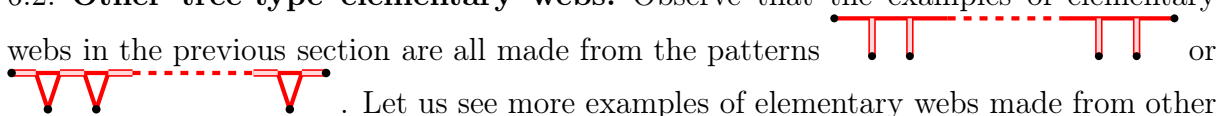

6.1. Web clusters adjacent to (I)–(V). Here are web clusters adjacent to the decorated triangulations (I)–(V) in the proof of Theorem 5.8. New elementary webs that do not come from any decorated triangulations appear in the replacement of e_3 or e_4 in each case, which are easily seen to be tree-type. Let us denote the mutation replacing e_3 (resp. e_4) starting from the web cluster (N) by $\mu_3^{(N)}$ (resp. $\mu_4^{(N)}$) for $N \in \{\text{I, II, III, IV, V}\}$.

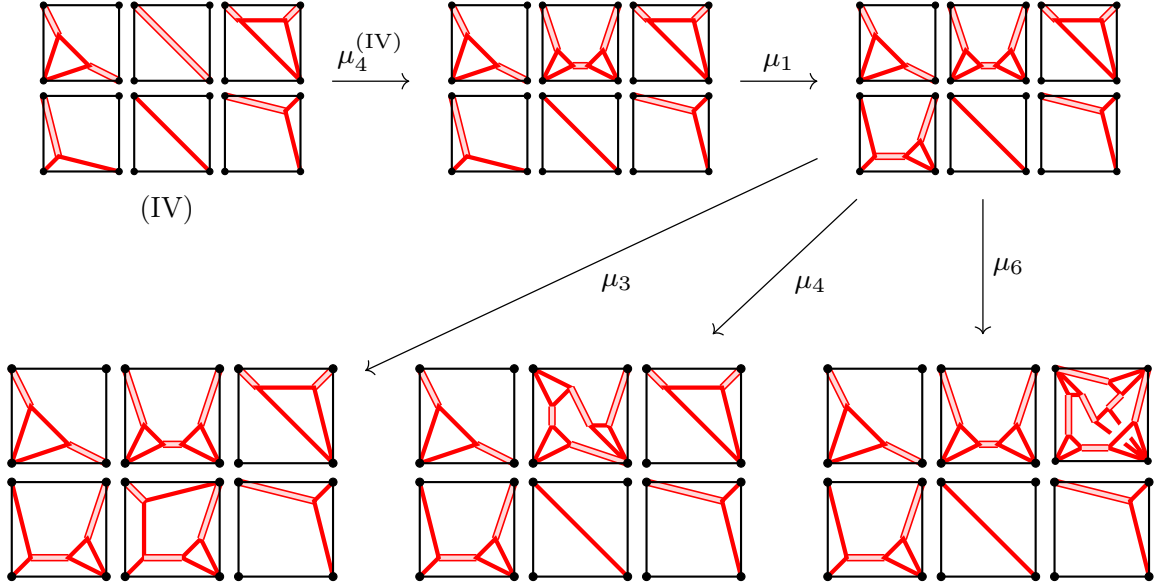


We have the following skein relations among them:

$$\begin{aligned}
\mu_3^{(I)} : e_3 e'_3 &= v[e_2 e_6] + [e_1 e_5 e_4], & \mu_4^{(I)} : e_4 e'_4 &= [e_2 e_6] + v^2[e_1 e_5 e_4], \\
\mu_3^{(II)} : e_3 e'_3 &= v^{\frac{1}{2}}[e_2 e_6] + v^{-\frac{1}{2}}[e_1 e_4 e_{11}], & \mu_4^{(II)} : e_4 e'_4 &= v^{-1}[e_2 e_5^2] + v[e_3^2 e_6 e_{10}], \\
\mu_3^{(III)} : e_3 e'_3 &= [e_1 e_5] + v[e_4 e_9 e_{13}], & \mu_4^{(III)} : e_4 e'_4 &= [e_2 e_6] + v^{-2}[e_3^2 e_8 e_{12}], \\
\mu_3^{(IV)} : e_3 e'_3 &= v^{-\frac{1}{2}}[e_5 e_7] + v^{\frac{1}{2}}[e_1 e_{13}], & \mu_4^{(IV)} : e_4 e'_4 &= [e_2 e_6] + v^2[e_1^2 e_{12}], \\
\mu_3^{(V)} : e_3 e'_3 &= [e_1 e_5] + v[e_2 e_{13}], & \mu_4^{(V)} : e_4 e'_4 &= v[e_6 e_{10}] + v^{-1}[e_2 e_{12}].
\end{aligned}$$

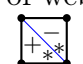
They are exactly the quantum exchange relations induced by $\mu_i^{(N)}$.

6.2. Other tree-type elementary webs. Observe that the examples of elementary webs in the previous section are all made from the patterns  or . Let us see more examples of elementary webs made from other types of trees. We start from the web cluster (IV).

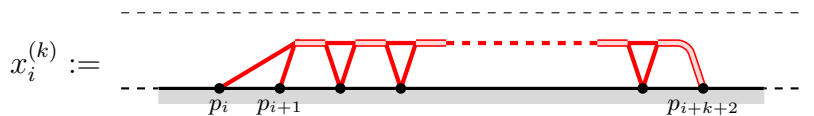


The skein/quantum exchange relations among them are:

$$\begin{aligned} \mu_1: e_1 e'_1 &= [e_6 e_7 e_9] + v^{-1} [e_3 e_4], & \mu_3: e_3 e'_3 &= [e_6 e_9 e_{13}] + v^{-1} [e_1 e_5], \\ \mu_4: e_4 e'_4 &= v^{-1} [e_1^2 e_2] + v [e_6 e_7^2 e_9^2 e_{12}], & \mu_6: e_6 e'_6 &= v^{-1} [e_3 e_4 e_{11} e_{13}] + v [e_1^2 e_5^2]. \end{aligned}$$

6.3. An infinite sequence of web clusters. We construct an infinite sequence of web clusters starting from the web cluster associated with the decorated triangulation . We denote by p_0, p_1, p_2, p_3 the special points in Σ in the counterclockwise order from the upper left corner. We represent an elementary web in Σ by a diagram in a band with infinitely many linearly ordered special points labeled by p_0, p_1, p_2, p_3 on its bottom side. See Figure 6.1. The band is viewed as an infinite cyclic covering of Σ , and the actual elementary web is obtained through the projection. At a crossing of the projection of the diagram, we draw the \mathfrak{sp}_4 -web in such a way that the right arc in the band becomes overpassing. If all the crossings in the projected diagram are arborizable or at special points, then we can uniquely determine the flat \mathfrak{sp}_4 -web representing this projected diagram.

For $i \in \mathbb{Z}$ and $k \in \mathbb{Z}_{\geq 0}$, let us consider the elementary webs $x_i^{(k)}$ and $y_i^{(k)}$ given by



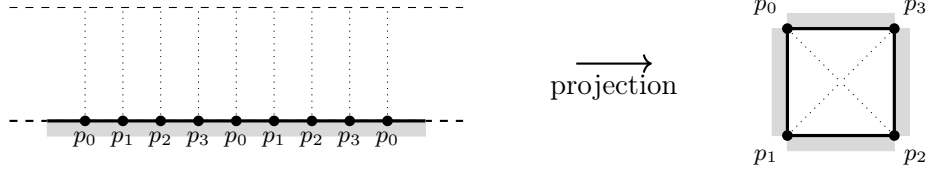
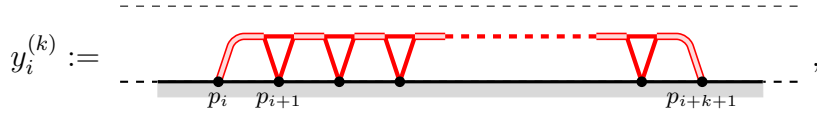


FIGURE 6.1. The bottom side corresponds to the boundary of Σ and the top side to the center of Σ .



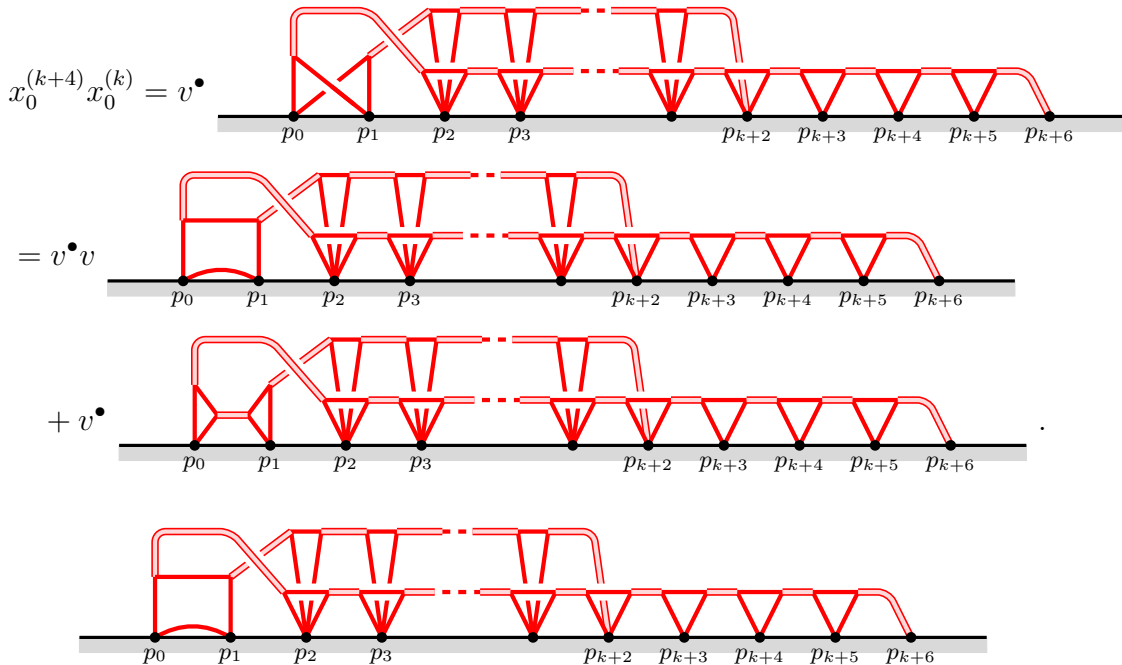
where subscripts i for p , x , and y are considered modulo 4. We denote by $e_{i,j}$ the simple arc of type 1 between the special points p_i and p_j for any distinct integers i and j .

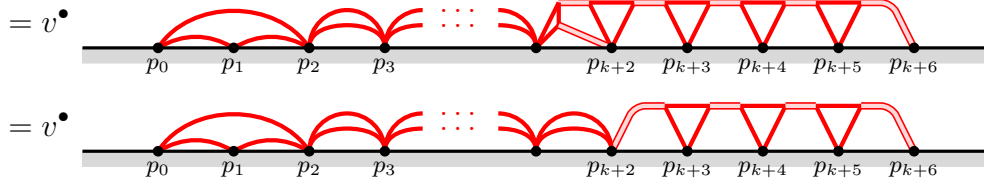
Proposition 6.1. *For $i, k \in \mathbb{Z}_{\geq 0}$, we have the relation*

$$\eta_i^{(k)} : x_i^{(k+4)} x_i^{(k)} = v^{m_k} \left[e_{i,i+2} e_{i,i+1} e_{i+1,i+2} \left(\prod_{j=i}^{k-1} (e_{j+2,j+3})^2 \right) y_{i+k+2}^{(3)} \right] + v^{n_k} (x_{i+2}^{(k+2)})^2, \quad (6.1)$$

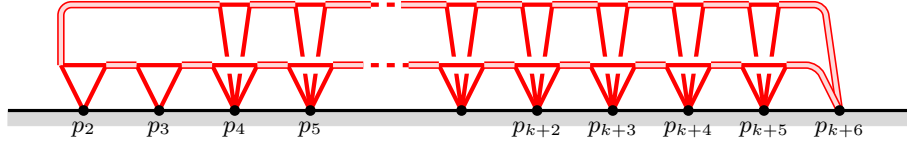
for some $m_k, n_k \in \frac{1}{2}\mathbb{Z}$. Moreover, the collections $\mathcal{C}_k := \{x_{2k+2}^{(2k)}, x_{2k}^{(2k+2)}, y_0^{(1)}, y_0^{(3)}, y_2^{(1)}, e_{0,3}\} \cup \partial_\Sigma$ are web clusters for any $k \in \mathbb{Z}_{\geq 0}$.

Proof. It suffices to show (6.1) for $i = 0$, since $x_i^{(k)}$ is obtained by shifting $x_0^{(k)}$ to the right by i special points. In the calculation below, we tacitly exchange over- and underpassing arcs when a crossing is arborizable or at a special points, discarding the explicit description of the exponents of v appearing in such exchanges.

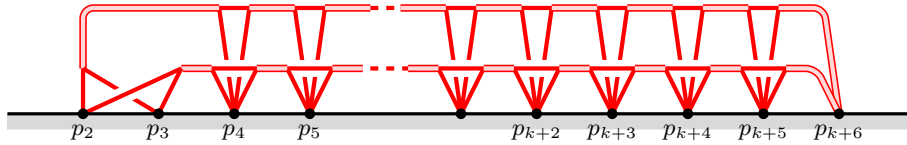




We can take another lift of \mathfrak{sp}_4 -web in the second term as



Furthermore, one can confirm the above \mathfrak{sp}_4 -web is the same as

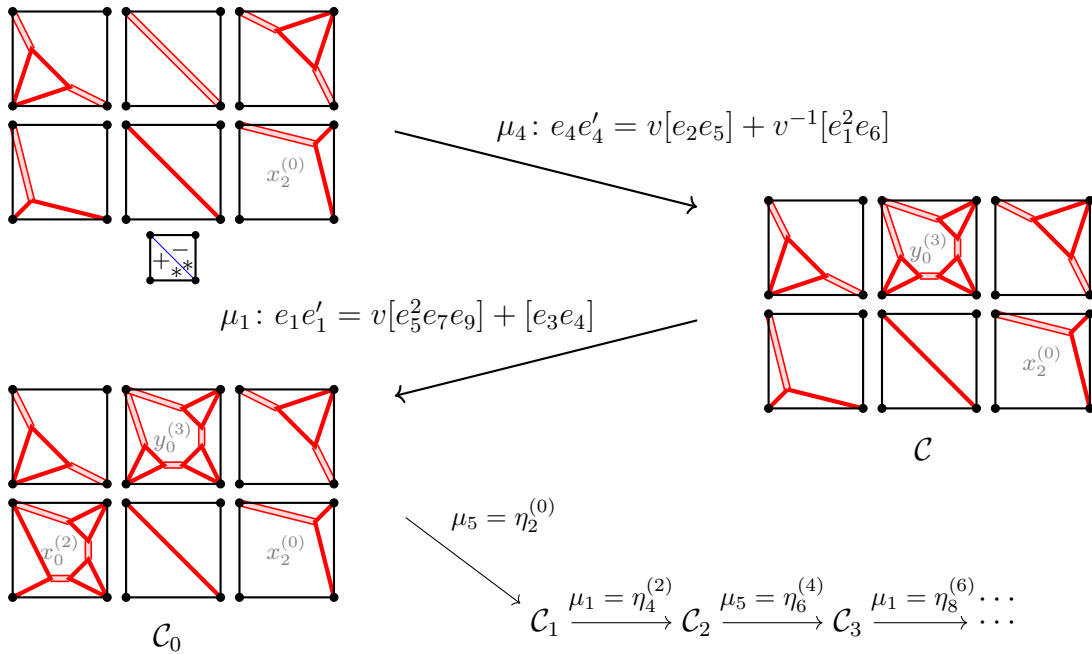


again by Lemma 2.20. Hence,

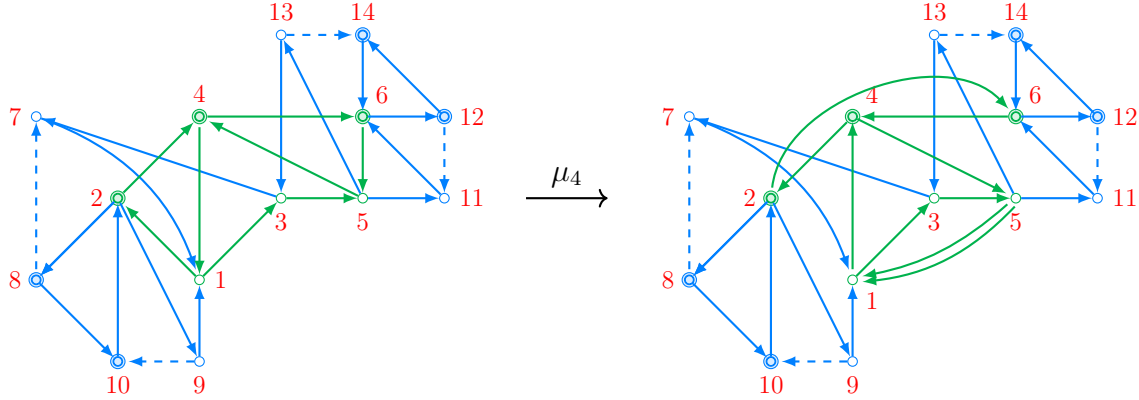
$$x_0^{(k+4)} x_0^{(k)} = v^\bullet \left[e_{0,2} e_{0,1} e_{1,2} \left(\prod_{j=2}^{k+1} (e_{j,j+1})^2 \right) y_{k+2}^{(3)} \right] + v^\bullet (x_2^{(k+2)})^2.$$

Firstly, it is easy to see that \mathfrak{sp}_4 -webs in \mathcal{C}_k are v -commutative by the arborization relations in Lemma 2.19, and that \mathcal{C}_k is related to \mathcal{C}_{k+1} by $\eta_{2k+2}^{(2k)}$ in (6.1). \square

The mutation sequence among the web clusters \mathcal{C}_k are the following:



One can verify that the relations $\eta_i^{(k)}$ are indeed quantum exchange relations. The quiver mutation for the first step μ_4 is given by



Then we find the Kronecker sub-quiver $\begin{matrix} 5 \\ \circ \implies \circ \\ 1 \end{matrix}$. It is well-known that the mutation sequences $(\mu_1\mu_5)^n$ for $n \geq 0$ on such a Kronecker quiver are non-trivial, and produce distinct quantum clusters. In this way, we obtain an infinite sequence of (web) clusters. Observe that $x_i^{(k)}$'s are all tree-type elementary webs which are not invariant under DT.

Remark 6.2. For a Kronecker quiver over vertices $\{i, j\}$ with a common weight and 2 arrows between them, it is known that the sequence of g -vectors along the mutation sequence $(\mu_i\mu_j)^n$ has linear growth, and its recurrence relation stabilizes to a linear one (see, for instance, [IK20, Proposition 6.6]). Hence the sequence $\deg[n] \in X^*(H_{\mathcal{A}})$ of ensemble degrees, which are projections of g -vectors, also has linear growth. Let us define $\deg_{\infty} := \lim_{n \rightarrow \infty} \deg[n]/n$, which we call the *asymptotic ensemble degree*.

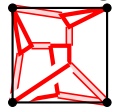
For the above sequence of (web) clusters, the elementary webs/cluster variables have weight 1 and the asymptotic ensemble degree can be easily seen to be

$$\deg_{\infty} = (2\varpi_1, 2\varpi_1, 2\varpi_1, 2\varpi_1) \in \mathbb{P}_+^{\oplus 4}. \tag{6.2}$$

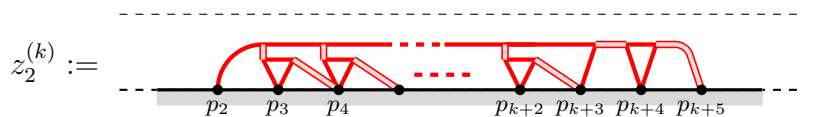
In a similar analysis, we can find a Kronecker sub-quiver over the weight 2 vertices $\{4, 6\}$, and hence an infinite sequence of (web) clusters of weight 2 starting from the cluster $\mathcal{D}_0 := \mu_2\mu_3\mu_4\mu_3 \left(\begin{matrix} \square \\ \hline \ast \end{matrix} \right)$. Its asymptotic degree is

$$\deg_{\infty} = (2\varpi_1 + \varpi_2, 2\varpi_1 + \varpi_2, 2\varpi_1 + \varpi_2, 2\varpi_1 + \varpi_2) \in \mathbb{P}_+^{\oplus 4}. \tag{6.3}$$

The corresponding web clusters until \mathcal{D}_0 has been confirmed, which are shown in Figure 6.2. The \mathfrak{sp}_4 -webs appearing here are all tree-type elementary webs, where



gives a lift of e_4 in the web cluster \mathcal{D}_0 . We believe that the \mathfrak{sp}_4 -webs $\{z_2^{(3)}, z_2^{(7)}, z_2^{(11)}, \dots\}$ give the corresponding sequence of web clusters of weight 2 from \mathcal{D}_0 , where



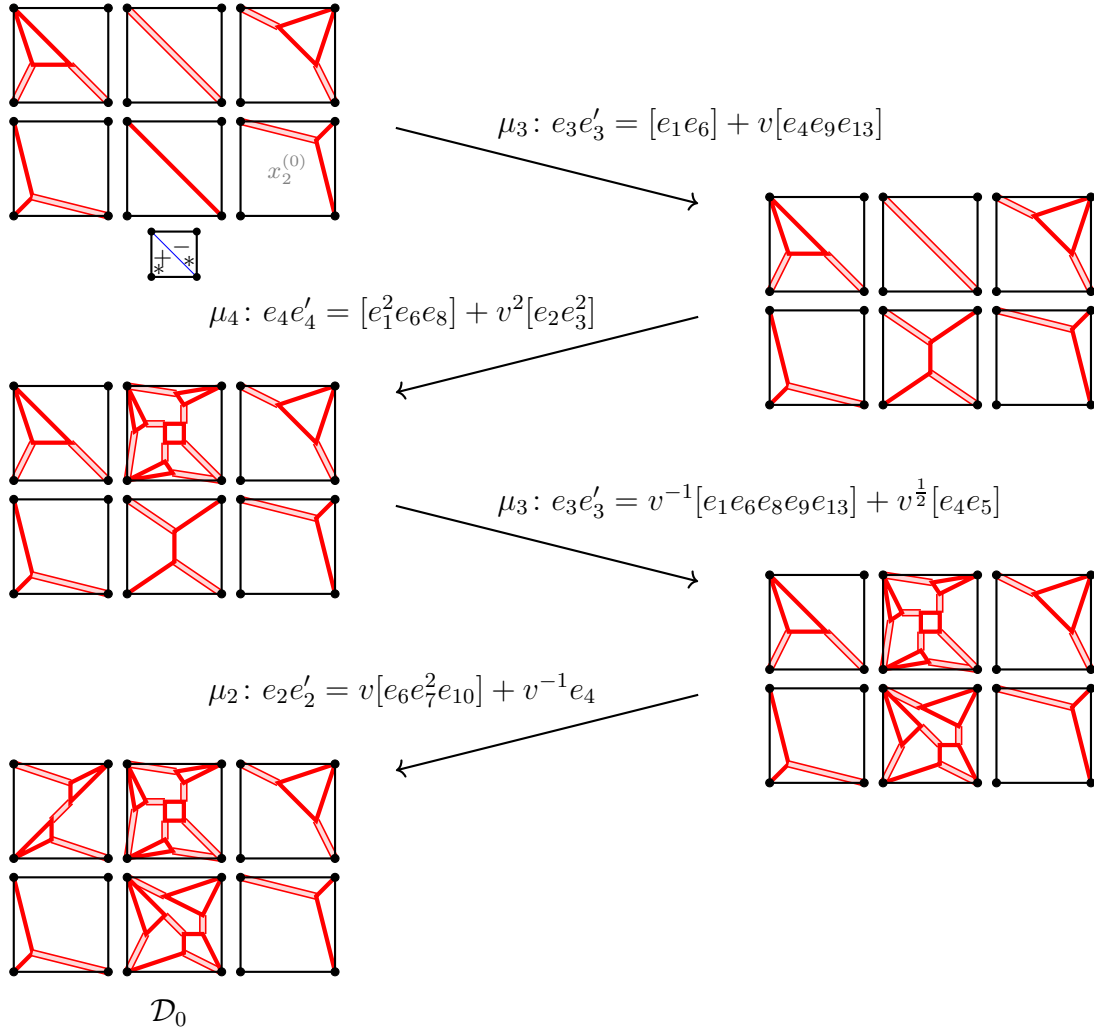


FIGURE 6.2. Web clusters along a weight 2 sequence.

We have verified the first two quantum exchange relations $e_4 z_2^{(3)} = v^\bullet [e_6^2 e_7 e_9^2 e_{11}^2 e_{12} e_{13} e_{14}] + v^\bullet [e_2 e_3^2]$ and $e_6 z_2^{(7)} = v^\bullet [e_2 e_3^2 e_{11}^2 e_{14}] + v^\bullet (z_2^{(3)})^2$, where the non-primed variables are elementary webs in \mathcal{D}_0 .

It is an interesting observation that the asymptotic ensemble degrees (6.2), (6.3) are invariant under rotations (*i.e.*, the cluster Donaldson–Thomas transformation). The authors do not know if a general theory exists behind this phenomenon.

REFERENCES

- [BZ05] A. Berenstein and A. Zelevinsky, *Quantum cluster algebras*, Adv. Math. **195** (2005), no. 2, 405–455. [31](#), [32](#), [33](#), [34](#)
- [BFZ05] A. Berenstein, S. Fomin, and A. Zelevinsky, *Cluster algebras III: Upper bounds and double Bruhat cells*, Duke Math. J. **126** (2005), no. 1, 1–52. [33](#)
- [Bod20] E. Bodish, *Web calculus and tilting modules in type C_2* , arXiv:2009.13786. [1](#)
- [Bod22] E. Bodish, *Triple clasp formulas for C_2 webs*, J. Algebra **604** (2022), 324–361. [1](#)

- [BERT21] E. Bodish, B. Elias, D. E. V. Rose, L. Tatham *Type C webs*, arXiv:2103.14997. [1](#)
- [FG06a] V. V. Fock and A. B. Goncharov, *Moduli spaces of local systems and higher Teichmüller theory*, Publ. Math. Inst. Hautes Études Sci., **103** (2006), 1–211. [1](#), [38](#)
- [FG06b] V. V. Fock and A. B. Goncharov, *Cluster \mathcal{X} -varieties, amalgamation and Poisson-Lie groups*, Algebraic geometry and number theory, volume 253 of Progr. Math., PP 27–68, Birkhäuser Boston, Boston, MA, 2006. [35](#)
- [FG09] V. V. Fock and A. B. Goncharov, *Cluster ensembles, quantization and the dilogarithm*, Ann. Sci. Éc. Norm. Supér., **42** (2009), 865–930. [39](#), [49](#)
- [FP16] S. Fomin and P. Pylyavskyy, *Tensor diagrams and cluster algebras*, Adv. Math. **300** (2016), 717–787. [1](#), [3](#), [14](#)
- [FS20] C. Frohman and A. S. Sikora, *$SU(3)$ -skein algebras and webs on surfaces*, Math. Z. **300** (2022), 33–56. [1](#)
- [GLS13] C. Geiss, B. Leclerc and J. Schröer, *Factorial cluster algebras*, Doc. Math. **18** (2013), 249–274. [49](#)
- [GS18] A. B. Goncharov and L. Shen, *Donaldson-Thomas transformations of moduli spaces of G -local systems*, Adv. Math. **327** (2018), 225–348. [4](#)
- [GS19] A. B. Goncharov and L. Shen, *Quantum geometry of moduli spaces of local systems and representation theory*, arXiv:1904.10491. [2](#), [5](#), [36](#), [37](#), [38](#), [39](#)
- [Hig20] V. Higgins, *Triangular decomposition of SL_3 skein algebras*, arXiv:2008.09419. [18](#)
- [IIO21] R. Inoue, T. Ishibashi, and H. Oya, *Cluster realizations of Weyl groups and higher Teichmüller theory*, Sel. Math. New Ser. **27**, 37 (2021). [34](#), [35](#)
- [IK20] T. Ishibashi and S. Kano, *Sign stability of mapping classes on marked surfaces II: general case via reductions*, arXiv:2011.14320. [54](#)
- [IOS22] T. Ishibashi, H. Oya and L. Shen, *$\mathcal{A} = \mathcal{U}$ for cluster algebras from moduli spaces of G -local systems*, arxiv:2202.03168. [2](#), [3](#), [20](#), [23](#), [39](#), [47](#)
- [IY21] T. Ishibashi and W. Yuasa, *Skein and cluster algebras of marked surface without punctures for \mathfrak{sl}_3* , arXiv:2101.00643. [1](#), [19](#), [26](#), [39](#), [48](#)
- [IY22] T. Ishibashi and W. Yuasa, *State-clasp correspondence for skein algebras*, in preparation. [18](#), [20](#)
- [Kup94] G. Kuperberg, *The quantum G_2 link invariant*, Internat. J. Math. **5** (1994), no. 1, 61–85. [7](#), [9](#)
- [Kup96] G. Kuperberg, *Spiders for rank 2 Lie groups*, Comm. Math. Phys. **180** (1996), no. 1, 109–151. [1](#), [6](#), [7](#), [9](#), [10](#), [12](#), [15](#)
- [Le19] I. Le, *Cluster structure on higher Teichmüller spaces for classical groups*, Forum Math. Sigma **7** (2019), e13, 165 pp. [1](#)
- [Lê18] T. T. Q. Lê, *Triangular decomposition of skein algebras*, Quantum Topol. **9** (2018), no. 3, 591–632. [18](#)
- [LS22] T. T. Q. Lê and A. S. Sikora, *Stated $SL(n)$ -skein modules and algebras*, arXiv:2201.00045. [18](#)
- [LY20] T. T. Q. Lê and T. Yu, *Quantum traces and embeddings of stated skein algebras into quantum tori*, arXiv:2012.15272. [18](#)
- [Mul16] G. Muller, *Skein and cluster algebras of marked surfaces*, Quantum Topol. **7** (2016), no. 3, 435–503. [1](#), [47](#)
- [SW07] A. S. Sikora and B. W. Westbury, *Confluence theory for graphs*, Algebr. Geom. Topol. **7** (2007), 439–478. [10](#), [12](#)

TSUKASA ISHIBASHI, MATHEMATICAL INSTITUTE, TOHOKU UNIVERSITY, 6-3 AOBA, ARAMAKI, AOBA-KU, SENDAI, MIYAGI 980-8578, JAPAN.

Email address: `tsukasa.ishibashi.a6@tohoku.ac.jp`

URL: `https://sites.google.com/view/tsukasa-ishibashi/home`

OSAKA CENTRAL ADVANCED MATHEMATICAL INSTITUTE, OSAKA METROPOLITAN UNIVERSITY, 3-3-138 SUGIMOTO, SUMIYOSHI-KU, OSAKA 558-8585, JAPAN.

Email address: `wyuasa@kurims.kyoto-u.ac.jp`

URL: `https://wataruyuasa.github.io/math/`